Microgrid based on photovoltaic energy for charging electric vehicle stations : charging and discharging management strategies in communication with the smart grid

Dian Wang

Par **Dian WANG**

Microgrid based on photovoltaic energy for charging electric vehicle stations : charging and discharging management strategies in communication with the smart grid

Thèse présentée
pour l'obtention du grade
de Docteur de l'UTC

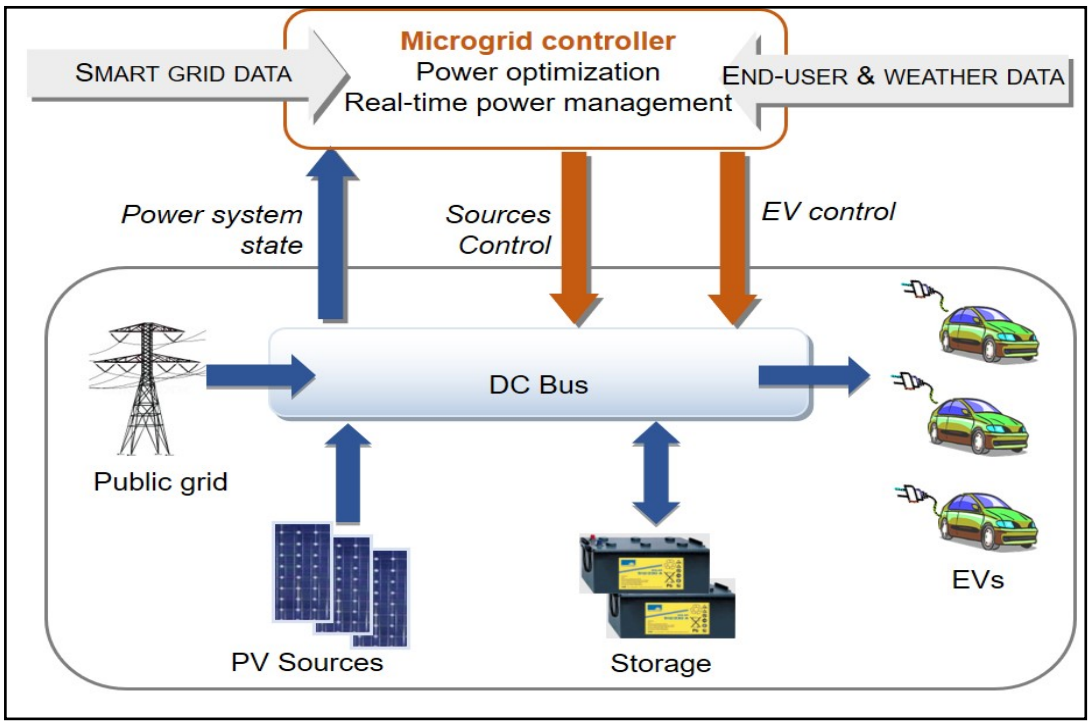

Soutenue le 26 janvier 2021
Spécialité : Génie Électrique : Laboratoire Avenues - EA-7284

D2584

UNIVERSITÉ DE TECHNOLOGIE DE COMPIÈGNE

THESE

Pour obtenir le grade de

DOCTEUR

Spécialité : Génie Électrique

Dian WANG

Microgrid based on photovoltaic energy for charging electric vehicle stations. Charging and discharging management strategies in communication with the smart grid.

Laboratoire AVENUES, EA 7284

Soutenance le 26 Janvier 2021 devant le jury composé de :

Rapporteurs :	Delphine RIU	G2ELab, Grenoble
	Brayima DAKYO	GREAH, Le Havre
Examinateurs :	Demba DIALLO	GeePs, Paris
	Arnaud HUBERT	Roberval, Compiègne
Directeur de thèse :	Fabrice LOCMENT	AVENUES, Compiègne
Co-Directeur de thèse :	Manuela SECHILARIU	AVENUES, Compiègne

Université de Technologie de Compiègne - AVENUES -
Rue Roger Couttolenc, 60203 Compiègne

Abstract

The rapid development of electric vehicles (EVs) increases the power demand, which causes an extra burden on the public grid increasing the load fluctuations, therefore, hindering the high penetration of EVs. A real-time rule-based algorithm for electric vehicle (EV) charging stations empowered by a DC microgrid is proposed to deal with the uncertainties of EV users' behaviour considering its arbitrary and random choices through the human-machine interface, meanwhile considering most of the users' choices. The simulation results obtained under MATLAB/Simulink verify the feasibility of the proposed management strategy that presents a good performance in terms of precise control.

In addition, EV shedding and restoration optimization algorithms (SROA) for battery charging power can be used to meet user needs while maintaining EV charging station power balance, taking into consideration the intermittency of the photovoltaic (PV) source, the capacity limitation of the storage, and the power limitation of the public grid. The simulation results show that compared with rule-based algorithm, the proposed SROA respect the user's choice while reducing total charging time, increasing the full rate, and maximizing the available power utilization, which shows the feasibility and effectiveness of SROA.

Furthermore, a PV based charging station for EVs can participate to solve some peak power problems. On the other hand, vehicle to grid (V2G) technology is designed and applied to provide ancillary services grid during the peak periods, considering the duality of EV battery "load-source". So, a dynamic searching peak and valley algorithm, based on energy management, is proposed for an EV charging station to mitigate the impact on the public grid, while reducing the energy cost of the public grid. Simulation results demonstrate the proposed searching peak and valley algorithm effectiveness, which can guarantee the balance of the public grid, meanwhile satisfy the charging demand of EV users, and most importantly, reduce the public grid energy cost.

Keywords: DC microgrid, EV charging station, power management strategy, searching peak and valley algorithm, vehicle to grid.

Résumé

Le développement rapide des véhicules électriques (EVs) augmente la demande de puissance, ce qui provoque une charge supplémentaire sur le réseau public et augmente les fluctuations de la charge. Par conséquent, la forte pénétration des EVs est freinée. Un algorithme simulé en temps réel et basé sur des règles est élaboré pour les bornes de recharge des EVs alimentées par un micro-réseau DC afin de faire face aux incertitudes du comportement des utilisateurs des EVs. L'algorithme prend en considération les choix arbitraires et aléatoires proposés via l'interface homme-machine. Les résultats de simulation sont

obtenus sous MATLAB / Simulink et vérifient la faisabilité de la stratégie de gestion proposée. Cette stratégie présente de bonnes performances en garantissant un contrôle précis.

Par ailleurs, les algorithmes d'optimisation de délestage et de la restauration des EVs (SROA) pour la recharge de la puissance de la batterie peuvent être utilisés pour répondre aux besoins des utilisateurs. Aussi les algorithmes SROA maintiennent l'équilibre de la puissance de la station de recharge des EVs. Les algorithmes SROA prennent en compte l'intermittence de la source photovoltaïque (PV), la limitation de capacité du stockage et la limitation de puissance du réseau public. En comparant les résultats de la simulation aux algorithmes basés sur les règles, les algorithmes SROA proposés respectent le choix de l'utilisateur, réduisent le temps de charge total, augmentent le plein débit et maximisent l'utilisation de la puissance disponible. Les résultats de la simulation montrent la faisabilité et l'efficacité des algorithmes SROA.

En outre, une station de charge basée sur le PV pour les EVs peut participer à la résolution de certains problèmes liés au pic de puissance. D'autre part, la technologie de véhicule à réseau (V2G) est conçue et appliquée pour fournir des services auxiliaires au réseau pendant les périodes de pointe, et V2G considère la dualité de la batterie des EVs «charge et source». Ainsi, un algorithme de recherche dynamique des pics et de vallées est proposé pour une station de recharge des EVs afin d'atténuer l'impact sur le réseau public. Cet algorithme réduit ainsi le coût énergétique du réseau public. Les résultats de la simulation démontrent bien l'efficacité de l'algorithme de recherche des pics et des vallées. L'algorithme peut garantir l'équilibre du réseau public, satisfaire la demande de charge des utilisateurs des EVs et, surtout, réduire le coût énergétique du réseau public.

Mots-clés : Micro-réseau DC, station de charge des EVs, stratégie de gestion de la puissance, algorithme de recherche dynamique de pic et de vallée, véhicule à réseau.

Acknowledgements

First of all, I would like to express my sincere gratitude to my supervisors, Prof. Fabrice LOCMENT and Prof. Manuela SECHILARIU, for their good guidance and great efforts throughout the research and the writing of the thesis. Thanks to this teamwork and their well-organized working style, this thesis has advanced well according to the plan, which has permitted that the thesis work can be published in each stage. Thanks to Prof. Fabrice LOCMENT for the great help in the progress of my French language, as well as the simulation operations. Thanks to Prof. Manuela SECHILARIU for the great advice and efforts in writing and revising of this thesis, as well as other publications.

I also express my very gratitude to Professor Delphine RIU and Professor Brayima DAKYO, who have made detailed reports and remarks on my thesis, which help a lot in improving the quality of my thesis for both research content and presentation. Thanks also to Professor Demba DIALLO, chairman of the thesis committee, and Professor Arnaud HUBERT for their interest in my work.

In addition, I would like to thank all the colleagues of the laboratory AVENUES and the department of GU (Génie Urban): Eduard ANTALUCA, Jean-louis BATOZ, Lydie DELETTRE, Carine HENRIOT, Fabien LAMARQUE, Gilles MOREL, Hipolito MARTELL-FLORES, Nassima MOUHOUS-VOYNEAU, Nathalie MOLINES and Cristina PRONELLO for the good ambiance during my PhD studies at UTC and in France.

I also thank my colleagues (PhD students) and friends: Jamila AOURIR, Amine BEN-DAOUED, Saleh CHEIKH-MOHAMAD, Raphael ROLIN, Soelarso SOELARSO, Ghada TAY, Hongwei WU and Changjie YIN for sharing the PhD and life experience, for discussions on culture and customs, as well as on the study.

I would like to thank my friends Dong Ding, Peng DU, Jishuai LI, Ke LI, Caiyun LIU, CongCong MA, Kaidi PENG, Guoqiang WEI, Xingyi WANG, Lu WANG, Maiqi XIANG, Deyang ZHAO and Rui ZHANG for their help during my PhD studies and daily life.

I am very grateful to my husband, Wenshuai BAI, for his help in my work, the care of my life, and deep love for me, which encourages me to face the work positively and complete the doctoral project successfully.

I would like to thank the China Scholarship Council for offering the opportunity to support my PhD study and life in France. I will treasure the experiences both academic and personal in my life. Finally, a special bunch of thanks goes to my parents and my brother for all their love and encouragement to support me in finishing the PhD studies.

Table of Contents

List of figures

List of tables

Abbreviations

AC	Alternating Current
CC	Constant Current
CV	Constant Voltage
CC/CV	Constant Current / Constant Voltage
CO_2	Carbon Dioxide
DC	Direct Current
DOD	Depth of Discharge
EV	Electric Vehicle
EVs	Electric Vehicles
ESR	Equivalent Series Resistance
ICDA	Immediate Charge/Discharge Algorithm
GHG	Greenhouse Gas
G2V	Grid to Vehicle
MPPT	Maximum Power Point Tracking
PV	Photovoltaic
RBA	Rule-Based Algorithm
SROA	Shedding and Restoration Optimization Algorithms
SPVA	Searching Peak and Valley Algorithm
STC	Standard Test Conditions
V2G	Vehicle to Grid
V2V	Vehicle to Vehicle
V2H	Vehicle to Home

Nomenclature

c_{PV}	Coefficient of PV power
c_{EV}	Coefficient of the energy that EVs can release
C	DC bus capacity (μF)
C_{ERF}	Battery storage capacity (Ah)
C_{PV}	PV capacitor (μF)
C_{EVs}	EV capacitor (μF)
D_{cp}	Completion degree of EVs
$D_{cp}(1)$	Completion degree of EVs under ICDA
$D_{cp}(2)$	Completion degree of EVs under SPVA
$E_{discharge}$	Maximum energy that EVs can discharge (kW)
E_{charge}	Maximum energy that EVs can be charged (kW)
f_{PV}	PV switching function
f_S	Battery storage switching function
f_{EVs}	EV switching function
f_A	AC/DC converter switching function
f_B	AC/DC converter switching function
f_C	AC/DC converter switching function
i	EV order
$i_{L_{PV}}$	PV converter's input side current (A)
$i'_{L_{PV}}$	PV converter's output side current (A)
i_S	Battery storage current before the converter (A)
i'_S	Battery storage current next to the DC bus (A)
i_{PV}	PV current (A)

J_{EV_ERF}	Battery energy of EV (kWh)
i'	Inverter current (A)
i_A	Three phases current (A)
i_B	Three phases current (A)
i_C	Three phases current (A)
$i_{L_{EVs}}$	EV converter's output side current (A)
i_{EVs}	EV current (A)
$i'_{L_{EVs}}$	EV converter's input side current (A)
I_{S_MAX}	Storage current limitation (A)
k	Distribution coefficient
L	Self-inductance (mH)
L_{PV}	PV inductor (mH)
L_S	Storage inductor (mH)
L_{EVs}	EV inductor (mH)
m_S	Storage control variable
m_A	Inverter control variables
m_B	Inverter control variables
$Ordinal_{EV}$	EVs ordinal number
p_{inject_G}	Grid injection power (kW)
p^*	Power reference (kW)
P_{PV_STC}	Estimated PV power under standard test conditions (kW)
p_{PV_MPPT}	PV power by MPPT algorithm (kW)
p_{PV_S}	PV shed power (kW)
p_{EVs_D}	EV demand power (kW)
p_{PV}	PV power (kW)

p_S	Storage power (kW)
p^*_S	Storage power control reference (kW)
P_{S_MAX}	Maximum storage power
p_G	Public grid power (kW)
p^*_G	Public grid power control reference (kW)
P_{G_MAX}	Grid power limit (kW)
p_{EV}	EV battery power (kW)
p_{EVs}	Total power of EVs (kW)
p_{EVs_D}	EV demand power (kW)
p_{EVs_lim}	EV charging station power limit (kW)
p_{EVs_S}	Shed EV power (kW)
p_{EV_total}	EVs output power (kW)
$p_{remaining}$	EV charging station remaining power (kW)
P_{FAST_MAX}	Maximal charging power by fast mode (kW)
P_{AVER_MAX}	Maximal charging power by average mode (kW)
P_{SLOW_MAX}	Maximal charging power by slow mode (kW)
p_{ST_AVA}	EV charging station available power (kW)
P_{DIS}	EV discharge power (kW)
soc	Storage state of charge (%)
soc_{EV}	EV state of charge (%)
SOC_{MIN}	soc lower limit (%)
SOC_{MAX}	soc upper limit (%)
SOC_{EV_in}	EV initial state of charge (%)
$SOC_{EV\_final\_lim}$	EV final state of charge limit (%)
$t_{EV\_charger\_1}$	Parking periods of EVs connected to charger 1 (s)

$t_{EV\_operate}$	EV start operating time (s)
t_{EV_arrive}	EV arrival time of (s)
t_{EV_depart}	EV departure time (s)
$t_{EV\_best\_st}$	EV optimal start operating time (s)
$t_{EV\_latest\_st}$	EV estimated latest operating time (s)
t	Time variable
T	Period
T_{arrive}	EV arrive time (s)
T_{depart}	EV leaves time (s)
T_{EV_FAST}	EV fast charging time for a period (s)
T_{EV_AVER}	EV average charging time for a period (s)
T_{EV_SLOW}	EV slow charging time for a period (s)
u_{AC}	Grid voltages between the phases A and C (V)
u_{BC}	Grid voltages between the phases B and C (V)
v_C	DC bus voltage (V)
v_C^*	DC bus voltage control reference (V)
v_{C_REF}	DC bus rated voltage (V)
v_{PV}	PV converter's input side voltage (V)
v'_{PV}	PV converter's output side voltage (V)
v'_S	Storage voltage next to the DC bus (V)
v_S	Storage voltage before the converter (V)
V_{S_RATED}	Rated voltage of the DC microgrid storage (V)
u'_{AC}	Output's inverter voltages between the phases A and C (V)
u'_{BC}	Output's inverter voltages between the phases B and C (V)
v_A	Simple voltage of the three phases (V)

v_B	Simple voltage of the three phases (V)
v_C	Simple voltage of the three phases (V)
v_{EVs}	EV converter’s output side voltage (V)
v'_{EVs}	EV converter’s input side voltage (V)
x	EV user possible choices

Publications associated with this PhD thesis

The works presented in thesis are validated by several publications which have been accepted or published in journals and conferences. The details of them are listed as below:

Article in international refereed journals:

1. **D. Wang**, F. Locment, M. Sechilariu. "Modelling, simulation and management strategy of an electric vehicle charging station based on a DC microgrid". *Applied Sciences*, vol. 10, no.6, pp 2053, MDPI Ed., 2020, Impact Factor 2.474, Scopus, WoS, https://doi.org/10.3390/app10062053.
2. **D. Wang**, M. Sechilariu, F. Locment. "PV-powered charging station for electric vehicles: power management with integrated V2G". *Applied Sciences*, vol. 10, no.6, pp 6500, MDPI Ed., 2020, Impact Factor 2.474, WoS, Scopus, https://doi:10.3390/app10186500.
3. **D. Wang**, H. Wu, F. Locment, M. Sechilariu: "Management strategy of an electric vehicle charging station under power limitation", Lecture Notes in Electrical Engineering, vol. 697, pp. 191, Springer Ed., 2020, DOI: 10.1007/978-3-030-56970-9_15.

Articles in proceedings at international conferences:

1. **D. Wang**, H. Wu, M. Sechilariu, F. Locment. "Management strategy of an electric vehicle charging station under power limitation". *ELECTRIMACS 2019 (International conference on theory and application of modeling and simulation in electrical power engineering including electric machines, power electronic converters and power systems)*, 21st-23rd, May 2019, Salerno, Italy.
2. **D. Wang**, M. Sechilariu, F. Locment. "Shedding and restoration algorithms for an EV charging station to maximize available power". *EPE'20 ECCE Europe (22nd European Conference on Power Electronics and Applications)* (virtual conference), 7-11, September 2020, Lyon, France.

National congress

1. **D. Wang**, H. Wu, M. Sechilariu, F. Locment "Stratégie de gestion d'une station pour véhicules électriques sous limitation de puissance", JCGE 2019 Conférence des Jeunes Chercheurs en Génie Électrique, Oléron, 11-14 juin 2019.

General introduction

Increased demand for transport called for more oil use, which caused an increase in carbon dioxide (CO_2) emissions which is a significant contributor to air pollution. Electrification is a key technological strategy to reduce air pollution, and it is also a promising option that helps countries achieve energy diversification and greenhouse gas (GHG) emission reduction goals. The benefits of EVs include zero tailpipe emissions, better efficiency than internal combustion engine vehicles, and large GHG emissions reduction potential. In 2010, there were only about 17,000 EVs on the world's roads. Just five countries could count more than 1 000 EVs on their roads: China, Japan, Norway, United Kingdom, and United States. However, by 2019, there were 7.2 million EVs on the world's roads. Nine countries had more than 100 000 EVs on the road [1]. The global stock remains concentrated in China, Europe, and United States, and it is worth noting that China has the largest number of EVs. With the continuous increase of EVs, the demand for charging infrastructure will increase accordingly. Governments have introduced a range of ambitious policies to support and structure a nascent EV industry, which include approaches to reduce adoption barriers and to promote the deployment of the needed charging infrastructure. By the end of 2019, 7.3 million EV chargers were installed worldwide, which increased by 40% from 5.2 million in 2018. Among them, the number of private slow chargers is the largest, followed by publicly accessible slow chargers, and the number of publicly accessible fast chargers is the least. The maximum number of private slow chargers indicates that EV users are more inclined to charge at home, while slow charging is conducive to protecting the battery life of EVs. The dramatic increase of EVs with the EVs' charging infrastructure shows the people's increased acceptance of EVs to prove the transformation from the transportation driven by traditional internal combustion engines to the new transportation driven by modern power electronic system.

As an electricity load, EVs have great randomness and uncertainty in the distribution of time and space. If random, massive, and unmanaged access to the public grid, it will inevitably cause a serious impact on the public grid. When the public grid is in the peak load period, a large number of EVs suddenly connected to chargers will bring a huge load impact to the public grid, and even cause the public grid to be paralyzed, threaten the reliability of residents' electricity use, and are extremely detrimental to maintaining the safety and stability of the power system. Therefore, how to coordinate and plan the energy flow between EVs and the public grid is an urgent problem to be solved.

With the continuous development of renewable energy, such as solar energy, wind energy, etc., more and more renewable energy sources are being integrated into the power system. Compared with traditional thermal power generation, new energy is affected by natural factors such as solar irradiation intensity and wind, and has strong uncertainty and discontinuity. There is an urgent need for other energy sources, such as storage systems, to smooth the intermittency of renewable energy.

V2G technology refers to the technology for EVs to send electricity to the public grid, and its core idea is to use a large amount of EV battery energy as a buffer for the public grid. V2G technology treats EVs as backup energy storage components and distributed power sources connected to the public grid at the same time, and participate in public grid regulation through a series of control and dispatching methods. By regulating the charging and discharging behaviour of EVs connected to the public grid in an area, the EVs can feed power to the public grid when the grid load peaks, and charge when the grid load is low, thereby alleviating the power supply pressure of the public grid during peak hours and improving the overall efficiency of the public grid. The V2G framework diagram is shown in Figure 1.

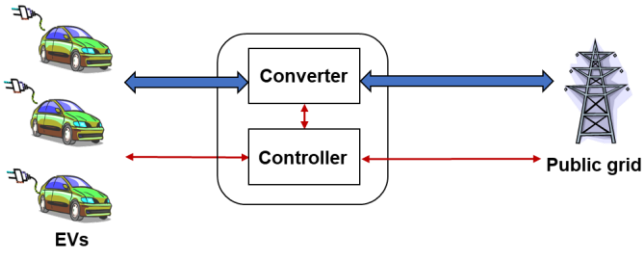

Figure 1. V2G framework diagram.

In the construction of the smart grid, the organic integration of EVs and renewable energy will promote the application of both, which will help improve the economic and environmental benefits of overall operation:

- Renewable energy power generation can reduce the dependence of EVs on fossil fuels and achieve true carbonization;
- EVs can also help solve the intermittent problems of renewable energy and reduce the cost of energy storage systems;
- The integrated system realizes the on-site consumption and utilization of renewable energy generation by EVs, which can reduce the adverse effects caused by the simple connection of the two to the public grid;
- Renewable distributed power sources serve the charging of EVs on-site, which will reduce the capacity of long-distance transmission of electric energy, so that the power loss caused by the long-line transmission process can be represented by renewable energy represented by wind and solar energy. Its essential feature is its dispersion of the spatial scale and strong random volatility of time scale.

Therefore, in-depth research on the orderly charging and discharging management strategies of a large number of EVs, and fully exerting its energy storage function through the public grid access technology of EVs, will reduce the charging cost of car owners. Providing auxiliary services such as voltage regulation, spinning reserve, load shifting, peak load shaving, and load levelling, as well as complimentary coordination with intermittent power supply, are extremely important.

According to this context, this thesis intends to make a further contribution on the power management of EV charging stations. This study presents a direct current (DC) microgrid consisting of EVs, an electrochemical storage system, a public grid connection, and PV sources.

The thesis structure is shown in Figure 2. The thesis is organized into five chapters. After the general introduction, Chapter I gives the research background and thesis objectives. First, the history of the development of EVs in the world is described, and then the encouragement policies for EVs in various countries are introduced. Then, the necessity of DC microgrid and the development of key technologies are presented. Subsequently, two charging methods for EV battery are introduced. At last, this chapter outlines the objectives of the thesis.

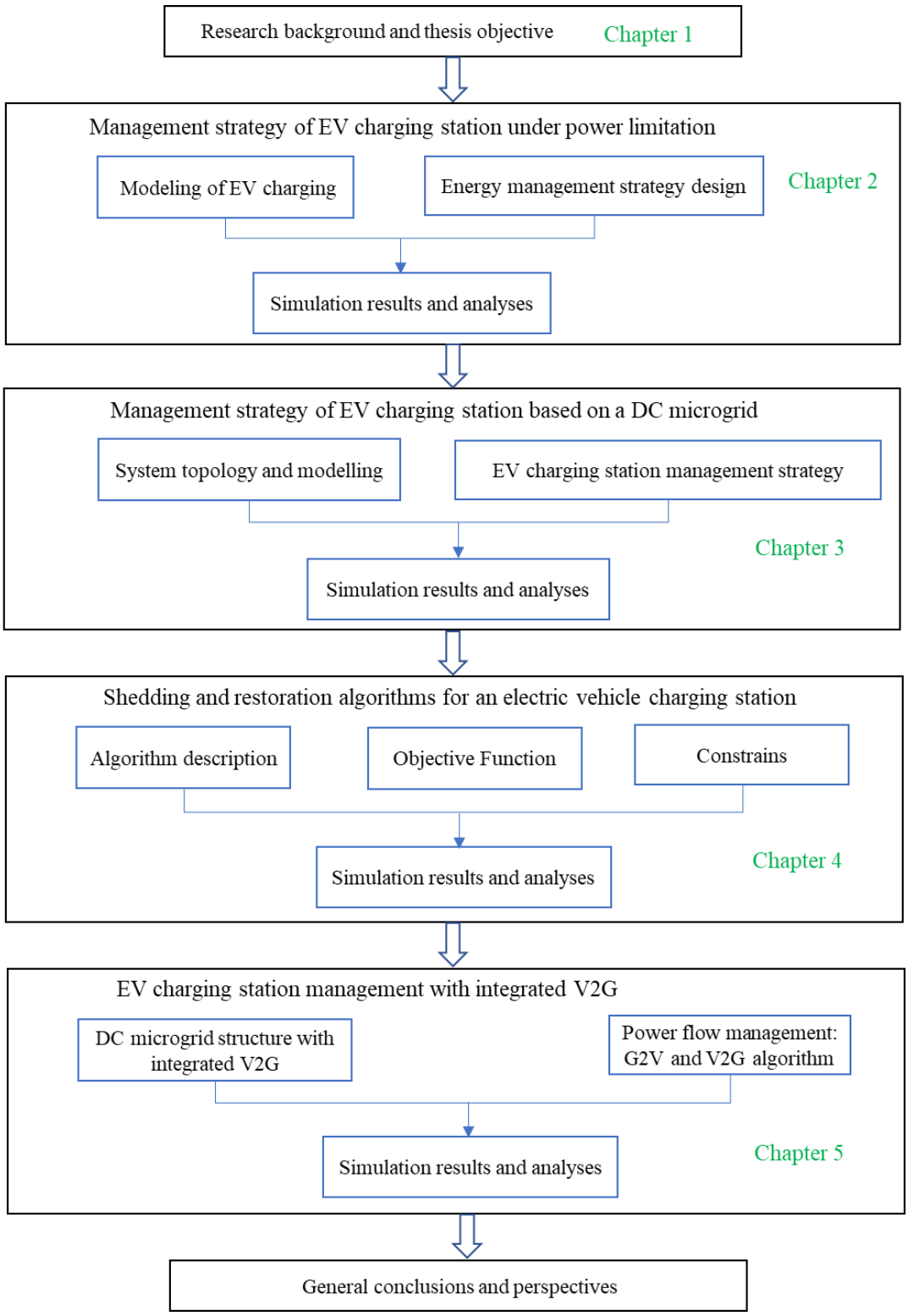

Figure 2. Thesis structure.

In Chapter II, a management strategy for an EV charging station under power limitation is investigated. Firstly, EV charging modelling is presented. Then, the EV charging station management strategy is proposed and common problems during an EV charging process are discussed. The simulation results obtained under MATLAB/Simulink verify the feasibility of the management strategy that presents a good performance in terms of precise control.

In Chapter III, a real-time management strategy of an EV charging station based on a DC microgrid is proposed and considering most of the users' needs from the perspective of combining theory with practice. Firstly, the topology and modelling of an EV charging station based on a DC microgrid are presented. Then, the EV charging station management strategy is proposed and common problems during an EV charging process are discussed. The management strategy is verified by simulation. The results show that the proposed management strategy can deal with the uncertainties of EV users' behaviour considering its arbitrary and random choices through the human-machine interface.

In order to better meet user needs while maintaining EV charging station power balance, Chapter IV further develops EV shedding and restoration optimization algorithms for an EV charging station which is based on a DC microgrid. The objective function is obtained by combining the optimization problem and constraints of shedding and restoration for the EV charging station to minimize the real-time remaining available power of the EV charging station. Simulation results show the increase in available power utilization and prove the technical feasibility of the proposed optimization algorithms.

In Chapter V, power management is proposed for the EV charging station with integrated V2G. Firstly, the structure of DC microgrid with integrated V2G and DC microgrid power flow are presented. Then, flow charts of the immediate charge/discharge algorithm (ICDA) and dynamic searching peak and valley algorithm (SPVA) are described. The proposed SPVA can determine the optimal charging/discharging start time of EV in consideration of all of the initial state of charge, namely SOC_{EV_in}, charging modes, arrival time, departure time, and the peak periods. Simulation results demonstrate the proposed SPVA effectiveness, which can guarantee the balance of the public grid, meanwhile satisfy the charging demand of EV users, and most importantly, reduce the public grid energy cost.

The scientific contribution of this thesis is mainly reflected in six aspects.

Firstly, the topological structure of an EV charging station based on a DC microgrid is proposed. The DC microgrid consists of 4 parts: PV sources, an electrochemical storage system, a public grid connection, and chargers associated with their parking spots.

Secondly, a real-time power management strategy for an EV charging station is proposed to meet the needs of users. This strategy fully considers the randomness of EV arrival, the unpredictability of user behaviour, and the randomness of the user's choice of charging modes.

Thirdly, two algorithms, rule-based algorithm (RBA) and SROA, are proposed for EV shedding and restoration. SROA respects the user's choice while reducing total charging time, increasing the full rate, and maximizing the available power utilization, which shows better performance than RBA.

Fourthly, the DC microgrid structure with integrated V2G is proposed. This structure provides the possibility for EV's "load-source" character.

Fifthly, an EV charging station management strategy with integrated V2G is proposed. In the management strategy, the SPVA is proposed to achieve the effect of peak shaving and valley filling, while meeting the charging requirements of EVs by calculating the optimal charging/discharging start time of EVs, and it also reduces the cost of the public grid.

Sixthly, a reasonable electricity price mechanism is set. The charge/discharge power limits are different in accordance with the “peak” periods and “valley” periods of the public grid, which protects the stability of the public grid.

General conclusions and perspectives of the proposed EV charging station based on DC microgrid are given in the end.

Chapter I. Research background and thesis objective

The shortage of energy and environmental pollution has become more and more serious, which has caused people to pay attention to their health and living environment. The increasing base of the automobile market has aggravated resource consumption, and brought greater pressure on the environment， thus, EVs become a trend due to their energy-saving and environmentally friendly characteristics [2, 3]. As the number of EVs continues to increase, the charging of EVs will become one of the problems that the public grid needs to solve [4]. The prerequisite for the popularization and application of EVs is the complete and large-scale construction of charging facilities, and management strategies are essential in the construction of charging facilities [5, 6]. Management strategies not only meet the needs of users according to their different choices, but also maintain the power balance of charging facilities, most importantly, they should benefit the safe and stable operation of the public grid.

The purpose of this chapter is to give research background and thesis objectives. The history of EVs and the support policies of EVs around the world are described in I.1. The concepts and structures of DC microgrid and smart grid are given in I.2, and the relationship between the two is explained. The battery charging modes existing in EV charging stations and the battery charging process are introduced in I.3. The thesis objectives are given in I.4. Conclusions are shown in I.5.

I.1. Electric vehicles around the world

Although renewable energy is the world’s fastest-growing form of energy, fossil fuels continue to meet much of the world’s energy demand [7]. Liquid fuels (mainly oil) remain the largest source of energy consumption in the world [8]. The rapid growth of energy demand will lead to excessive CO_2 emissions and energy crisis. In many countries, GHG emissions reduction plans have been implemented and one of the promising solutions is transport electrification [9]. Transport electrification is an effective way to mitigate the phenomenon of GHG emissions. EVs used to be the first choice for transportation [10].

The origin of EVs goes back a long time. The Scotsman Robert Anderson developed the first crude EV around 1832, but it was not applied until the 1870s or later [11]. Around 1889, William Morrison created the first successful EV in the U.S, which sparked an interest in EVs. EVs were quickly becoming with urban residents because of its advantages: quiet, easy to drive, and odorless. Between 1900 and 1912, EVs reached their heyday in the U.S, accounting for about one-third of all vehicles on the road. The world's first hybrid EV was invented by Ferdinand Porsche around 1901, which was empowered

by electricity stored in batteries and gasoline engines. Between 1908 and 1912, with gas-powered EVs widely available and affordable, model T dealt a blow to EVs. In 1912, the electric starter was introduced, which further promoted the sales of gasoline-powered EVs. By 1935, EVs had almost disappeared. In the next 30 years or so, there is almost no demand for alternative fuel vehicles because of cheap abundant gasoline and the continuous improvement of internal combustion engines.

But in the 1960s and 1970s, the soaring price of gasoline once again aroused interest in EVs. Around the same time, the first manned vehicle drove on the moon empowered by electricity, which helped to increase the visibility of EVs, then many automakers began to explore alternative fuel vehicles. Between 1974 and 1977, Sebring-Vanguard became the leader in EV Sales. The interest in EVs faded by 1979 with drawbacks, for example, limited drive range. New regulations renewed EV interest around 1990. In the year 1996, EV1 released by GM gained a cult following, and in 1997, Toyota introduced the first mass-produced hybrid EV. In 2006, Silicon Valley startup, Tesla Motors, takes on EVs. In 2010, GM released the Chevy Volt, and made it the first commercially available plug-in hybrid EV. Nissan released the LEAF, an all-electric, zero-emission vehicle in December 2010. Since 2010, the cost of EV batteries has plummeted, and various other major automobile brands have also begun to develop their own long-range, road-use vehicles, such as Nissan, Bavarian Motor Works, and Volkswagen, etc.

Many countries in the world have introduced corresponding measures to encourage the development of EVs [12]. In May 2016, the German Federal Cabinet formally adopted a resolution to introduce a series of preferential policies such as EV subsidies and tax relief to stimulate the development of EVs in Germany. According to regulations, from May 18, 2016, consumers who purchase pure EVs in Germany will receive a subsidy of 4,000 euros, and the purchase of gasoline-electric hybrid vehicles will receive a subsidy of 3,000 euros. Consumers who purchase EVs will also enjoy the preferential policy of exempting the car tax for 10 years. The tax exemption policy can be traced back to the buyers of EVs starting from January 1, 2016. In 2008, the French government's subsidy policy began to be implemented. The subsidies were raised twice in 2014 and 2016, and consumers' purchase costs were gradually reduced. France formulated different subsidy standards, that is, EVs and gasoline-electric hybrid vehicles with a displacement of less than 20g/km can receive a discount of 6,300 euros; purchases of gasoline-electric hybrid vehicles with a displacement of 21g/km to 60g/km can enjoy a discount 1,000 euros; purchase of a hybrid EV with a displacement of 61g/km to 110g/km can enjoy a discount of up to 750 euros; abandoned diesel vehicles with a vehicle age of more than 10 years can be subsidized by 6,300 euros a when they switch to pure EVs and a subsidy of 2500 euros for the purchase of plug-in hybrid vehicles. In order to encourage consumers to purchase new energy vehicles, the U.S. government has given preferential policies in several aspects. In May 2007, the U.S. Bureau of Internal Revenue adjusted the personal income tax relief for consumers of new energy vehicles. For vehicles that meet the subsidy standard, with the cumulative sales of 60,000 vehicles as the boundary, consumers will enjoy a 50% tax reduction after reaching 30,000 vehicles; more than 45,000 vehicles will enjoy a 25% tax reduction; after more than 60,000 vehicles, no enjoy any tax cuts. In 2008, the "Emergency Economic

Stability Act" also stipulates that starting January 1, 2009, the first 250,000 consumers who purchase new energy vehicles will enjoy tax deductions of US $2500 to US $7500.

The environment ministry of South Korea announced on January 25, 2017 that 101 cities across the country can enjoy new energy vehicle subsidies. Compared with 2016, 70 new cities were added. The subsidies in 2017 also increased compared with 2016. The state subsidies 14 million won, and localities vary from 3 to 12 million won according to their economic conditions. In terms of purchase, consumers will enjoy tax reductions in terms of personal consumption tax, registration tax, acquisition tax, education tax, etc. When purchasing hybrid vehicles. Buying a hybrid vehicle can save up to 3.3 million won. For the purchase of a pure EV, government subsidies at all levels are up to 23 million won, and consumers will also enjoy 4.2 million won in tax relief.

The British subsidy policy began in 2011. It stipulated that British consumers who purchased EVs with CO_2 emissions less than 75g/km can receive up to 5,000 pounds of vehicle purchase subsidies, and were exempt from automobile fuel taxes and automobile consumption taxes. In 2016, the government announced that the policy extension would continue until 2018, and the British government continued to maintain its incentives for EVs. The British Ministry of Transport introduced a new subsidy policy for plug-in EVs and trucks, stipulating that British consumers who purchased electric trucks with CO_2 emissions less than 75g/km can receive a maximum of 8,000 pounds in purchase subsidies.

In Sweden, plug-in hybrid vehicles with CO_2 emissions not exceeding 50g/km can receive a subsidy of 20,000 kronor, and pure EVs can enjoy a subsidy of 40,000 kronor. The Belgian subsidy policy is that purchase of EVs in Flanders can enjoy a subsidy of 5,000 euros [13]. This subsidy cost is relatively high among countries. Spain stipulated that electric passenger cars can enjoy up to 5,500 euros in subsidies, electric trucks can enjoy 8,000 euros in subsidies, and electric buses can enjoy 20,000 euros in subsidies. Portugal provided a subsidy of 2,250 euros for pure EVs and 1,125 euros for plug-in hybrid vehicles. Denmark stipulated that municipal units and companies can enjoy subsidies ranging from US $1,470 to US $3,675 per vehicle. Norway, like the United States, used tax breaks to subsidize consumers. Norway began to implement an incentive policy in 2013, exempting the first 50,000 new energy vehicles from road tax and purchase tax. Consumers need to pay more than 50% less tax on the purchase of new energy vehicles than ordinary cars of the same price. In 2015, Norway completed the target of 50,000 vehicles, and the government retained the incentive policy until 2017, which ensured the growth momentum of Norwegian new energy vehicle sales.

In China, the state adopted a series of policies to support EV development [14, 15]. On July 10, 2012, the State Council issued the “Development Plan on Energy Saving and New Energy Vehicles Industry (2012–2020)”, emphasizing the industrialization process of pure EVs and plug-in hybrid EVs. On April 22, 2015, the Ministry of Finance issued “Notice on the Financial Support Policy for the Promotion of New Energy Vehicles in 2016–2020”. On November 18, 2015, the National Development and Reform Commission issued the “Guide for the Development of Electric Vehicle Charging

Infrastructure (2015–2020)" to guide the construction of EV charging infrastructure and promote the rapid development of the EV industry.

Based on the vehicle hybridization ratio, EVs could be classified into several categories, hybrid electric vehicles, plug-in hybrid electric vehicles, fuel-cell electric vehicles, and battery electric vehicles [16]. Hybrid electric vehicles are driven by a combination of internal combustion engines and electric motors and they cannot accept electricity from external energy sources. Plug-in hybrid electric vehicles are similar to hybrid electric vehicles with additional features such as larger battery packs and charging from the distribution network. Fuel-cell electric vehicles use the electricity generated from the reaction of hydrogen with oxygen to form water in a process which is the reverse of electrolysis. However, battery electric vehicles rely on a large battery power purely.

The battery is the core component of EVs. Current EV batteries have a lower energy density, which directly affects the maximum full electric drive range of the EV [17, 18].

In order to invent batteries of high energy density, high power density, low cost, safety, and durability, EV battery technology has gone through several stages of development [16]. The first battery technology used in transportation was the lead-acid battery. Lead-acid battery technology is mature and cheap. However, the obvious disadvantages of lead-acid batteries, such as low energy density, heavy weight and require checking electrolyte levels are not environmentally friendly. Lead-acid batteries were quickly replaced by nickel-based batteries, which are considered relatively mature technologies and have higher energy densities than lead-acid batteries. However, this battery technology has serious drawbacks such as poor charge-discharge efficiency, high self-discharge rate, has memory effect, and poor performance in cold weather.

Sodium–nickel chloride (Zebra) batteries have high energy density and power density, which is suitable for EV application. However, extreme operating temperatures bring a lot of pressure for its thermal management and safety issues. Lithium-based batteries are one of the promising battery technologies, which have a high energy density, high power density, light weight, low cost, non-toxic, and acceptably fast charge.

However, lithium–sulfur battery has high discharge rate and short life cycle. Zinc–air battery is a potential candidate for future EV battery, which has a higher energy density than lithium-based battery. At present, the main disadvantage of Zinc-air battery is the low power density and short life cycle. However, it can compete with traditional combustion engine vehicles because of the theoretical high energy density in excess of 1700Wh/kg [19]. Current research focuses on the development of this compelling battery technology in order to extend the driving range of EV.

I.2. DC Microgrid and smart grid

The global energy crisis is becoming increasingly severe, and the shortage of traditional fuels and the caused environmental pollution problems are becoming increasingly serious [20, 21]. At the same time, the continuous improvement and maturity of renewable energy technologies, e.g., PV source, provides a new path for solving the energy crisis [22, 23]. Therefore, many countries are focusing on distributed power generation with renewable energy as the energy source [24]. Compared with the traditional large-scale centralized generation and distribution mode, distributed generation technology has advantages of independence, real-time control of the power quality and performance of the regional grid, less investment, flexible installation locations, short construction periods, and high energy utilization and low environmental pollution [25, 26]. However, the large-scale application and access of renewable distributed energy sources bring huge challenges and impacts to the public grid [27, 28].

Smart grid is a fully automated power transmission network that monitors and controls each end-user and power grid node, which guarantees the bidirectional flow of information and power between all nodes from the power grid to the end-user throughout the transmission [29, 30]. The possible smart grid topology evolution is shown in Figure 3.

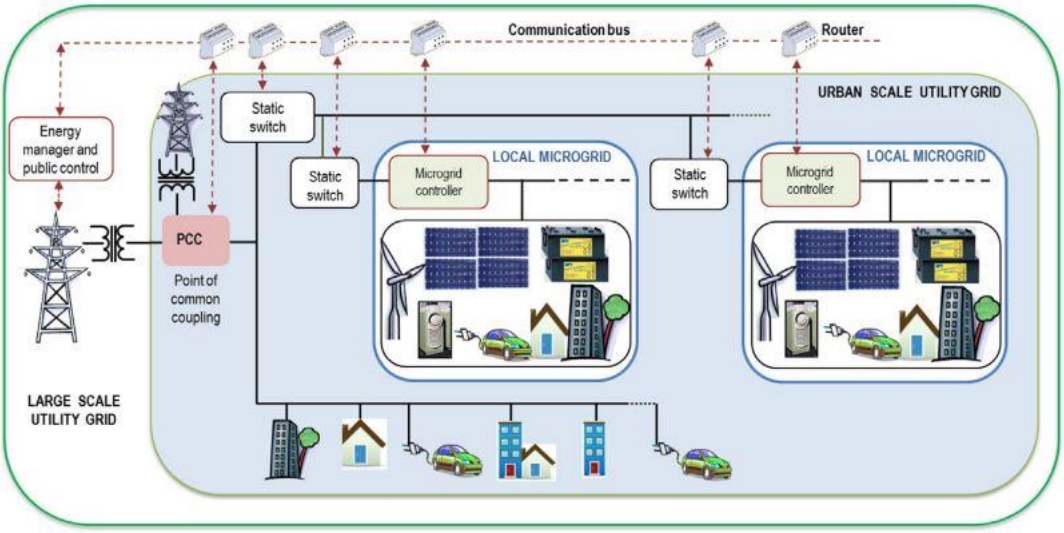

Figure 3. Smart grid topology [31].

An interesting feature of smart grids is that consumers can actively participate in grid operations [32, 33]. By changing the mode of electricity consumption, consumers can help balance energy supply and demand. Self-healing smart grids will take immediate corrective action to recover their outages, even if the problem occurs，such as isolated specific faulty lines. The implementation of smart grids can improve grid power quality. Smart grid is a new type of power grid that utilizes advanced information and communication technologies to optimize power system management in real-time, enabling bidirectional power flows and information flows interactions and increasing grid efficiency and security

[16]. Compared with the traditional centralized power generation system, distributed energy has the advantages of cleanliness, environmental protection, and flexibility [34, 35]. Renewable energy will become one of the important energy sources for the smart grid. However, a large number of distributed energy grid-connected operation will bring great challenges to the stability of the power system. In the research of smart grid technology, how to effectively dispatch distributed energy in the environment of the smart grid while ensuring the dynamic stability of the grid is an important issue.

Based on the above analyses, in order to reduce the adverse impact of distributed power access on the public grid, while combining the characteristics and advantages of renewable energy sources, researchers propose a more flexible, intelligent, and more reliable system—microgrid [36, 37]. The microgrid shown in Figure 4 integrates advanced information technology, control technology, and power technology, while providing a reliable power supply to meet the various needs of users and, it can maximize energy, economic and environmental benefits [37]. At the same time, microgrid can support the public grid, improve energy efficiency, save energy and, reduce consumption. Therefore, a microgrid is an indispensable and important part in the construction of smart grids. The DC microgrid is an important part of the future intelligent power distribution system, and is of great significance for promoting energy-saving and emission reduction and achieving sustainable energy development. Compared with the alternating current (AC) microgrid, the DC microgrid can more efficiently and reliably receive distributed renewable energy power generation systems such as wind and solar, energy storage units, EVs, and other DC power loads.

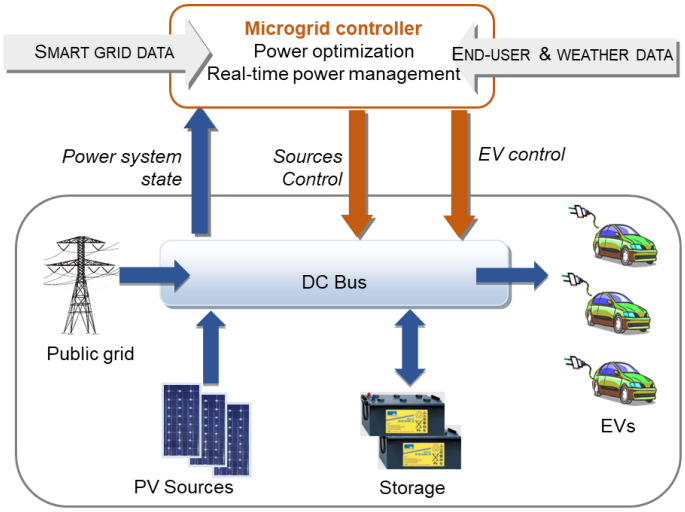

Figure 4. DC microgrid.

The key technology development of DC microgrid is in the following three aspects.

1. At present, distributed energy sources, energy storage units, and loads are all connected to the DC microgrid through conventional power electronic devices that exist common problems such as single function and lack of plug-and-play. More efficient, reliable, modular, and intelligent electrical energy exchangers will be worthy of in-depth exploration in the industry and academia.

2. In terms of operation control, how to improve the robustness, reliability, flexibility, and scalability of the control system, and to coordinate operation control technology and intelligent protection technology comprehensively, is an important theory for future DC microgrid energy management.

3. In terms of DC microgrid protection technology, research, and development of more efficient and reliable DC circuit breakers; new DC distribution protection technology based on fault current limitation, etc., are all frontier topics worth exploring.

I.3. EV charging stations

An EV charging station is a system and technology for charging EVs [38]. With the popularity of EVs, EV charging stations will surely become the focus of the development of the automobile industry and energy industry [39].

Charging stations generally provide three charging modes for users to choose: fast mode, average mode, and slow mode. EV chargers are a scarce resource. Users all hope that EVs can quickly complete charging needs. If users choose fast mode, the charging power needs to increase, and the construction cost of chargers will increase. If users choose average mode or slow mode, the charging power is relatively small, which is better for the battery life, and the charging cost is low. At present, the battery charging process include constant current (CC) charging, constant voltage (CV) charging, and constant current/constant voltage (CC/CV) [40, 41]. The battery charging process curve is shown in Figure 5.

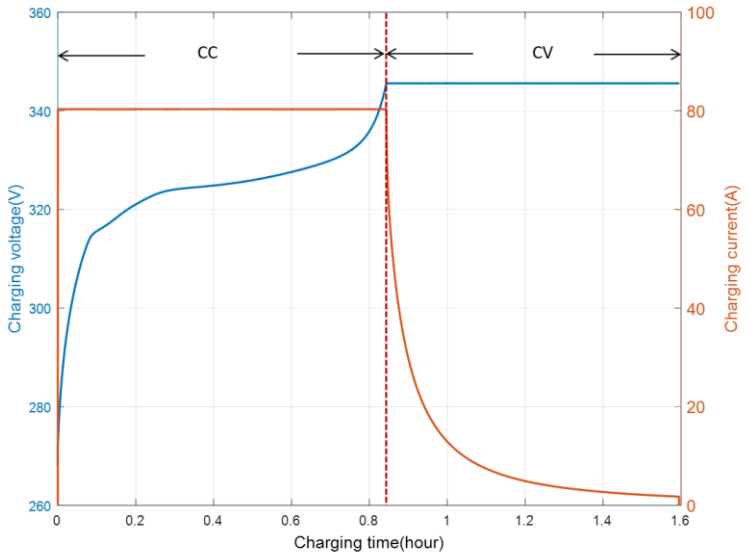

Figure 5. Battery charging process curve.

1. CC charging method

CC charging means that the battery is charged in a CC manner when charging, and the current can be adjusted by the charging device [42]. The main feature of this charging method is that it has greater adaptability, and the charging current can be arbitrarily selected and adjusted, so it can charge batteries in various situations and states. The main disadvantage of this charging method is that the charging current in the initial stage is relatively small, and the charging current is relatively too large in the later stage of the charging, so the entire charging process takes a long time, consumes a lot of energy, and requires special management.

2. CV charging method

CV charging means that the battery is charged in a CV mode when charging. Its main characteristics are that the initial charging current is quite large, as the charging continues, the charging current gradually decreases, and there is only a small amount at the end of charging. Compared with CC charging, this charging method has a shorter charging time. Generally, the battery can obtain more than 90% of its capacity after a few hours, and the charging process does not require special management. However, in actual applications, the charging time is still too long, and a better and faster-charging method is needed.

3. CC/CV charging method

At present, the most commonly used is CC/CV charging [43, 44]. In the beginning, CC charging is used until the terminal voltage of the battery reaches the CV charging voltage, and then the CV charging is changed to the CV charging until the battery is fully charged. When fully charged, it is necessary to check whether the charging current is reduced to the charging termination current.

An intelligent management strategy is necessary for EV charging stations [45, 46]. On the one hand, since users will go to EV charging stations according to their habits and actual needs, this requires the EV charging station to meet the fluctuation of electricity consumption in real-time. On the other hand, a large number of EV charging will cause excessive pressure on the public grid, so the stability of the public grid needs to be ensured.

I.4. Thesis objectives

The rapid development of EVs increases the power demand, which causes an extra burden on the public grid increasing the load fluctuations and, therefore, hindering the high penetration of EVs. The research, through this thesis, aims to study, design, and develop charging/discharging management strategies in communication with the smart grid for DC microgrid based on PV energy for EV charging stations.

The first step is to build a DC microgrid model which consists of EVs, an electrochemical storage system, a public grid connection, and PV sources, and then propose a management strategy for an EV charging station under power limitation to simulate various realistic situations including the interaction with the EV users, such as charging modes, real-time charging power, power limitation, and especially the various options of users in case of lacking power for the EV charging.

The second step is to propose a real-time management strategy of an EV charging station based on a DC microgrid. In the management strategy, common problems during an EV charging process should be discussed, e.g. disconnection operation, standby mode, shedding and restoration operation. Furthermore, the proposed power management should deal with the uncertainties of EV drivers' behaviour considering its arbitrary and random choices through the human-machine interface.

In order to better meet user needs while maintaining EV charging station power balance, the third step is to develop algorithms for an EV charging station which is based on a DC microgrid to minimize the real-time remaining available power of the EV charging station.

The fourth step is to build DC microgrid model with integrated V2G, and then propose a power management strategy for the EV charging station with integrated V2G. In order to guarantee the balance of the public grid, meanwhile, satisfy the charging demand of EV users, and most importantly, reduce the public grid energy cost, algorithms should be proposed to determine the optimal charging/discharging start time of EV in consideration of soc_{EV}, charging modes, arrival time, departure time, and the peak periods.

I.5. Conclusions

The reason and necessity of the proposed microgrid are introduced in detail in this section, especially the shortcomings of distributed renewable energy and the relationship between smart grid and microgrid. The types of EVs and batteries are introduced. The advantages and development prospects of EVs are introduced, and the framework of EV charging stations based on a microgrid is displayed, which gives the conclusion that studying the management for EV charging stations based on a DC microgrid is necessary. Therefore, this thesis focuses on the DC microgrid system consisting of PV sources, battery storage, public grid, and EV charging stations. Under this academic and industrial circumstance, it describes the research purposes, motivations, and research contributions. The first objective of this thesis, the management strategy of EV charging station under power limitation, is studied in the next chapter.

Chapter II. Management strategy of EV charging station under power limitation

This chapter focuses on the management strategy of an EV charging station under power limitation, which can deal with the power availability and interact with the EV users and discusses the common problems during the EV charging process. The simulation results obtained under MATLAB/Simulink verify the feasibility of the management strategy that presents a good performance in terms of precise control. Literature review is described in II.1. The modelling of EV charging is shown in II.2. The EV charging station management strategy is introduced in Section II.3. The simulation results and analyses are presented in Section II.4. Conclusions are given in Section II.5.

II.1. Literature review

In many countries, GHG emission reduction plans have been implemented and one of the promising solutions is transport electrification. EV is a transport means that emits zero GHG and produces minimal noise. The powertrain of the EV depends on the electric motors and battery storage, which has greater efficiency and lower operating costs compared with the traditional internal combustion engine [47]. The continuous development of lithium-ion battery and rapid charging technology will be the driver for EV popularity in the near future [48].

However, the current EV industry has encountered many technical limitations, such as high initial cost, limited charging facilities, limited driving range, long battery charging time, and short battery life [29]. In addition, frequent charging of EVs by grid power causes the problem of power quality as well as power system stability. Moreover, when the EV charging process is consistent with the peak load of the public grid, the impact of the charging load will be more serious [49].

The swapping of batteries is proposed in [50, 51] and optimal pricing algorithm and strategy are given [52, 53] for charging EVs. The author of [49] discussed three main charging patterns of EV users from observations on measured data and proposed a novel schedule strategy based on “valley filling” concept to manage EV charging behaviours in order to relieve its impact on the grid; however, this strategy is based on probability and it cannot completely prevent public grid overload if the charging of EVs is unscheduled. Thus, a complete management strategy for an EV charging station is essential.

The main difficulty in arranging EV charging is that each EV arrives for charging randomly according to its respective requirements for charging power, which is not known in advance [45]. A closed-form solution to optimally schedule time-shiftable loads with uncertain deadlines is proposed, which focuses on charging EVs with uncertain departure times, but it assumes the future load demand

is perfectly known a priori [54]. Decentralized optimal scheduling is proposed for EVs in [55], and all EVs are assumed to arrive at the same time, meanwhile, the future load demand is assumed to be known. A complete management strategy should deal with the randomness of EVs arriving at charging stations.

Generally, EV charging stations provide three charging modes: fast mode, average mode, and slow mode. For fast mode, it usually lasts for about 30min with large power consumption [56]. For average mode, it usually lasts for a period of about 1h and 30min with average power consumption. For slow mode, it usually lasts for a period of about 4h with low power consumption. Different charging modes correspond to different charging powers. Users' choices will not be known until EVs reach the charging station, so EVs power demand cannot be predicted. In order to ensure the safety of the public grid and reduce the cost of the spinning reserve, the power of the EV charging station needs to be limited. A management strategy for EV charging station under power limitation should be proposed. The management strategy aims to minimize the potential impact of large-scale EV integration into the public grid, while the power limitation aims to minimize the cost of power generation subject to operational constraints and meeting demand.

II.2. Modelling of EV charging

The protocol of charging lithium batteries in EVs is the CC/CV process [56, 57]. During the CC mode, the charging current remains constant until the voltage rises to a cut-off voltage. During the CV mode, the voltage remains constant while the current drops. This CC/CV procedure is supposed to be controlled by a battery management system already integrated into the EV battery system. When the EV just starts charging, the EV battery voltage is relatively low. If the charging current is not constant, the battery lifecycle and the charger lifecycle will be shortened. When the battery is nearly fully charged, the procedure goes into the CV phase, whose goal is to prevent the battery from overcharging. In this chapter, it is assumed that three charging modes exist: the fast mode, the average mode, and the slow mode. The EV battery power p_{EV} and its state of charge noted soc_{EV} for the same EV are presented in Figure 6. These curves are based on experimental testing of the element: A123 LiFePo4. In Table 1, the maximal charging power demanded by the fast mode P_{FAST_MAX} is 83kW; the maximal charging power demanded by the average mode P_{AVER_MAX} is 27kW; the maximal charging power demanded by the slow mode P_{SLOW_MAX} is 7kW, and the EV battery energy is about 24kWh.

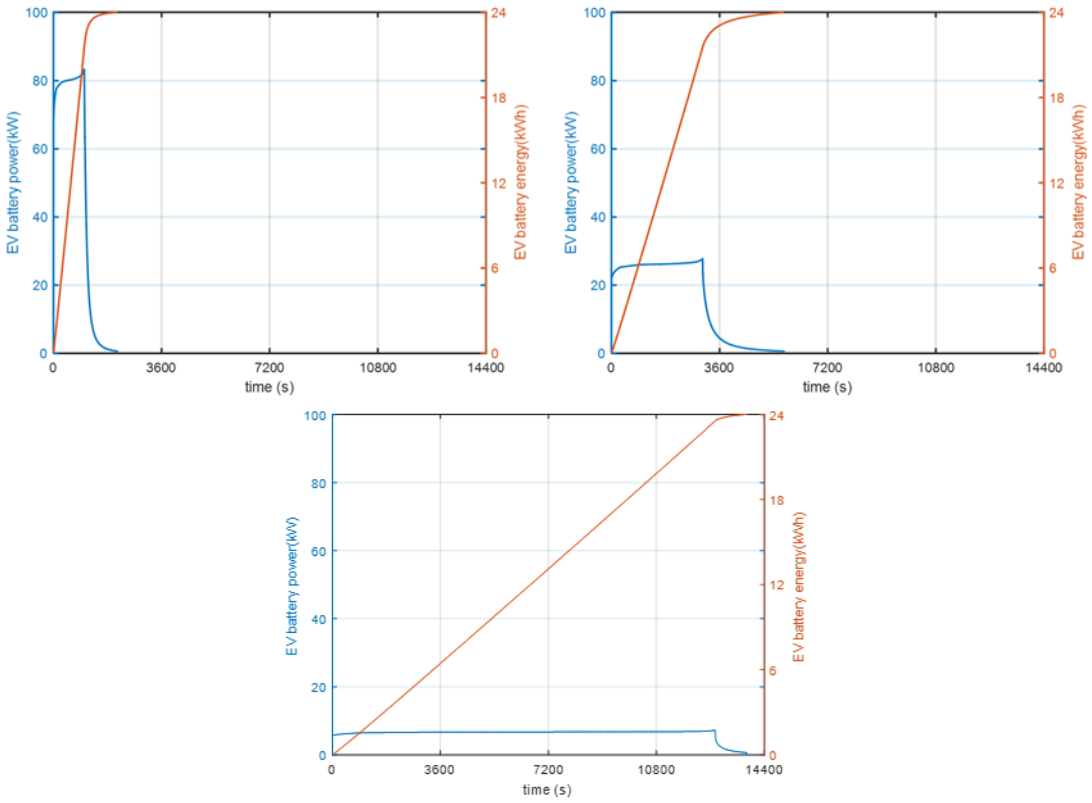

Figure 6. EV battery power and EV battery energy during EV charging: (a) Fast charging mode; (b) Average charging mode; (c) Slow charging mode.

Table 1. Charging mode and demanded maximal charging power.

Charging mode	**Maximal charging power**
Fast charging mode	P_{FAST_MAX}
Average charging mode	P_{AVER_MAX}
Slow charging mode	P_{SLOW_MAX}

II.3. Energy management strategy design

The management strategy of the EV charging station mainly depends on the charging choice of the EV users. Different charging modes correspond to different charging costs. If the users choose the fast mode, they will save time along with relatively high fees. On the contrary, if users choose average mode or slow charge, the cost will be lower.

In order to facilitate users, a human-machine interaction interface is suggested including a management strategy of interaction which is based on the questions for users. The questions for the users are listed in Table 2.

Table 2. Question lists.

Sign	Question
Q1	Which charging mode? The fast mode, the average mode, or the slow mode.
Q2	The power is insufficient for the fast mode. Which do you choose among the average mode, waiting and departure?
Q3	The power is insufficient for average mode. Which do you want to choose among the slow mode, waiting and departure?
Q4	The power is insufficient for any recharging mode. Which do you want to choose between waiting and departure?
Q5	The EV is being charged. Do you want to stop charging and leave?

The available power and options are presented in Table 3. In order to keep the power balance in the microgrid, it is necessary to set up a power limitation for the charging station, there are 3 possible cases to be considered when a new EV is connected to an available charger.

Table 3. Available power test and options.

Condition	Option
$p_{EVs\_lim} > P_{FAST\_MAX}$	The fast mode, the average mode, or the slow mode.
$p_{EVs\_lim} < P_{FAST\_MAX}$ and $p_{EVs\_lim} > P_{AVER\_MAX}$	The average mode, waiting or departure.
$p_{EVs\_lim} < P_{AVER\_MAX}$ and $p_{EVs\_lim} > P_{SLOW\_MAX}$	The slow mode, waiting or departure.
$p_{EVs\_lim} < P_{SLOW\_MAX}$	Waiting or departure.

The flowchart of the management strategy for the EV charging station is shown in Figure 7, where p_{ST_AVA} is the available power of the EV charging station. As shown in Figure 7, when a new EV arrives, the user chooses a charging mode. If the power demanded by the chosen charging mode is less than the available power of the EV charging station, the EV is connected to the charger. If the power demanded by the chosen charging mode is greater than the available power of the EV charging station, the user can choose waiting or departure. If the user's choice is waiting, when the available power is greater than the demanded power, the EV starts to be charged. During the charging process, the user can disconnect the

EV at any time and leave the EV charging station. Therefore, this strategy provides the user with the possibility to choose the charging mode.

In the proposed EV charging station management strategy, the disconnection of the EV from the charger is always possible, permitting these users to stop charging and leave immediately. The EV charger is in standby mode if the user chooses to wait for the power availability. In standby mode, the EV is not charged until the available power is enough for the chosen charging mode.

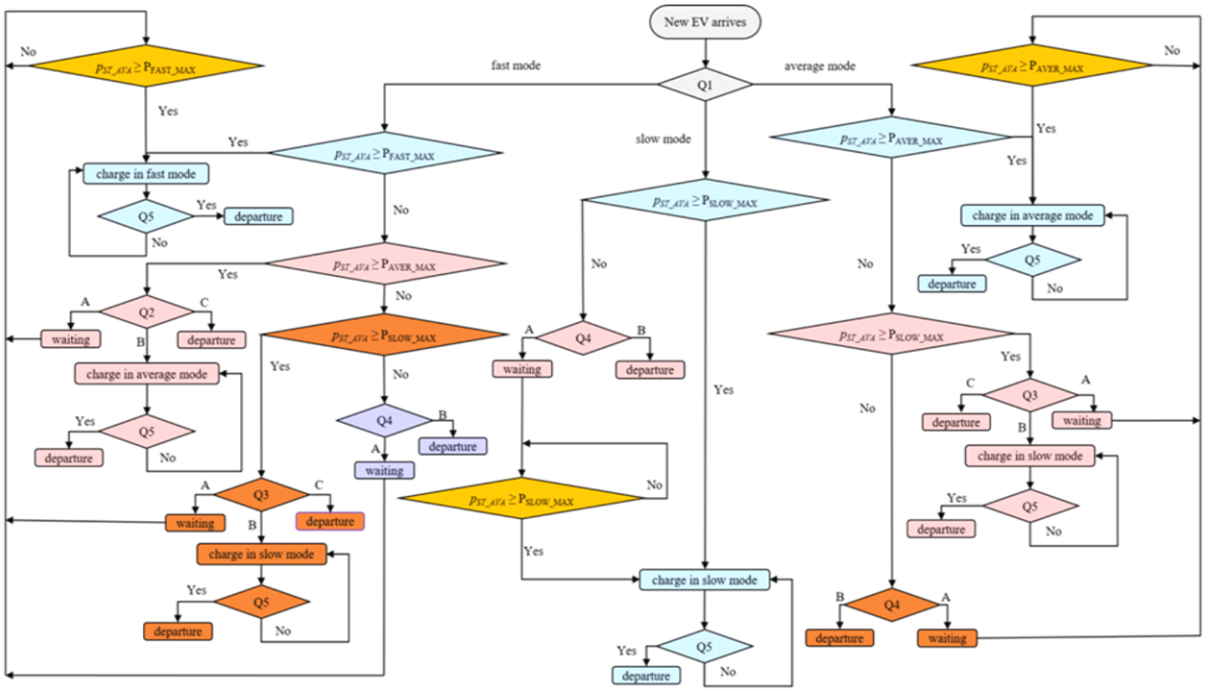

Figure 7. Flow chart of the EV charge station.

II.4. Simulation results and analyses

The EV charging station management strategy simulation is performed with MATLAB/Simulink, in which the process CC/CV with three charging modes is implemented. When an EV arrives, the user chooses the charging mode. Under the power limitation, if the charging station available power is greater than the maximal power demanded by the charging mode chosen by the user, the EV charges directly. If not, the system offers options for users.

Five EV chargers are set in the simulation model. In order to better emulate the real situation, the arrival time of EVs and the initial state of charge soc_{EV} are randomly generated in the simulation. Different users will take the charging price and charging time into account to choose the charging mode they need, and to emulate this action, the charging mode is also randomly generated.

The simulation time period is from 9:00 to 18:00. In order to better analyze the simulation results, the simulation can be divided into three time slots: 9:00-11:00, 11:00-13:00, and 13:00-18:00. The number of records for the EV charging station is listed in Table 4.

Table 4. Number of records.

Number	9:00-11:00	11:00-13:00	13:00-18:00
Arrive	6	5	5
Being charged	4	4	4
Waiting	1	1	1
Departure	1	0	0

The output power of each charger is shown in Figure 8, where p_charger_n is the output power of charger n.

In the first time slot 9:00-11:00, 6 EVs arrive at the station: 4 EVs choose to be charged followed in turn by charging mode: fast mode, fast mode, average mode, and slow mode; 1 EV chooses waiting, and 1 EV chooses departure. The power requested by charger 1 and charger 2 with peak values close to 90kW represent that the charging mode chosen by users is fast mode. The power requested by charger 3 and charger 4 with peak values close to 30kW indicate that the charging mode chosen by users is average mode. The power requested by charger 5 represents that the charging mode chosen by the user is slow mode. In addition, the curve shape of the power requested by charger 5 is rectangular, because the EV disconnects the charger before fully charged, while the other EVs charging curves are complete CC/CV.

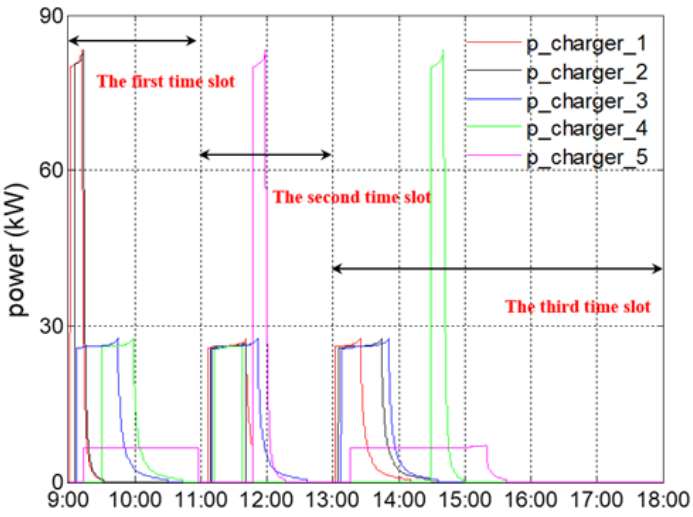

Figure 8. Output power of each charger.

In the second time slot 11:00-13:00, 5 EVs arrive at the station: 4 EVs choose to be charged by average mode; 1 EV chooses waiting. In the third time slot 13:00-18:00, 5 EVs arrive at the station: 4 EVs choose to be charged followed in turn by charging mode: average mode, average mode, average mode, and slow mode; 1 EV chooses waiting. The curve shape of the power requested by charger 5 is a complete CC/CV process, which means that the EV is disconnected from the charger after being fully charged.

As shown in Figure 8, in the first time slot, because the user has an emergency and needs to leave immediately, the EV connected to the charger 5 disconnects the charger before fully charged. In the second time slot, the EVs connected to charger 4, charger 2, charger 1 disconnect respectively in order when not fully charged because of the users' needs. In the first time slot, after the EV connected with the charger 1 fully charged represented, the EV on waiting connected with charger 4 is starting to be charged by average mode.

In the second time slot, as the EVs connected with charger 4, charger 2, charger 1 leaves urgently in order, thus, p_{ST_AVA} is greater than P_{FAST_MAX}, the EV connected with charger 5 on waiting is automatically starting to be charged followed by fast mode. In the third time slot, after the EVs connected with charger 1 and charger 2 fully charged, the EV on waiting connected with charger 4 is starting to be charged followed by fast mode.

The PV sources, the storage, and the public grid can be considered as a multi-source system that impose a total charging power limitation for EVs. Total recharging power is shown in Figure 9. The public grid load is variable according to different time of one day. For example, it is considered that after 11:00, the power consumption suddenly increases because the public grid load increases. To ensure public grid power balance, therefore, the power limitation of the EV charging station is required. In order to emulate this reality, the initial power limitation of the station is 120kW, but at 9:05, the power limitation is set to 210kW. Thus, 120kW can guarantee the EV charging station to provide users with one fast mode, one average mode, and one slow mode and 210kW can guarantee the EV charging station to provide users with two fast modes, one average mode, and one slow mode.

The simulation results show that the EV charging station can operate normally under variable power limitations, which proves the effectiveness of the power management strategy.

The EV charging load is inherently more random than traditional power loads. For future planning and deployments of the charging station, recording of EV behaviour is necessary. For example, how many EVs arrive at the charging station every day, how many EVs choose to wait when the available power of the charging station cannot meet the power demanded by the charging mode chosen by users, and how many EVs choose to leave. To continuously develop the charging station, it is necessary to adjust strategies through the recorded data to maximize the benefits of the charging station.

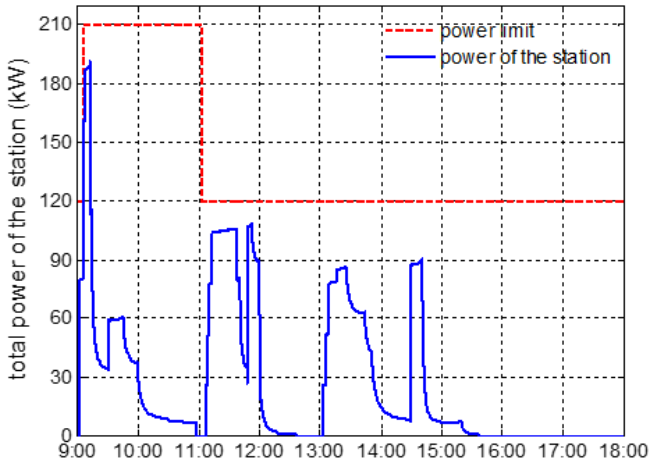

Figure 9. Total output power of the charging station.

The recording of EV behaviour in different situations during the simulation are shown in Figure 10.

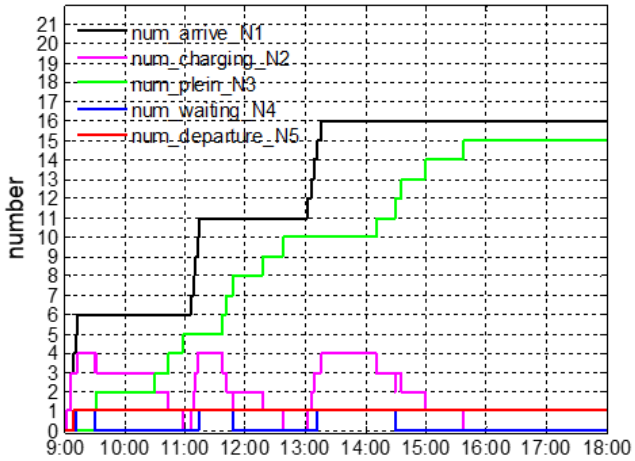

Figure 10. Recording of EV behaviour.

Real-time data is recorded in the system, including the total number of EVs arrived at the charging station N1 (num_arrive), the total number of EVs being charged N2 (num_charging), the total number of EVs fully charged N3 (num_plein), the total number of EVs on waiting N4 (num_waiting), the total number of EVs choose departure N5 (num_departure).

As can be seen from Figure 10, N1 is the sum of N2, N3, N4, and N5, which satisfy (2. 1), and is one of the ways to verify whether the system is working properly or not.

$$N1 = N2 + N3 + N4 + N5 \tag{2. 1}$$

As can be seen from Figure 10, most of the EVs arrived at the charging station choose to be charged. When the available power of the charging station is insufficient, the users are more inclined to wait, and only a small number of users choose to leave directly. Thus, the current planning of this charging station is reasonable and the management strategy shows a significant control effect. If most of EVs arrived at

the charging station choose to leave due to power limitation, the charging station should consider adjusting its management strategy, such as adjusting the power limitation, or appropriately reducing the charging price according to the waiting time of users.

II.5. Conclusions

The rapid development of EVs increases the power demand, which causes an extra burden on the public grid, and most importantly increases the load fluctuations to the public grid. The object of this chapter is to design a management strategy for an EV charging station under power limitation.

Firstly, the modelling of EV charging is presented. Then, a management strategy is proposed to simulate various realistic situations including the interaction with the EV users. The simulation results verify the feasibility of the management strategy and show in detail the management strategy of the EV charging station, such as charging modes, real-time charging power, power limitation, and especially the various options of users in case of lacking power for the EV charging, which presents excellent control effects.

Chapter III. Management strategy of EV charging station based on a DC microgrid

This chapter focuses on strategy charging management taking users' needs and power limitations into consideration. A real-time management strategy of an EV charging station is proposed under power limitation and considering most of the users' need from the perspective of combining theory with practice, in which users' choices, the disconnection operation, the standby mode, the shedding operation, and the restoration operation are included. Meanwhile, the arrival time of EVs, the initial state of charge, and users' choices are random, which emulates the uncertainty of the EV charging behaviour, and provides users' interface with the largest right to choose the charging modes. The intelligent shedding operation and the restoration operation based on the same theory as computer stack are proposed. The simulation results obtained under MATLAB/Simulink verify the feasibility of the proposed management strategy that presents a good performance in terms of precise control.

Literature review is described in III.1. The topology and modelling of the studied system are described in Section III.2. The EV charging station management strategy is introduced in Section III.3. The simulation results and analyses are presented in Section III.4. Conclusions are given in Section III.5.

III.1. Literature and review

The increased number of EVs can have a significant impact on the power distribution system [49]. Frequent charging of EVs using the public grid causes problems in power quality as well as power system stability [58]. Moreover, when the EV charging process is consistent with the peak load of the public grid, the impact of the charging load will be more serious [59].

In order to reduce the impact on the public grid, researchers have developed a number of possible solutions. A two-stage charging strategy for solving charging control issues of EVs is proposed [60], which is proved to reduce load peak and smooth transformers load profile. A three-level (provincial level, municipal level, and charging station level) EV charging strategy is proposed in [61]; it jointly optimizes system load profile and charging costs while satisfying customer charging requirements, which reduces system peak demand charging costs. A robust energy management strategy for EV charging stations is proposed in [62]; it is based on randomized algorithms and determines a day-ahead upper bound profile on the power consumption of EV charging stations and strictly respected in real-time, guarantying the grid stability in a more efficient and less costly manner. However, no additional storage unit could be used to compensate for EV uncertainties.

Although various charging strategies have been employed to design different EV charging protocols in existing work, the current research outcomes are still limited to the interactions and power transfer between EVs and the public grid. The distributed energy generation system has attracted wide attention because of its on-site power consumption, which improves the peak performance of the public grid without increasing the grid capacity [63, 64]. Due to its simple operation, the PV source is considered to be the most effective choice for on-site sources. However, PV power has intermittent properties, thus, an energy storage system is used to complement the PV sources to overcome and sustain PV power output [56, 65]. A social acceptance study of microgrids dedicated to EV charging stations is presented in [66], which shows that a large majority of EV users accept the intelligent charging station based on PV energy for recharging EVs powered by the microgrid. Economic analysis is an essential point for decision-makers. EV charging stations empowered by PV-based microgrid can work in a self-consumption mode so that reducing the impact on the public grid. In terms of PV and storage sources, the investment and initial installation costs are high and the means to reduce these costs are to extend the service life and improve the energy conversion rate. However, in operation, the energy costs for recharging EVs are minimized by the use of renewable PV energy. Regarding the public grid, taking into account a power limit reduces the negative impact on the stability of the system. EV charging stations empowered by PV-based microgrid have been supported by government departments and achieved social acceptance [67].

Considering the EV charging station modelling proposed in [68, 69], this paper presents an EV charging station model empowered by a DC microgrid. The DC microgrid aggregates EVs, a storage system, a public grid connection, and a PV source, aiming at power balancing of the system [70], and bringing various interests [16], such as the peak power of the public grid is lowered, the profits of the charging station are increased, and the EV users' charging cost is reduced. Due to the intermittency of the PV power, the capacity limitation of the storage, and the power limitation of the public grid, the power of an EV charging station can be reduced. In addition, this power limitation of an EV charging station is variable in different situations, according to the weather and the charging time slots.

Users without private chargers must go to public charging stations. EV charging stations mainly includes three types of charging systems: single cable with a single charger, multiple cables integrated in a single charger, multiple cables with multiple chargers. The second and the third are considered suitable for installation in residential areas or near workplaces taking investment costs into consideration [71]. Intelligently controlled charging can reduce manual maintenance, and more importantly, can meet the users' needs and overcome the intermittency of the PV power. The EV charging station requires precise management taking users' needs and power limitations into consideration. It should be noted that in real life, charging modes chosen by users are impossible to predict. The choices of the same users are not necessarily the same at different times and in different conditions. Meanwhile, the arrival time and its initial state of charge SOC_{EV_in} are random. In the EV charging process, the user has the possibility to leave at any time. When the power of the station is insufficient, the shedding operation

should be considered. The restoration operation should be considered if there are EVs on waiting because of EV shedding operation.

A spatial and temporal model of EV charging demand for a rapid charging station is developed in [72], and the charging demand is forecasted by the queueing theory with the arrival rate of discharged vehicles. The paper [73] proposes a mathematical model for the spatial-temporal charging demand for EVs, which helps to obtain the charging spatial-temporal parameters: charging mode, charging location, and charging time based on the input parameters. EV parameters include the number of EVs, EV charging power, and battery capacity. However, load shedding and load restoration are not considered in this model. A load shedding/restoration real-time optimization for DC microgrid building-integrated is presented [74, 75], which solves the load shedding and load restoration when the available microgrid power is less than the load demanded power and provides a reference for the shedding operation and restoration operation of the EV charging station. However, designing a complete power management strategy for an EV charging station remains an open issue [45].

III.2. System topology and modelling

The studied system is designed on the basis of a DC microgrid. As shown in Figure 11, it is composed of the PV sources, an electrochemical storage system, a public grid connection, and an EV charging station, which includes five EV chargers.

The DC microgrid's sources are connected to the common DC bus. The electricity produced by PV sources is primarily for EV charging. Storage is an additional energy source to supply the EVs or to absorb excessive energy produced by PV sources. The public grid is used as a back-up source, which allows PV sources to sell excessive energy. If PV power is lower than the power demanded by the EVs, the additional power needed to charge EVs is provided primarily by the storage and then by the public grid. In contrast, the excess energy primarily feeds the storage, then is injected into the public grid [56, 69]. Based on the above analyses, the EVs are the only loads, as shown in Figure 11 and p_{PV}, p_S, p_G, and p_{EVs} are respectively the power of the PV, the storage, the public grid, and EVs.

The flow chart of the power management strategy of the DC microgrid is shown in Figure 12, which focuses on power system control.

The management strategy, responsible for ensuring instant power balance, interacts with the EV shedding and EV restoration. (3. 1) expresses p^* that is the power reference to keep the stability of the DC bus voltage in a steady state:

$$p^* = \left(p_{PV\_MPPT} - p_{PV\_S}\right) - \left(p_{EVs\_D} - p_{EVs\_S}\right) \quad (3.\ 1)$$

where p_{PV_MPPT} is the PV power imposed by MPPT algorithm, p_{PV_S} is the PV power needed to be shed, p_{EVs_D} is the power demand of EVs, and p_{EVs_S} is the EV power needed to be shed.

In the power management strategy of the DC microgrid, p^* is provided by the public grid power reference p^*_G and the storage power reference p^*_S, as presented in (3. 2):

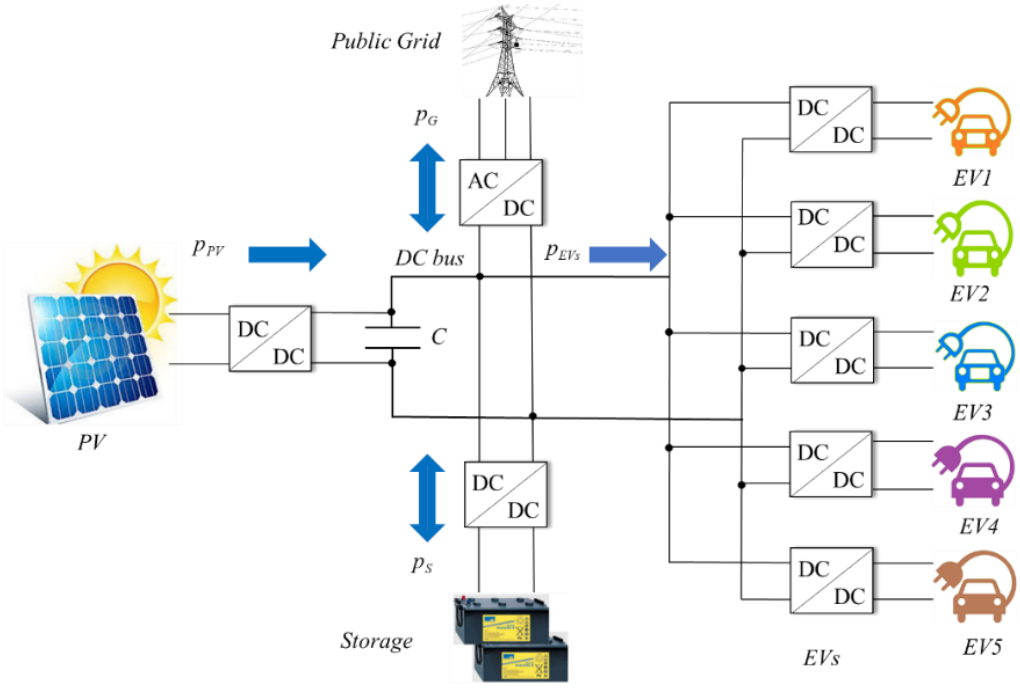

Figure 11. The EV charging station based on a DC microgrid.

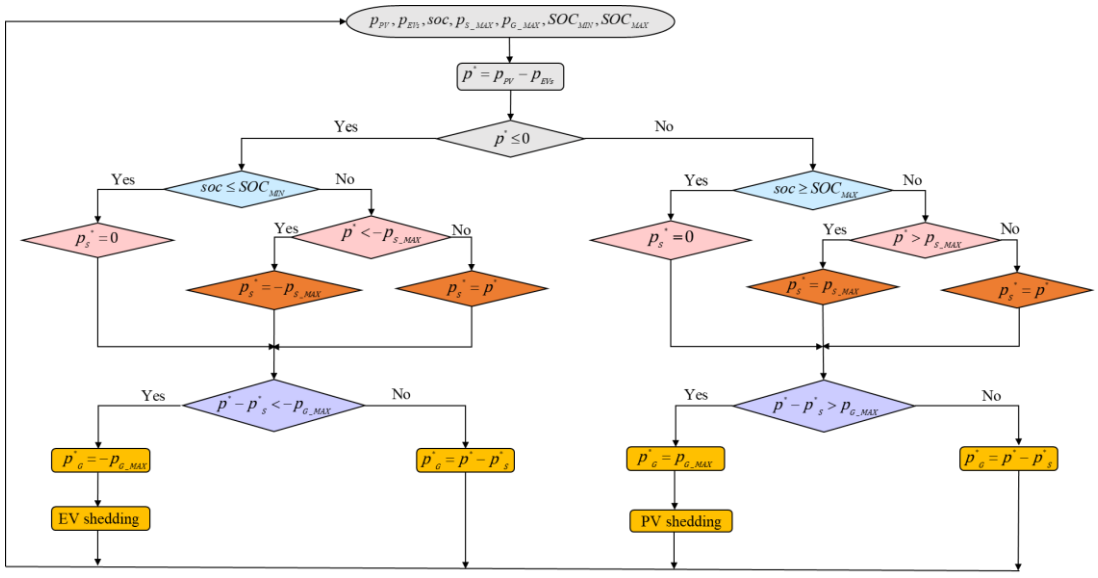

Figure 12. Flow chart of the power management strategy of the DC microgrid.

$$p^* = p^*_G + p^*_S \quad (3.\ 2)$$

A distribution coefficient, named k, is introduced in (3. 3):

$$SOC_{B\_MIN} \le SOC_B(t) \le SOC_{B\_MAX} \tag{3. 3}$$

The distribution coefficient k does not only take binary values, but also fractional values between zero and one.

The power p_S* is calculated by (3. 4) and p_G* is calculated by (3. 5).

$$p_S* = k \cdot p*,\ k \in [0,1] \tag{3. 4}$$

$$p_G* = (1-k)\,p* \tag{3. 5}$$

To avoid storage damage by overcharging and over-discharging, the state of charge of the storage, namely soc, is limited: SOC_{MIN} is the soc lower limit and SOC_{MAX} is the soc upper limit. Also, maximum storage power P_{S_MAX} is considered. Regarding the public grid, P_{G_LIM} is the absolute value of the grid injection power limit (positive) and grid supply power limit (negative).

The electrical scheme of the DC microgrid power architecture is given in Figure 13. PV sources, the storage system, and EVs are connected to the common DC bus through their dedicated static converters whose switching functions are f_{PV}, f_S, and f_{EVs} respectively. The rated DC bus voltage is considered to be 400V. In order to properly charge EVs and the storage, static converters are required. The public grid connection is carried out by a three-phase bidirectional AC/DC converter with the following switching functions: f_A, f_B, and f_C.

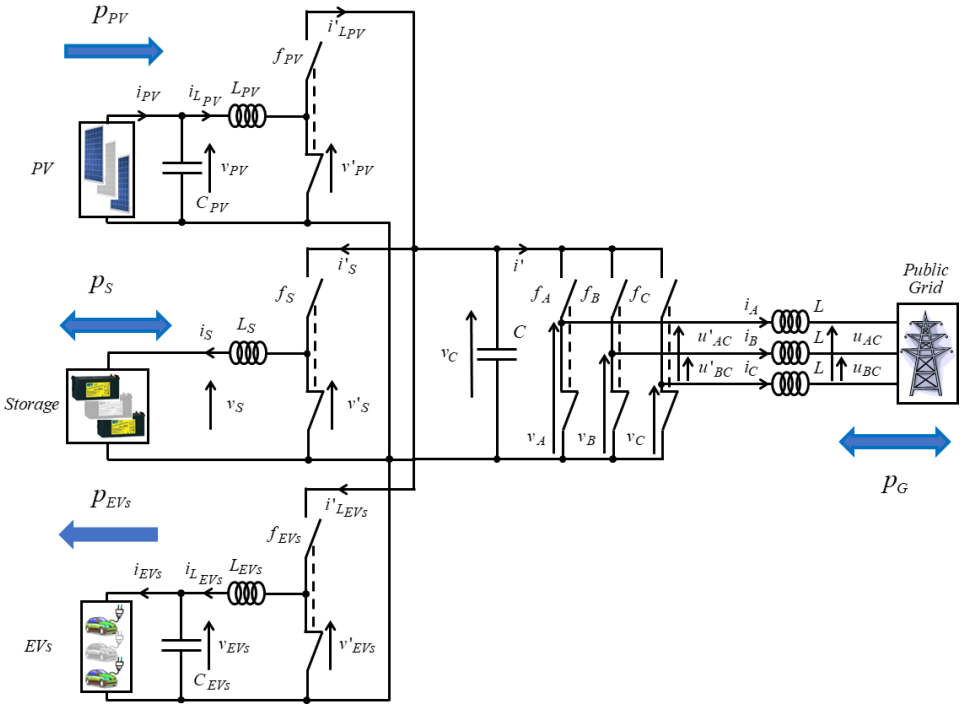

Figure 13. Electrical scheme of the DC microgrid power architecture.

Assuming that the system is ideal in terms of energy conversion, and neglecting the total losses of the power converter, the DC microgrid power balancing is given in (3. 6):

$$p_G + p_S = p_{PV} - p_{EVs} - v_{PV} \cdot C \frac{dv_C}{dt} \tag{3. 6}$$

where v_C represents the voltage of DC bus and C is the capacity of DC bus. In order to make the system work properly, it must always be respected.

III.2.1. Photovoltaic modelling

The proposed EV charging station is based on 400 PV panels (AIGPSMONO250W, AIGER), whose power is 100kW under the standard condition of the solar irradiance of 1000W/m^2 and cell temperature of 25°C, and it is composed of 40 parallel branches of 10 serial panels by branch. The voltage is imposed by the MPPT algorithm: perturb and observe [32]. The PV modelling equations are expressed by (3. 7):

$$\begin{aligned}
&\frac{dv_{PV}}{dt} = \frac{i_{PV} - i_{L_{PV}}}{C_{PV}} \\
&\frac{di_{L_{PV}}}{dt} = \frac{v_{PV} - v'_{PV}}{L_{PV}} \\
&\begin{bmatrix} v'_{PV} \\ i'_{L_{PV}} \end{bmatrix} = f_{PV} \begin{bmatrix} v_C \\ i_{L_{PV}} \end{bmatrix} \Rightarrow \begin{bmatrix} v'_{PV} \\ i'_{L_{PV}} \end{bmatrix} = m_{PV} \begin{bmatrix} v_C \\ i_{L_{PV}} \end{bmatrix} \\
&m_{PV} = \frac{1}{T}\int_0^T f_{PV} dt \text{ with } m_{PV} \in [0;1]
\end{aligned} \tag{3. 7}$$

where v_{PV} and $i_{L_{PV}}$ are the voltage and current of the PV converter's input side, L_{PV} and C_{PV} are the PV inductor and capacitor, respectively, i_{PV} represents the current provided by PV sources, v'_{PV} and $i'_{L_{PV}}$ are the voltage and current of the PV converter's output side, T is the period, and t is the time variable.

III.2.2. Electrochemical storage modelling

In this chapter, the electrochemical storage is a system characterized by 300V voltage and 300Ah capacity. The storage system modelling equations are expressed by (3. 8):

$$\frac{di_S}{dt} = \frac{v'_S - v_S}{L_S}$$

$$\begin{bmatrix} v'_S \\ i'_S \end{bmatrix} = f_S \begin{bmatrix} v_C \\ i_S \end{bmatrix} \Rightarrow \begin{bmatrix} v'_S \\ i'_S \end{bmatrix} = m_S \begin{bmatrix} v_C \\ i_S \end{bmatrix} \quad (3.\ 8)$$

$$m_S = \frac{1}{T}\int_0^T f_S dt \text{ with } m_S \in [0;1]$$

where v'_S and i'_S represent the voltage and current of the storage next to the DC bus, v_S and i_S are the voltage and current of the storage before the converter, m_S is the storage control variable, and L_S is the storage inductor.

III.2.3. Public grid modelling

The public grid used is considered to be a low voltage three-phase network with the 50Hz frequency, whose network connection is traditional. It is considered: i' the inverter current, i_A, i_B, i_C the currents of the three phases, L the self-inductance, and u_{AC} and u_{BC} the public grid voltages between the phases A and C, and B and C respectively. The public grid modelling equations are expressed by (3. 9):

$$\begin{bmatrix} u'_{AC} \\ u'_{BC} \end{bmatrix} = \begin{bmatrix} v_A - v_C \\ v_B - v_C \end{bmatrix}; \begin{bmatrix} v_A \\ v_B \\ v_C \end{bmatrix} = \begin{bmatrix} f_A \\ f_B \\ f_C \end{bmatrix} v_C$$

$$\begin{bmatrix} v_A \\ v_B \\ v_C \end{bmatrix} = \begin{bmatrix} f_A - f_C \\ f_B - f_C \end{bmatrix} v_C \Rightarrow \begin{bmatrix} v_A \\ v_B \\ v_C \end{bmatrix} = \begin{bmatrix} m_A \\ m_B \end{bmatrix} v_C \quad (3.\ 9)$$

$$\begin{bmatrix} m_A \\ m_B \end{bmatrix} v_C = \frac{1}{T}\int_0^T \begin{bmatrix} f_A - f_C \\ f_B - f_C \end{bmatrix} dt \text{ with } \begin{bmatrix} m_A \\ m_B \end{bmatrix} \in [-1;1]$$

where u'_{AC} and u'_{BC} are the output's inverter voltages between the phases A and C, and B and C respectively, v_A, v_B, and v_C are the simple voltages of the three phases, and m_A and m_B are the inverter control variables.

III.2.4. EV Modelling

The EV charging modelling equations are expressed by (3. 10) where v_{EVs} and $i_{L_{EVs}}$ are the voltage and current of the EV converter's output side, L_{EVs} and C_{EVs} are the EV inductor and capacitor, respectively, i_{EVs} represents the input current for EVs, and v'_{EVs} and $i'_{L_{EVs}}$ are the voltage and current of the EV converter's input side. v_{EVs} and $i_{L_{EVs}}$ are the voltage and current of the EV converter's output

side, L_{EVs} and C_{EVs} are the EV inductor and capacitor, respectively, i_{EVs} represents the input current for EVs, v'_{EVs} and $i'_{L_{EVs}}$ are the voltage and current of the EV converter's input side.

$$\begin{aligned}
&\frac{dv_{EVs}}{dt} = \frac{i_{L_{EVs}} - i_{EVs}}{C_{EVs}} \\
&\frac{di_{L_{EVs}}}{dt} = \frac{v'_{EVs} - v_{EVs}}{L_{EVs}} \\
&\begin{bmatrix} v'_{EVs} \\ i'_{L_{EVs}} \end{bmatrix} = f_{EVs} \begin{bmatrix} v_C \\ i_{L_{EVs}} \end{bmatrix} \Rightarrow \begin{bmatrix} v'_{EVs} \\ i'_{L_{EVs}} \end{bmatrix} = m_{EVs} \begin{bmatrix} v_C \\ i_{L_{EVs}} \end{bmatrix} \\
&m_{EVs} = \frac{1}{T}\int_0^T f_{EVs} dt \text{ with } m_{EVs} \in [0;1]
\end{aligned} \tag{3. 10}$$

III.3. EV charging station management strategy

The management strategy of the EV charging station mainly depends on the charging choice of the EV users. Different charging modes correspond to different charging costs. If the users choose the fast mode, they will save time along with relatively high fees. On the contrary, if users choose an average mode or a slow mode, the cost will be lower. The interaction diagram between sources and the EV charging station is shown in Figure 14.

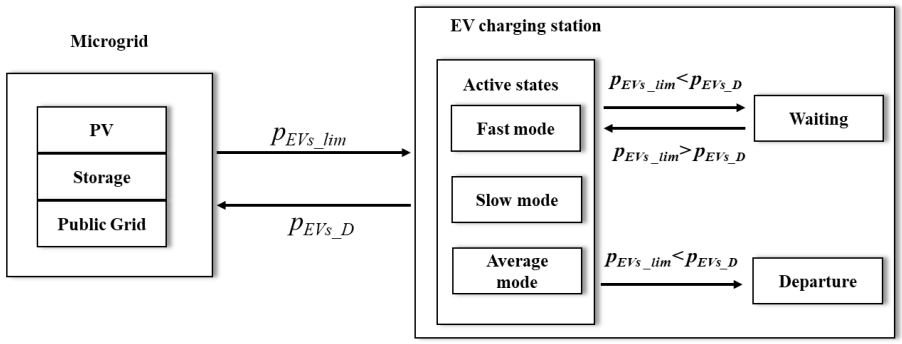

Figure 14. Interaction diagram between sources and EV charging station.

The DC microgrid's sources provide the available power p_{EVs_lim}, namely power limitation for the EV charging station. The EV charging station outputs the power demand p_{EVs_D} to the DC microgrid, which is a closed-loop. EV charging depends on the charger priority, and, in this chapter, the EVs are assigned on a first-come-first-serve method.

The EV charging station power limitation $p_{EVs\_\lim}$ is provided by p_{PV_MPPT}, P_{G_LIM}, and P_{S_MAX}, as expressed by (3. 11):

$$p_{EVs\_\lim} = p_{PV\_MPPT} + P_{G\_LIM} + P_{S\_MAX} \tag{3. 11}$$

III.3.1. Disconnect EV

The EV disconnection from the charger is always possible, permitting the user to stop charging and leave immediately.

III.3.2. Standby mode

The EV charger is in standby mode if the user chooses to wait for the power availability. In standby mode, the EV is not charged until the available power is enough for the chosen charging mode. There are two cases of standby modes. In the first case, when the EV just arrives at the station, the EV enters the initial waiting mode due to insufficient power. In the second case, the EV enters the waiting mode from the charging mode due to insufficient power, and it is a state between EV shedding operation and EV restoration operation.

III.3.3. EV shedding operation

The EV restoration algorithm operates following the scheme presented in Figure 15.

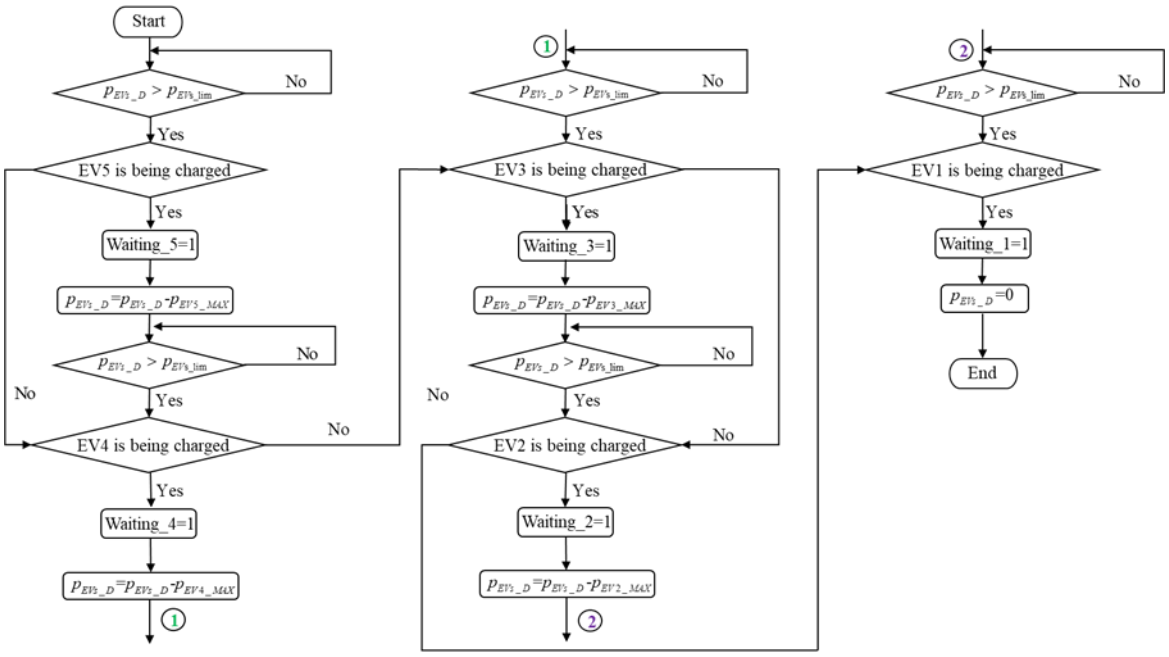

Figure 15. Flowchart of EV shedding.

In the beginning, the value of EV charging station power limitation and the power demand are read and a decision is made. If the power demand is less than the power limitation, the algorithm does not perform the EV shedding operation. Otherwise, when the power limitation is insufficient to attend the EV power demand, the EV charging station automatically performs the EV shedding operation in the order from EV5 to EV1, respecting the priority order first come first serve. For example, when p_{EVs_D} is greater than p_{EVs_lim}, if EV5 is being charged, it enters a waiting state after shedding operation.

The simulation is designed considering that the EV number "n" is connected to charger number "n", where "n" takes values from 1 to 5.

III.3.4. EV restoration operation

The EV restoration algorithm operates following the scheme presented in Figure 16.

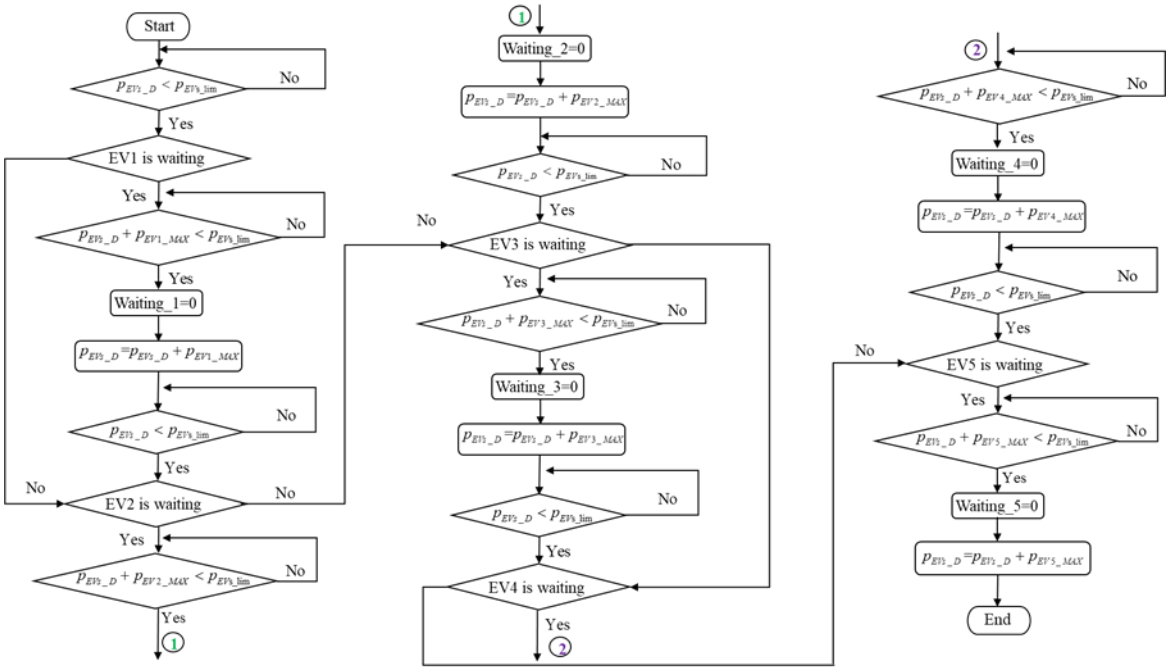

Figure 16. Flowchart of EV restoration.

If the power demand is more than the EV charging station power limitation, the algorithm does not perform the EV restoration. Otherwise, when the power limit is sufficient to attend the EV power demand, the EV charging station automatically performs the EV restoration operation in the order from EV1 to EV5, if there are EV on waiting connected to a charger. For example, when the p_{EVs_D} is less than the p_{EVs_lim}, if EV1 is on waiting, therefore the EV1 will be charged first during the restoration operation.

III.4. Simulation results and analyses

Five EV chargers are set in the simulation model, according to the priority order, namely from charger 1 to charger 5, the order from top to bottom in Figure 11. The EV charging station management strategy simulation is performed with MATLAB/Simulink, in which the process CC/CV with three charging modes is implemented. An integral proportional controller controls the current and voltage of EVs during the EV charging process. The simulated scenario follows the described EV charging station based on a DC microgrid and under power limitation. When an EV arrives, the user chooses the charging mode. Under the power limitation, if the charging station available power is greater than the maximal power demanded by the charging mode chosen by the user, the EV charges directly. If not, the system offers options for users.

III.4.1. Simulation conditions

In order to better emulate real situations, assuming that all EVs have the same battery characteristics, the arrival time of each EV is random and different and the initial SOC_{EV} is randomly generated in the simulation. Different users will take the charging price and charging time into account to choose the charging mode they need, and to emulate this action, the charging mode is also randomly generated. The parameters of the PV, EV, battery storage, public grid, and DC bus are detailed in Table 5,Table 6, Table 7, Table 8, and Table 9, respectively. In Table 5, P_{PV_STC} is the estimated PV power under standard test conditions (STC). In Table 6, T_{EV_FAST} is the EV fast charging time for a period of 0.5h; T_{EV_AVER} is the EV average charging time for a period of 1.5h; T_{EV_SLOW} is the EV slow charging time for a period of 4h. In Table 7, V_{S_RATED} is the rated voltage of the DC microgrid storage and C_{REF} is its capacity. The rated DC bus voltage was chosen as 400V [32].

Table 5. Parameters of the PV AIGPSMONO250 (10 PV in series, 40 branches in parallel).

Parameter	**Value**
P_{PV_STC}	10*40*250=100kW

Table 6. Parameters of the EV 26650 LiFePO4 (120 cells in series, 28 branches in parallel).

Parameter	Value	Parameter	Value
T_{EV_FAST}	0.5h	P_{FAST_MAX}	83kW
T_{EV_AVER}	1.5h	P_{AVER_MAX}	27kW
T_{EV_SLOW}	4h	P_{SLOW_MAX}	7KW
Stored energy	24kWh	Number of chargers	5

Table 7. Parameters of the battery storage.

Parameter	Value	Parameter	Value
V_{S_RATED}	300V	SOC_{MIN}	20%
C_{ERF}	300Ah	SOC_{MAX}	80%
I_{S_MAX}	115A	V_{S_RATED}	300V

Table 8. Parameters of the public grid.

Parameter	Value
P_{G_MAX}	50kW

Table 9. Parameters of the DC bus.

Parameter	Value
v_{C_REF}	400V

III.4.2. Simulation results

Figure 17 shows the real solar irradiance and PV cell temperature during the day of 28 May 2019 at Compiegne, France.

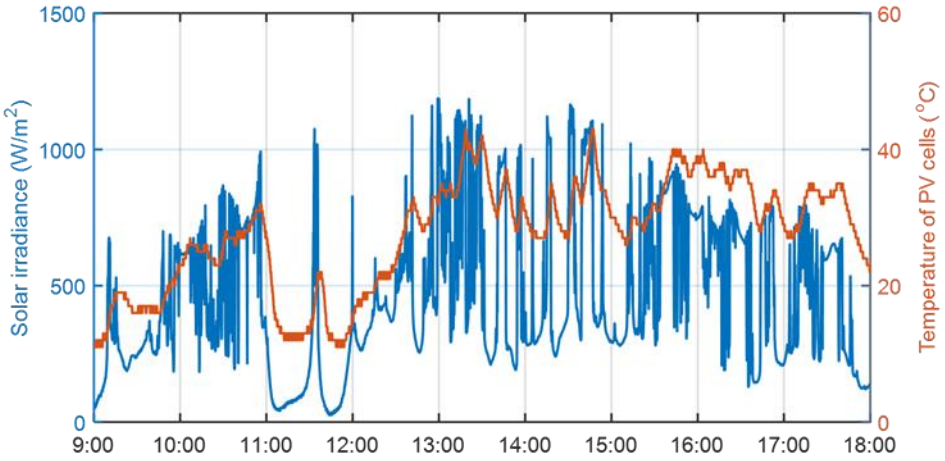

Figure 17. Solar irradiance and PV cell temperature.

The voltage of DC bus, namely v_C, is shown in Figure 18. The steady DC bus voltage is 400V and v_C reaches a steady state at 9:05, which proves that the strategy works well to balance the powers.

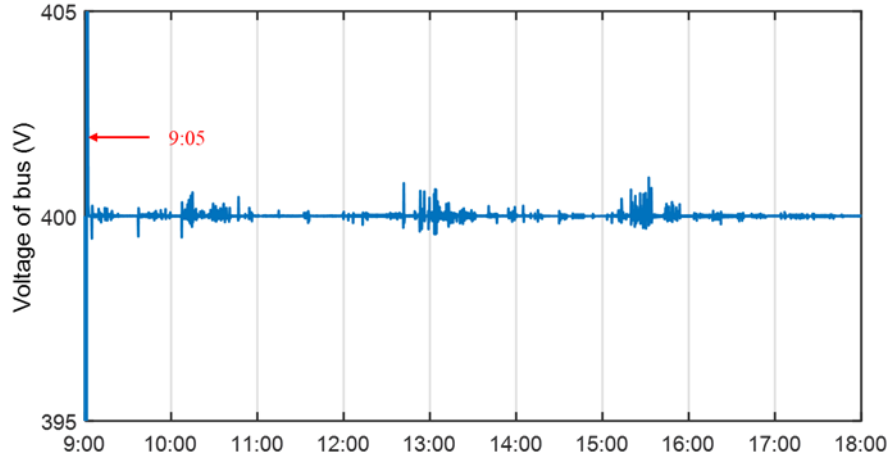

Figure 18. DC bus voltage evolution.

To extend battery life, the storage current should be limited. Figure 19 presents the storage current limitation for a value of 115A.

Storage *soc* and distribution coefficient k are shown in Figure 20 where $k=1$ if only the storage is working and $k=0$ if only the public grid is working. If k is between 0 and 1, the power is shared simultaneously between the storage and the public grid during the current limitation periods. To reduce storage damage *soc* upper limit is 80% and *soc* lower limit is 20%.

The powers' evolution is recorded and the powers' flow is shown in Figure 21. PV sources work in two modes: PV-constrained production control and PV-MPPT control. When the storage and the public grid reach their upper limits, the PV production should be constrained [76].

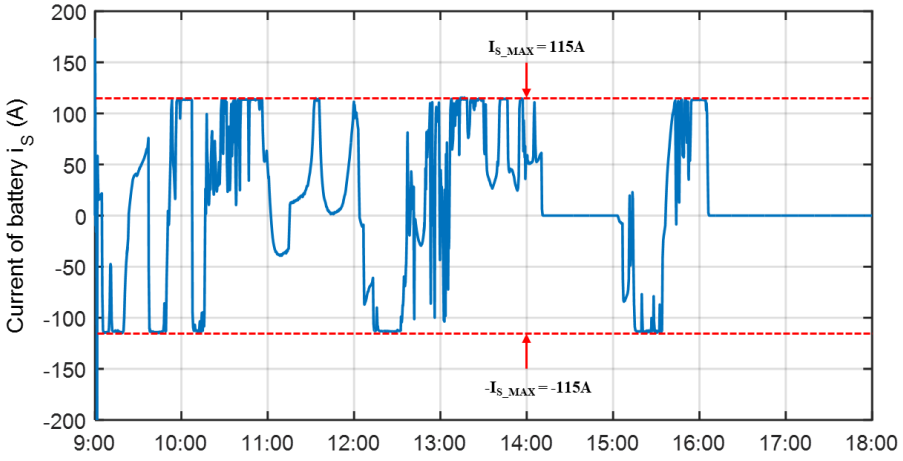

Figure 19. Storage current evolution.

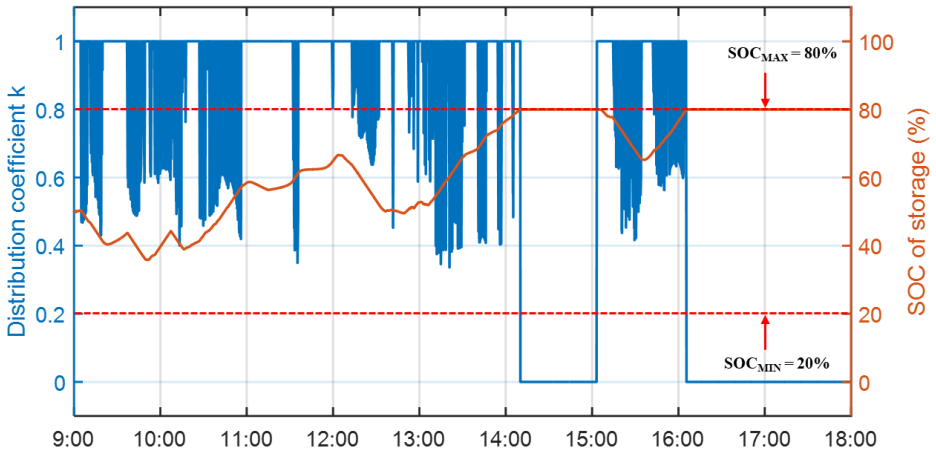

Figure 20. Storage *soc* and distribution coefficient *k* .

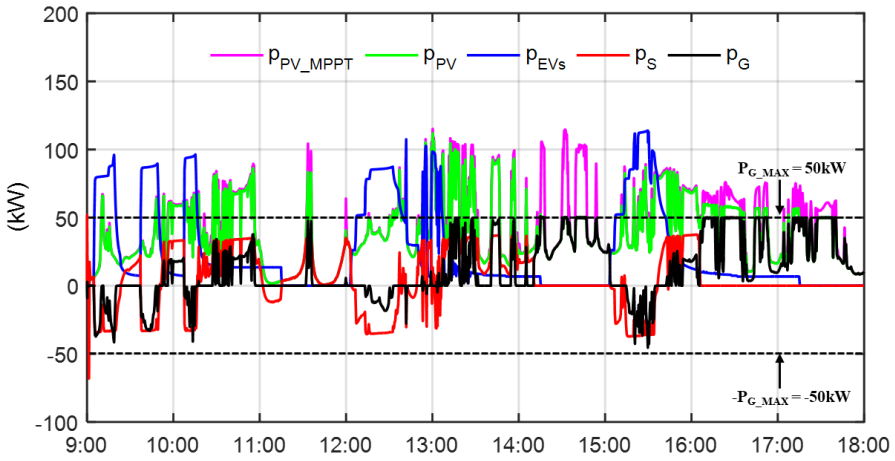

Figure 21. The power flow of DC microgrid.

Furthermore, $p_S < 0$ means that the storage charges EVs, $p_S > 0$ represents that PV sources inject excess energy into the storage, $p_G < 0$ shows that PV sources and the storage cannot provide sufficient energy for EVs so that the public grid needs to inject electricity into EVs, and $p_G > 0$ illustrates that the storage has reached its upper limit so that the excess PV energy is sold to the public grid.

The results show that the power management strategy is well respected.

III.4.2.1 Users' choices

In order to better analyze the simulation results, they can be divided into three-time slots: 9:00-12:00, 12:00-15:00, and 15:00-18:00. The number of records for the EV charging station is listed in Table 10. In the first time slot 9:00-12:00 five EVs arrive at the station; three EVs choose to be charged respectively as fast mode, slow mode, and slow mode, while the other two EVs choose to wait. In the second time slot 12:00-15:00, five EVs arrive at the station; four EVs choose to be charged respectively as average mode, average mode, average mode, and slow mode, while one EV chooses to wait. In the third time slot 15:00-18:00, six EVs arrive at the station: five EVs choose to be charged respectively as average mode, average mode, average mode, slow mode, and average mode, while one EV chooses departure.

Table 10. Number of records.

Number	9:00-12:00	12:00-15:00	15:00-18:00
Arrive	5	5	6
Being charged	3	4	5
Waiting	2	1	0
Departure	0	0	1

Charge evolution refers to the display SOC_{EV}, but it is not the real storage capacity of EV batteries. The original battery capacity is 100%, but it only can be used about 80%-90% taking battery safety and service life into consideration. If the charging is too full, once the charging system is faulty, it may cause a safety accident due to overcharging. The battery management system generally reserves a certain bottom line on redundancy as a guarantee, which is used for the situation that the EV is not used for a long time; it must have a small amount of residual electricity when the user thinks that the power reaches 0%.

EV charging power and SOC_{EV} evolution connected to charger 1 are shown in Figure 22. The power requested by charger 1 in the first time slot with peak values close to 90kW indicates that the charging

mode chosen by users is fast mode; the power requested by charger 1 in the second time slot with peak values close to 30kW indicates that the charging mode chosen by users is an average mode.

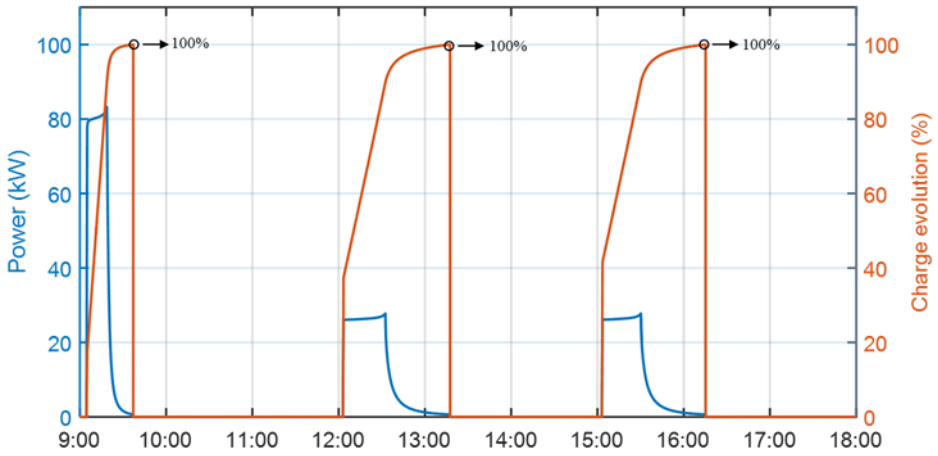

Figure 22. EV charging power and SOC_{EV} evolution connected to charger 1.

EV charging power and SOC_{EV} evolution connected to charger 2 are shown in Figure 23.

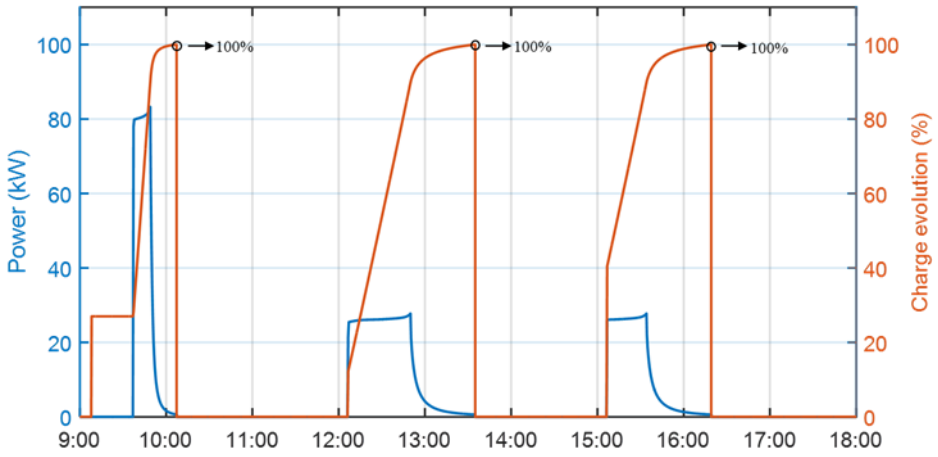

Figure 23. EV charging power and SOC_{EV} evolution connected to charger 2.

EV charging power and SOC_{EV} evolution connected to charger 3 are shown in Figure 24. The curve shape of the power requested by charger 3 in the second time slot is high frequency oscillating because the EV switches frequently between waiting and charging due to the power limitation.

EV charging power and SOC_{EV} evolution connected to charger 4 are shown in Figure 25. The power requested by charger 4 in the first and third time slots with peak values close to 10kW, indicates that the charging mode chosen by users is slow mode. The curve shape of the power in the first and third time slot is rectangular, because the EV disconnects from the charger before fully charged. The power

requested by charger 4 in the second time slot suddenly becomes zero because the EV enters a waiting state due to power limitation.

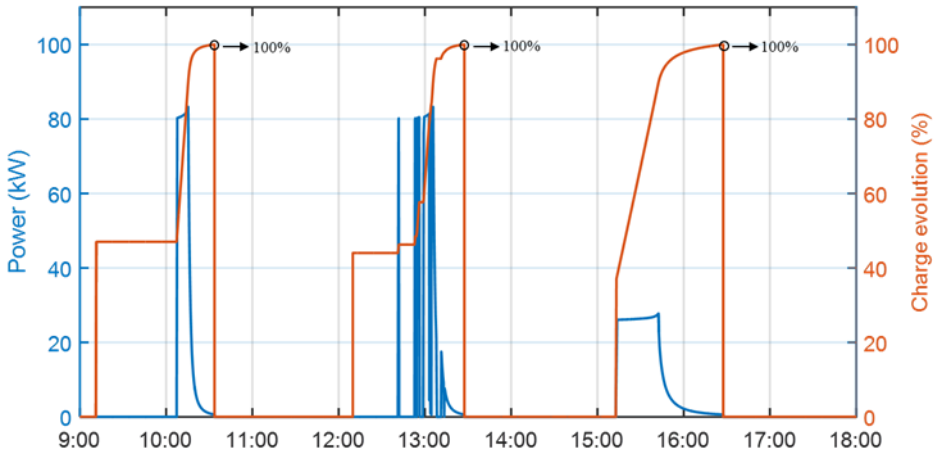

Figure 24. EV charging power and SOC_{EV} evolution connected to charger 3.

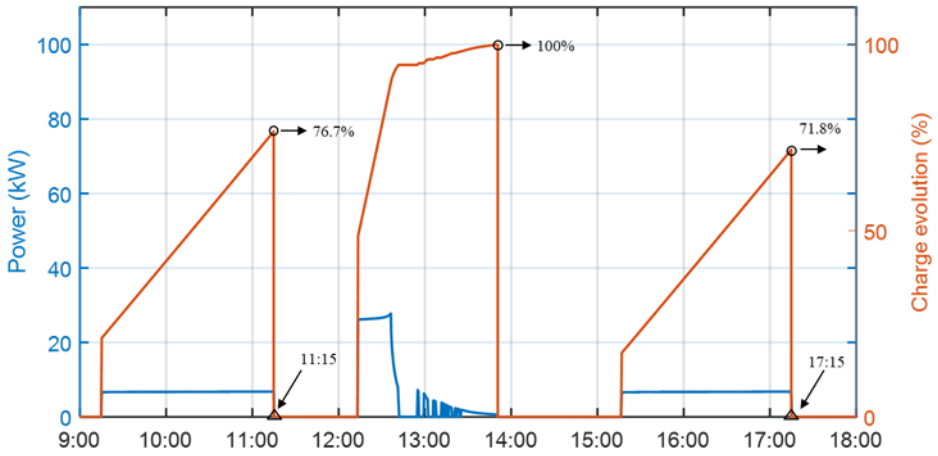

Figure 25. EV charging power evolution connected to charger 4.

EV charging power and SOC_{EV} evolution connected to charger 5 are shown in Figure 26. The power requested by charger 5 in the first and second time slots with peak values close to 10kW indicates that the charging mode chosen by users is slow mode; the power requested by charger 5 in the third time slot with peak values close to 30kW indicates that the charging mode chosen by users is average mode. The power requested by charger 5 in the first time slot suddenly becomes zero because the EV enters a waiting state due to power limitation. The curve shape of the power requested by charger 5 in the second and third time slots is high frequency oscillating because the EVs switch frequently between waiting and charging due to power limitation.

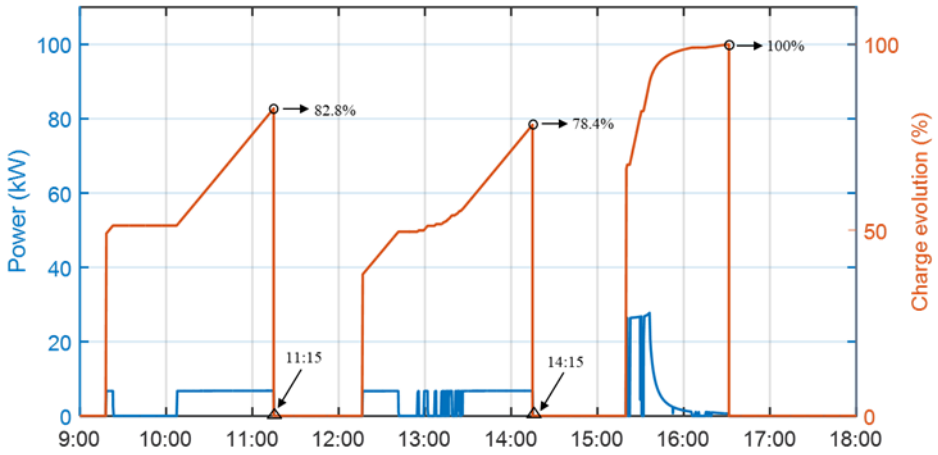

Figure 26. EV charging power and SOC_{EV} evolution connected to charger 5.

III.4.2.2 Disconnection

In the first and third time slots of Figure 25, the EVs connected to the charger 4 disconnect from the charger at 11:15 and 17:15 respectively, because the users have an emergency and need to leave immediately and the charging evaluation values are 76.7% and 71.8% respectively. In the first and second time slots of Figure 26, the EVs connected to the charger 5 disconnect from the charger at 11:15 and 14:15 respectively, before fully charged. Their charging evaluation values are 82.8% and 78.4% respectively. The other EVs have completed the full charging process and no EVs leave before fully charged.

III.4.2.3 EVs on waiting

In the first time slot of Figure 23, and in the first and second time slots of Figure 24, the charging evaluation values of EVs are constant at the beginning of the period, because the initial choices of the EVs are waiting.

In the second time slot of Figure 24, in the second time slot of Figure 25, and in the first, second and third time slots of Figure 26, when $p_{EVs\_\lim}$ is less than P_{EVs_D}, the EV connected to chargers enter a waiting state.

III.4.2.4 EV shedding operation

In the first time slot of Figure 23, and in the first and second time slots of Figure 24, the charging evaluation values of EVs are constant at the beginning of the period, because the initial choices of the EVs are waiting.

In the second time slot of Figure 24, in the second time slot of Figure 25, and in the first, second, and third time slots of Figure 26, when $p_{EVs\_\lim}$ is less than P_{EVs_D}, the EV connected to chargers enter a waiting state.

III.4.2.5 EV restoration operation

After EV shedding operation, there are EVs on waiting. When the power is available, restoration priority is from EV1 to EV5, in which situation the EV continues to be charged with the original chosen charging mode, and the SOC_{EV} is continuous. In the first and third time slots, the EVs connected to charger 5 switches back and forth between shedding operation and restoration operation. In the second time slot, the EVs connected to charger 3, charger 4, charger 5 are recharged in sequential order when the power is sufficient.

III.4.2.6 Recording of EV charging

It is necessary that the EV charging station has the function of recording data in real-time, which will provide a data base for adjustment and future planning of the station. The recording of EV charging station is shown in Figure 27. It can be seen, N1, N2, N3, N4, and N5 are the number of EVs arrived at the station, the number of EVs being charged, the number of EVs fully charged, the number of EVs on waiting, and the number of departure EVs, respectively.

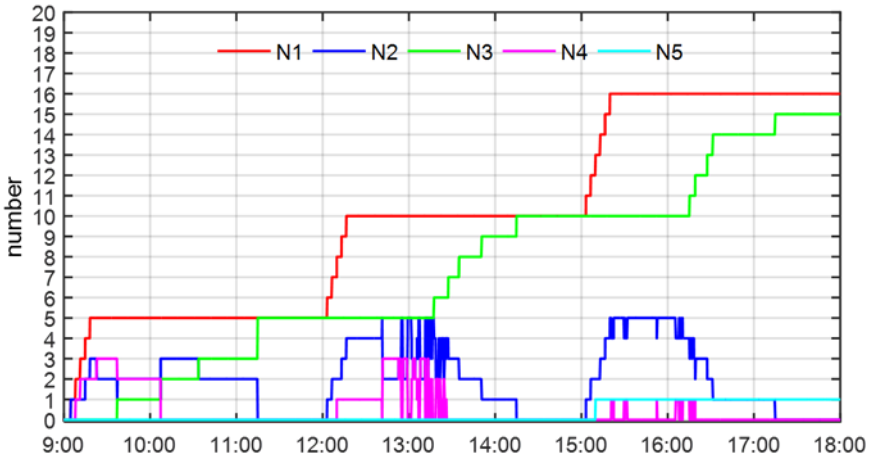

Figure 27. Recording of EV charging station.

The results show that most of the EVs arrived at the charging station choose to be charged. When the available power of the charging station is insufficient, the users are more inclined to wait or choose other charging modes. Thus, the current planning of this charging station is reasonable.

The management strategy has strong applicability in real life. At the physical level, EV charging stations based on a DC microgrid, consisting of PV source, storage system, public grid connection, are

easy to design and implement in shopping malls, school parking lots, community parking lots, etc. The PV-based EV charging station fully takes advantage of renewable energy that PV sources provide, improves peak performance of the public grid without increasing the grid capacity, and most importantly, it has succeeded in social acceptance during a social acceptability study [66, 67]. In addition, the proposed power management deals with the uncertainties of EV user's behaviour considering its arbitrary and random choices through the human-machine interface, which considers most of the users' choices and is easy to be accepted by users.

III.5. Conclusions

The charging station stability and users' satisfaction are of great value for the future development of EVs, which requires managing an EV charging station in a reliable and intelligent way. The object of this chapter is to propose a management strategy for an EV charging station empowered by a DC microgrid under power limitation to emulate various realistic scenarios, including the interaction with EV users.

Firstly, the microgrid-based EV charging station topology and modelling are proposed. The microgrid is composed of PV sources, an electrochemical storage system, a public grid connection, five chargers associated with their parking spots, and a DC common bus. Then, a real-time power management strategy for an EV charging station and a real-time interface is proposed. The management strategy fully considers the randomness and unpredictability of users' choices based on power availability. Meanwhile, the real-time power management strategy considers the constraints of the physical components of the microgrid. The real-time interface can deal with microgrid's sources and interact with users. An EV charging algorithm is presented to deal with the uncertainties of EV user behaviours. Users may choose three charging modes: fast mode, average mode, and slow mode. In addition, it is also considered that the user can disconnect the EV from the charger at any time. A simple EV shedding and restoration method is applied according to the available power of the proposed microgrid and the EV power demand. Simulation results verify the efficiency of the proposed management strategy in handling user choices and ensuring power balance under power limitation, which provides a theoretical basis for the future construction of EV charging stations based on a DC microgrid.

The rapid development of EVs increases the power demand and, how to meet the needs of as many EV users as possible is a very critical issue under the premise of ensuring the stability of the public grid. Thus, in further work, SROA will be developed to maximize available power. In addition, V2G technology will be designed and applied for ancillary services for the public grid during the "peak" periods, considering the duality of EV battery "charge-source". In order to reduce the high operation

costs of the EV charging station, optimization algorithms based on the proposed energy management strategy will be applied to minimize the total operation energy costs of EV charging stations.

Chapter IV. Shedding and restoration algorithms for an electric vehicle charging station

This chapter focuses on SROA for an EV charging station based on a DC microgrid to maximize the utilization of available power to meet user needs, meanwhile, taking into consideration the intermittency of the PV source, the capacity limitation of the storage, and the power limitation of the public grid. The simulation results show that compared with RBA, the proposed SROA respects the user's choice while reducing total charging time, increasing the full rate, and maximizing the available power utilization, which shows the feasibility and effectiveness of SROA.

Literature review is described in IV.1. The structural frame of an EV charging station is given in Section IV.2. Two algorithms for EV shedding and restoration are described in Section IV.3. The optimization problem and objective function are presented in Section IV.4. The constraints of shedding and restoration for the EV charging station are given in Section IV.5. The simulation results and analyses are presented in Section IV.6. The conclusions of this chapter are given in Section IV.7.

IV.1. Literature review

To reduce the consumption of fossil fuels and achieve the true meaning of low-carbon life, accompanied by sharp cost reductions for PV sources, in particular, grid-connected PV sources systems like EV charging stations centered on a microgrid based PV sources generation are proposed [56, 66].

The management of the EV charging station should consider both the needs of users and the revenue of the charging station. An optimization model for EVs scheduling in a smart grid is proposed in [77], which considered a problem including the economic cost of energy production/acquisition from the public grid and the cost relevant to the delay in the satisfaction of the customers' demand. A multi-objective function is introduced to balance the trade-off between maximizing the microgrid revenue and minimizing the microgrid operating cost [78]. An optimal scheduling mathematical model for a DC microgrid consisted of PV system and EV charging station is proposed [79], and solves the model to acquire the Pareto solution with the cost of electricity purchasing and energy circulation of storage batteries. In addition, the state management of each EV should be fully considered, especially EV shedding and EV restoration. The practical experience achieved with the operation of ten EVs and solar station during two years is presented [50], taking different states of EVs into consideration: "EV is waiting", "EV is scheduled", "EV is charging", and "EV charging is finished". On the other hand, a load shedding/restoration real-time optimization for DC microgrid building-integrated is presented in [75] . The objective of this optimization is solving the problem of selection and controlling loads in the

emergency conditions and/or limitation of available power by fixing a priority coefficient to each load that needs to be controlled. However, in this case, the load types and power demand are deterministic while the EV power demand varies according to the user's need, i.e. charging modes and state of charge in real-time [80].

IV.2. The structural frame of an EV charging station

A microgrid is a multi-source and multi-load system based on renewable energy sources and storage. Compared with the AC microgrid, the DC microgrid may be the main power supply structure for EV charging stations in the future due to its simplicity, economy, and high efficiency.

The studied EV charging station is designed based on a DC microgrid [45]. As illustrated in Figure 28, it is composed of PV sources, an electrochemical storage system, a public grid connection, and EV charging terminals. These components are all connected directly to the DC bus.

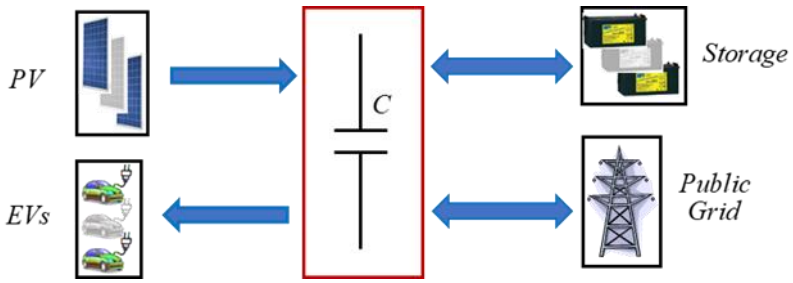

Figure 28. DC microgrid for an EV charging station.

IV.3. Algorithm description

This chapter presents two algorithms for EV shedding and restoration: RBA and SROA, which are demonstrated in an EV charging station to simultaneously support five EVs.

IV.3.1. RBA algorithm

EV shedding and restoration decisions of the RBA are obtained by comparing the value of the power demand, p_{EVs_D}, and the power limitation of the EV charging station. Flow chart of RBA is shown in Figure 29. When the power limitation is insufficient to attend the EV power demand, the EV charging station automatically performs the EV shedding operation in the order from the 5th EV, i.e. EV5, to 1st EV, i.e. EV1. When the power limitation is sufficient to attend the EV power demand, the EV charging station automatically performs the EV restoration operation in the order from EV1 to EV5, if there are EVs on waiting connection to the charger.

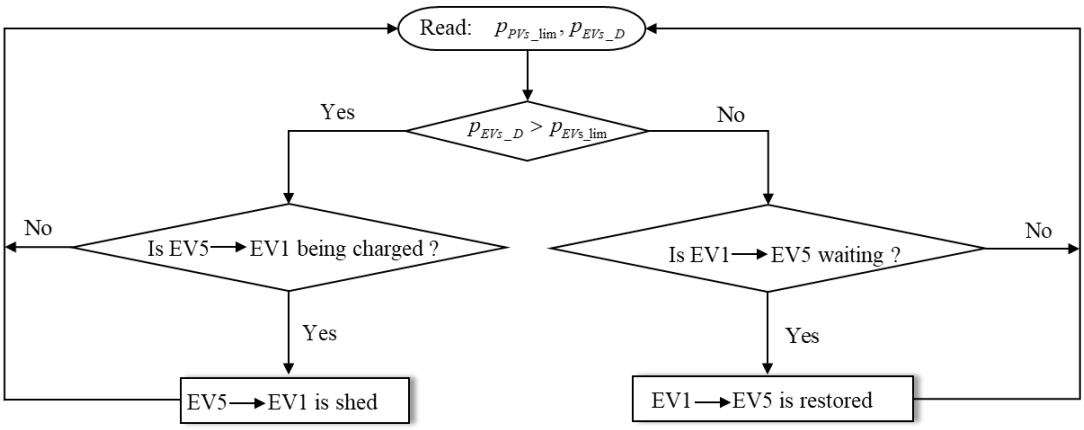

Figure 29. Flow chart of RBA.

IV.3.2. SROA algorithm

The goal of the SROA is to maximize the utilization of available power from the microgrid. The optimal EV shedding and restoration decisions are gained according to the power demand and the power limitation of the EV charging station. Flow chart of SROA is shown in Figure 30.

When the power limitation is insufficient to attend the EV power demand, the algorithm calculates the charging power that needs to be reduced, and then, the algorithm calculates the power value of which EV downshifts or stops charging is closest to and greater than the power value needed to be reduced. In order to maximize the available power, the algorithm performs the downshift or stopping the charging of the EV. When the power limitation is sufficient to attend the EV power demand, the algorithm calculates the remaining power value. If there are EVs on waiting or downshifted, the algorithm performs the EV restoration operation or upshift whose power value is closest to and less than the remaining power value.

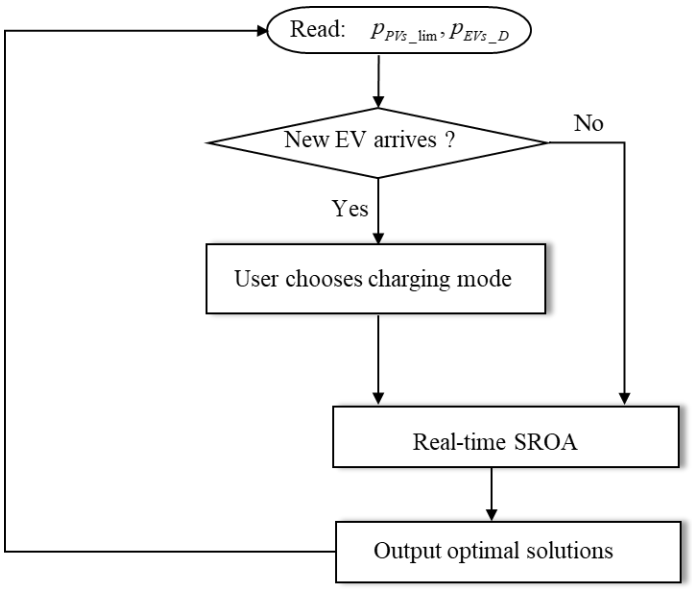

Figure 30. Flow chart of SROA.

IV.4. Objective Function

The optimization problem, objective function, and constraints of shedding and restoration for the EV charging station, are presented by following. Regarding the charging modes, it is considered that each EV has four choices corresponding to the following powers: P_{FAST_MAX} is the maximal charging power demanded by the fast mode, P_{AVER_MAX} is the maximal charging power demanded by the average mode, P_{SLOW_MAX} is the maximal charging power demanded by the slow mode, and 0 for waiting. The objective function to minimize the real-time remaining available power of the EV charging station that should be greater than or equal to zero is expressed by (4. 1):

$$p_{\text{remaining}} = p_{EVs\_\text{lim}} - p_{EVs\_D} \geq 0 \tag{4. 1}$$

where $p_{\text{remaining}}$ is the real-time remaining available power of the EV charging station, p_{EVs_D} is calculated by (4. 2), i represents the EV order and x represents the EV user possible choices as constrained in (4. 3):

$$p_{EVs\_D} = \sum_{i=1}^{5}(P_{FAST\_MAX} \cdot x_{(i-1)\cdot 4+1} + P_{AVER\_MAX} \cdot x_{(i-1)\cdot 4+2} + P_{SLOW\_MAX} \cdot x_{(i-1)\cdot 4+3} + 0 \cdot x_{(i-1)\cdot 4+4}) \tag{4. 2}$$

$$x_{(i-1)\cdot 4+1} + x_{(i-1)\cdot 4+2} + x_{(i-1)\cdot 4+3} + x_{(i-1)\cdot 4+4} = 1,\ i \in \{1,2,3,4,5\} \tag{4. 3}$$

where $x_{(i-1)\cdot 4+1}, x_{(i-1)\cdot 4+2}, x_{(i-1)\cdot 4+3}, x_{(i-1)\cdot 4+4}$ are the choices, i.e. fast mode, average mode, slow mode, and waiting, for EV1, EV2, EV3, EV4, and EV5; the domains of $x_{(i-1)\cdot 4+1}, x_{(i-1)\cdot 4+2}, x_{(i-1)\cdot 4+3}, x_{(i-1)\cdot 4+4}$ are set to $\{0\}$ or $\{0,1\}$ by the users when an EV is coming.

IV.5. Constrains

In order to calculate the real-time remaining available power of the EV charging station, five constraints should be considered: photovoltaic constraints, electrochemical storage constraints, public grid constraints, power balance constraints, and EV charging station constraints.

IV.5.1. Photovoltaic constraints

To operate a PV source within its maximum power point, whatever the solar irradiance and cell temperature variations, a MPPT algorithm is needed to find and maintain the peak power. Conversely, when the storage and public grid reach their upper limits, the PV production should be constrained. Therefore, in this study, PV sources work in two modes, PV-constrained production control, and PV MPPT control, and p_{PV} is expressed by (4. 4).

$$SOC_{B\_MIN} \le SOC_B(t) \le SOC_{B\_MAX} \tag{4. 4}$$

where p_{PV_S} is the shedding power of PV sources, p_{PV_MPPT} is the MPPT power of PV sources.

IV.5.2. Electrochemical storage constraints

To avoid storage damage or overcharging/over-discharging, the microgrid storage constraints are expressed by (4. 5) for the power and by (4. 6) for its state of charge soc .

$$-P_{S\_MAX} \le p_S \le P_{S\_MAX} \tag{4. 5}$$

where $\left|P_{S\_MAX}\right|$ is limited by the maximum current I_{S_MAX} of the storage charging or discharging.

$$SOC_{B\_MIN} \le SOC_B(t) \le SOC_{B\_MAX} \tag{4. 6}$$

where SOC_{MIN} is the soc lower limit and SOC_{MAX} is the soc upper limit.

IV.5.3. Public grid constraints

The public grid power p_G is constrained by (4. 7):

$$-P_{G\_LIM} \le p_G \le P_{G\_LIM} \tag{4. 7}$$

where the maximum output power of the public grid P_{G_LIM} is the absolute value of grid injection power limitation (positive) and grid supply power limitation (negative).

IV.5.4. Power balance constraints

The power balance of the microgrid is expressed by (4. 8):

$$p_{EVs} = p_{PV} + p_S + p_G \tag{4. 8}$$

where p_{EVs} is the power demanded by the EVs, p_{PV} is the power of PV sources, p_S is the power of the storage, p_G is the public grid power.

IV.5.5. EV charging station constraints

Fully considering the public grid constraints and the storage constraints, this multi-source system provides an available power, $p_{EVs\_\lim}$, namely the power limitation for the EV charging station and expressed by (4. 9):

$$p_{EVs\_\lim} = p_{PV\_MPPT} + P_{G\_LIM} + P_{S\_MAX} \quad \text{with} \quad (soc > SOC_{MIN}) \tag{4. 9}$$

where the storage can output power only when soc is greater than SOC_{MIN}.

When the EV arrives at the charging station, the user selects the charging mode or departures according to the available power of the charging station. After an EV is connected to the charger, the soc_{EV} is detected in real-time and the relative power and voltage are set according to soc_{EV} and the charging mode, and then charging is started. Once the users choose to charge, it means that when the power is insufficient, they can accept the downshift or waiting; also, the user can choose the departure at any time.

IV.6. Simulation results and analyses

The simulation for SROA is performed with MATLAB/Simulink and CPLEX that is an optimization software package for solving mixed-integer linear programming. Five chargers are considered. The simulation parameters are detailed in Table 11, where P_{PV_STC} is the estimated PV power under STC and v_C^* is the reference voltage of the DC bus.

Table 11. Parameters of DC microgrid

Parameters	Values	Parameters	Values
P_{FAST_MAX}	83kW	I_{S_MAX}	115A
P_{AVER_MAX}	27kW	SOC_{MIN}	20%
P_{SLOW_MAX}	7kW	SOC_{MAX}	80%
P_{PV_STC}	100kW	Number of chargers	5
P_{G_LIM}	50kW	v_C^*	400V

Figure 31 shows the DC bus voltage evolution v_C by using the RBA and SROA, respectively. The voltage deviation in Figure 31(a) is 0.23%, and in Figure 31(b) is 0.35%, because the calculation speed of SROA is faster than that of RBA. The standard deviation of voltage is 5.75V both in Figure 31(a) and Figure 31(b), so the voltage stability is the same.

Figure 32 shows the soc_{EV} evolution of each EV by using the RBA and SROA, respectively. The waiting time of EVs in Figure 32(b) is significantly less than that of Figure 32(a), because when the power is insufficient, the EV in Figure 32(a) directly chooses to wait, and the EV in Figure 32(b) first selects the downshift. Fifteen EVs with the same battery characteristics choose to charge both in the RBA and SROA. Eleven EVs in Figure 32(a) are fully charged and, four EVs are not fully charged, thus, the full rate is 73.3%. Twelve EVs in Figure 32(b) are fully charged and, three EVs are not fully charged, thus, the full rate is 80%. The SROA effectiveness is therefore shown.

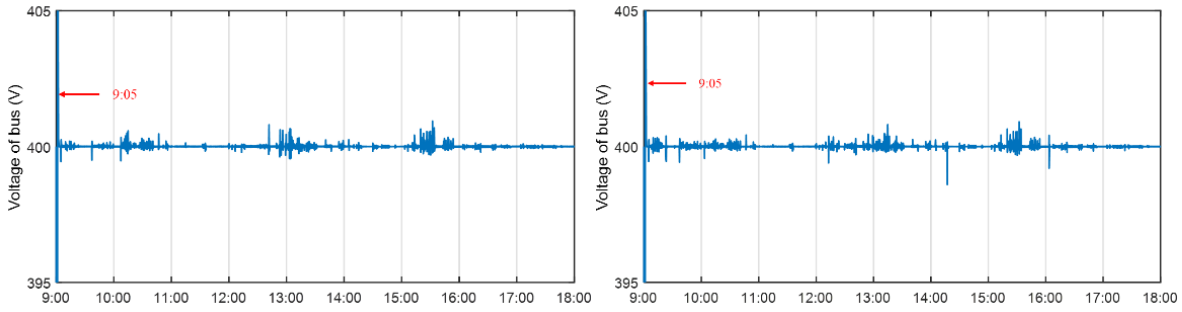

Figure 31. (a) DC bus voltage after RBA. (b) DC bus voltage after SROA.

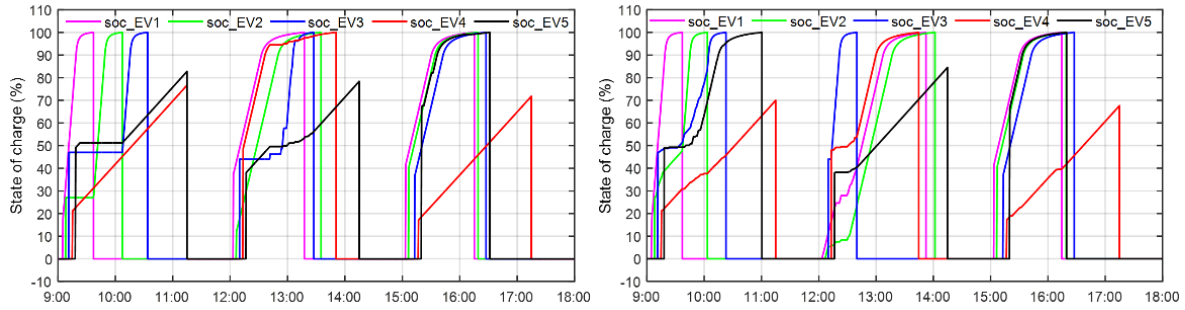

Figure 32. (a) SOC_{EV} evolution of each EV after RBA. (b) SOC_{EV} evolution of each EV after SROA.

Figure 33 shows the power evolutions of PV MPPT and PV by using the RBA and SROA, respectively. The same meteorological conditions are considered for RBA and SROA. The PV energy produced remains a priority for EVs. In case of insufficient energy, system security is ensured thanks to the storage system and public grid connection.

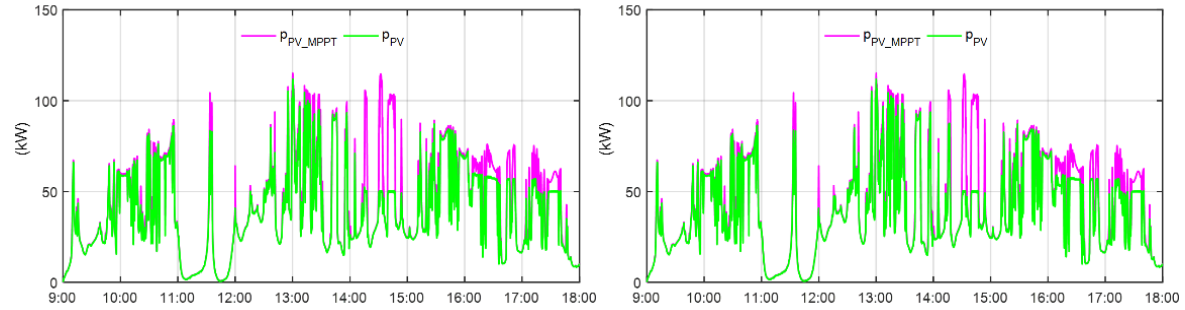

Figure 33. (a) PV MPPT and PV powers after RBA. (b) PV MPPT and PV powers after SROA.

Figure 34(a) and Figure 34(b) show the power evolutions of power limitation and EVs' total power by using the RBA and SROA, respectively. The total power variation after SROA is smaller than that of RBA, because when the power is insufficient, downshift is considered firstly instead of waiting under SROA. The total charging time in Figure 34(a) and Figure 34(b) are 21.3h and 20.7h, respectively. The power utilization in Figure 34(a) and Figure 34(b) are 20.5% and 21.8%, respectively. So, the SROA shortens the total charging time and improves power utilization.

Figure 35(a) and Figure 35(b) show power evolutions of storage and public grid by using the RBA and SROA, respectively, where the public grid power limitation is 50kW. The grid power is positive means that the public grid receives power; the grid power is negative means that the public grid supplies power to EVs. Figure 36 shows storage current by using the RBA and SROA, respectively, and present the storage current limitation for a value of 115A.

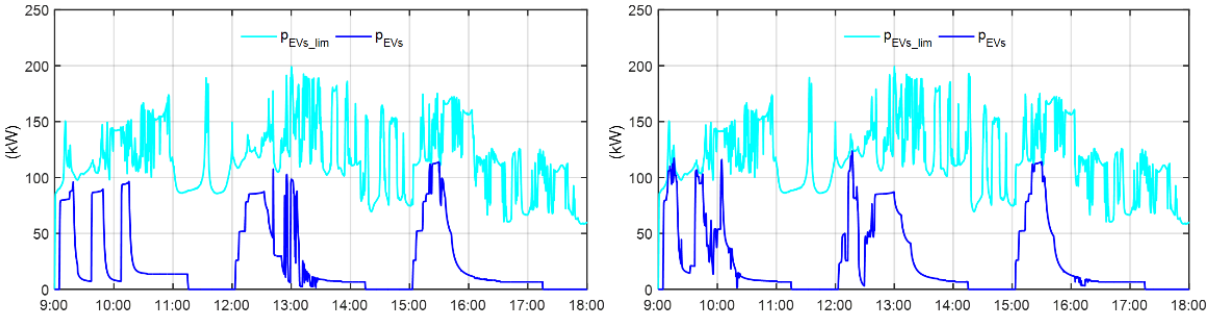

Figure 34. (a) EVs' power limitation and total power after RBA. (b) EVs' power limitation and total power after SROA.

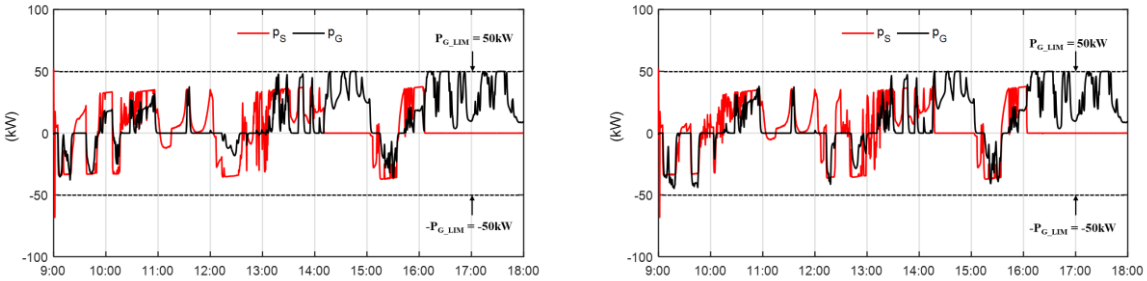

Figure 35. (a) Storage and public grid powers after RBA. (b) Storage and public grid powers after SROA.

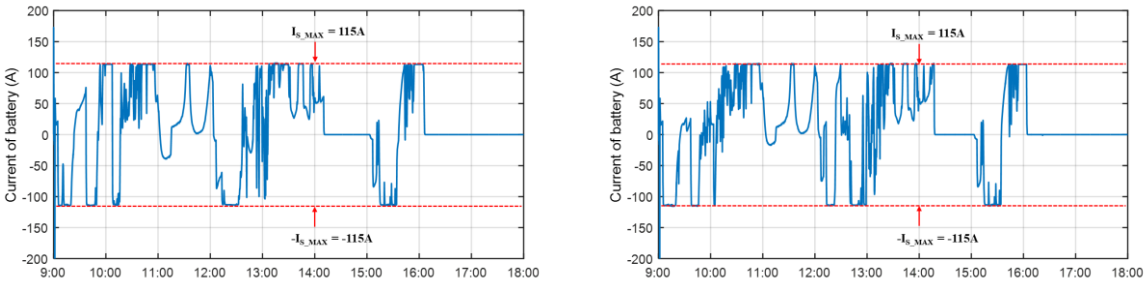

Figure 36.(a) Storage current after RBA. (b) Storage current after SROA.

The comparison of results obtained by using the RBA and SROA are detailed in Table 12. Due to the faster voltage regulation, the voltage deviation value by using SROA is greater than the voltage deviation value by using RBA, but the standard deviation of voltage is the same, so voltage stability has not been changed. The total charging time is shortened, the full charging rate becomes higher, and the utilization of available power becomes larger, demonstrating the availability and effectiveness of SROA.

Table 12. Comparison of results by using RBA and SROA

Algorithm	Voltage deviation	Standard deviation of voltage	Total charging time	Full rate	Power utilization
RBA	0.23%	5.75	21.3h	73.3%	20.5%
SROA	0.35%	5.75	20.7h	80%	21.8%

IV.7. Conclusions

As a low-noise, zero-direct emission vehicle, EVs have received unprecedented popularity. The explosive growth in the number of EVs causes an increase in power demand, resulting in the energy challenges of EV charging stations. The object of this chapter is to propose an optimization algorithm to maximize the available power of the EV charging station under the high EVs' penetration, and then to verify it.

Firstly, the structural frame of an EV charging station is presented. Then two algorithms for EV shedding and restoration: RBA and SROA are proposed. After then, the objective function is introduced considering all the system constraints. The simulation results show that compared with the RBA, the proposed SROA respects the user's choice while reducing total charging time, increasing the full rate, and maximizing the available power utilization, which provides an effective technical means for the stable operation of an EV charging station based on the microgrid. In addition, the SROA has certain reference significance for reducing the impact of EV charging on the peak load of the public grid.

Chapter V. EV charging station management with integrated V2G

This chapter focuses on the power management of a PV-powered charging station with integrated V2G from two aspects of energy scheduling and real-time control. A dynamic SPVA, based on energy management, is proposed for an EV charging station to mitigate the impact on the public grid, while reducing the energy cost of the public grid. The proposed SPVA can determine the optimal charging/discharging start time of EV in consideration of all of the initial state of charge SOC_{EV_in}, charging modes, arrival time, departure time, and the peak periods. Simulation results demonstrate the proposed SPVA effectiveness, which can guarantee the balance of the public grid, meanwhile satisfy the charging demand of EV users, and most importantly, reduce the public grid energy cost.

Literature review is described in V.1. The concept, major benefits, and challenges of V2G are given in Section V.2. DC microgrid structure with integrated V2G is introduced in Section V.3. Power flow management: grid-to-vehicle (G2V) and V2G algorithm are described in Section V.4. Simulation results and analyses are presented in Section V.5. Conclusions are given in Section V.6.

V.1. Literature review

In order to reduce the peak loads, a real-time dynamic pricing model is proposed for EVs charging/discharging service and building energy management [81]. In practice, many EVs are traveling on the road for only 4–5% of the day, while they are parked for the rest of the time [82]. Research on bidirectional on-board chargers makes EV discharge possible [83]. EVs can discharge into the public grid during its “peak” periods and can be charged during its “valley” periods to achieve the purpose of peak shaving and valley filling [84]. When EVs need an energy supply, they are connected to the public grid as charging loads; when EVs are idle, i.e., EVs are seen as distributed power sources, EV battery energy can be injected into the public grid. This is the V2G operation. Thus, V2G technology makes it possible for EVs to have a mobile battery function [85]. Moreover, compared with common loads, EVs have greater flexibility and dispatchability. When reasonable scheduling strategies for V2G technology are designed, and the charging/discharging behaviour of EVs is planned, EV charging costs will be reduced, most importantly, the load curve of the public grid will be improved. The paper [86] proposes a time-based charging group dispatching approach to schedule the charging of numerous EVs, which enables EVs to play an important role in peak shaving and valley filling, meanwhile solving the stability problem of the microgrid system brought by the penetration of renewable energy. EV batteries and related power electronics can be used to mitigate PV sources’ impact and support the public grid with

appropriate control strategies. The paper [87] develops a controllable charge/discharge pattern to optimize the limitation of EV battery capacity and the impacts of PV sources. Most importantly, EVs can provide instant power, which is much faster than starting a standby power source. So, V2G technology enables EVs to act as emergency power sources in the event of a power outage [85, 88]. V2G can bring economic benefits to EV users, offset part of the EV costs, promote communication between the public grid and EVs, meanwhile, protect the environment, and solve the shortage of fossil energy. V2G services are important for reducing environmental pollution, mainly referring to the GHG emission, such as CO_2 [89].

With the continuous development of renewable energy, such as PV sources, more and more renewable energy is being integrated into the power system in large quantities. Considering the intermittency and distribution of PV sources, microgrids are proposed to achieve small-scale renewable energy penetration while reducing the public grid stress [90, 91]. Surveys show that most EV users can accept the intelligent EV charging station based on a microgrid [66, 67]. The paper [56] proposes the model for an EV charging station. However, the above microgrid models and simulations do not consider V2G. Traditional V2G technology mainly refers to EVs directly connected to the public grid for the energy exchange. Generally, two types of control exist in systems: centralized control and decentralized control [92]. The former has high construction costs, while the latter has the problem of difficult control. Therefore, the V2G based on a DC microgrid control mode is proposed, which makes EVs connect to the public grid through a DC microgrid, moreover, it effectively integrates renewable energy, whilst meanwhile saving the cost of buying electricity from the public grid. V2G based on the microgrid is used for multi-objective optimization coordination between EVs and the public grid to minimize grid load fluctuation, maximize renewable energy utilization, and maximize the benefits for the EV users [93]. The paper [94] proposed a centralized model to co-optimize the transformer loss-of-life with benefits for EV users on charging/discharging management. As an optimal energy cost solution, cyber insurance was introduced to guarantee the best price for charging/discharging, which is effective not only in dealing with cyber risks but also in maximizing revenue for EV users [82]. The paper [95] develops a model predictive control-based approach to address joint EV charging scheduling and power control to minimize both EV charging cost and energy generation cost in meeting both residence and EV power demands.

A DC microgrid with integrated V2G has also been examined in other papers [93, 96]. The paper [96] proposes an optimal day-ahead operation planning procedure that aims to minimize microgrid operation daily costs, according to suitable load demand and source availability forecast without involving MATLAB/SIMULINK modeling. The review paper [97] focuses on the charging system components, architecture, operational modes, and control, including the interaction between the PV sources, public grid, energy storage unit, and power electronics, however, it does not take into account the management of multiple EVs. In addition, V2G was characterized as a comparatively advantageous means of peak load shaving [82]. The paper [92] proposes an optimal logical control algorithm based

on V2G to reduce the average charging cost of EVs, which is dedicated to the French energy billing system within the peak/base hour's contract. The algorithm can minimize the EV charging cost and maximize energy selling by using daily energy price profiles, considering constraints and disruptions: EV arrival/departure times, and the desired state of charge (soc_{EV}) for the next use. However, this algorithm has not yet involved a PV-powered charging station and research in the microgrid field.

In a V2G system, the EV charging station can obtain the optimal charging/discharging start time by reading the EV's arrival time, departure time, initial state of charge namely SOC_{EV_in}, and the state of charge limit at the time of departure, namely $SOC_{EV\_final\_\lim}$. Based on the above, this paper proposes an EV charging station management with integrated V2G, in which the optimal charging/discharging start time for EVs can be achieved to perform the purpose of peak and valley filling through a dynamic SPVA. Compared with the power limit of the public grid in the "valley" period, the power limit of the public grid absorbed from the microgrid is larger, while the power limit of the public grid released to the microgrid is smaller during the "peak" period. Therefore, when EVs connect to discharge, the charging station will select a time point near the "peak" periods for EVs; when EVs connect to charge, the charging station will choose a time point far away from the "peak" periods, which can not only relieve the pressure on the public grid but also reduce unnecessary charging costs [98]. In order to protect the stability of the public grid, the energy injected into the public grid needs to be limited, namely the self-protection mechanism of the public grid. To better ensure the stability of the public grid, the power limit of the power grid is set to different values according to the "peak" periods and "valley" periods.

V.2. Vehicle to grid

EVs with V2G function can provide energy back to the public grid. Electricity companies will be willing to purchase electricity from clients during peak power consumption or use the capacity of EV batteries to assist the public grid, such as load balancing or grid frequency control. Therefore, V2G has great commercial potential.

V.2.1. The concept of vehicle to grid

There are three emerging concepts of grid-connected EV technologies, which are the V2G, Vehicle to home (V2H), and Vehicle to vehicle (V2V). The framework of V2G, V2H, and V2V is shown Figure 37. V2G refers to the power provider company or aggregator to control and manage the EV load through the communication between the vehicle and the power grid [99]. V2H refers to the exchange of power between the EV battery and the home power network [100]. In this case, EV battery can be used as energy storage to provide backup energy for home appliances. V2V is the so-called vehicle-to-vehicle mutual charging technology, which can charge the power battery of another EV through a charging gun.

In general, V2H, V2V, and V2G relate to components such as power supplies, power loads, grid aggregators, transmission systems, communications systems, EVs, and V2G chargers. The concept of V2G will become viable through the bidirectional communications infrastructure by controlling and managing the energy exchange between the power grid and the EV battery. The V2G system consists of intelligent interactive terminals, energy storage bidirectional converters, on/off-grid automatic switching devices, and accessories to enable dynamic interaction between the EVs and the grid. Recently, the popularity of EVs has brought a revolutionary change to the grid. EVs can be considered as distributed energy storage because EVs can charge the grid and discharge power into the public grid through V2G technology [101, 102].

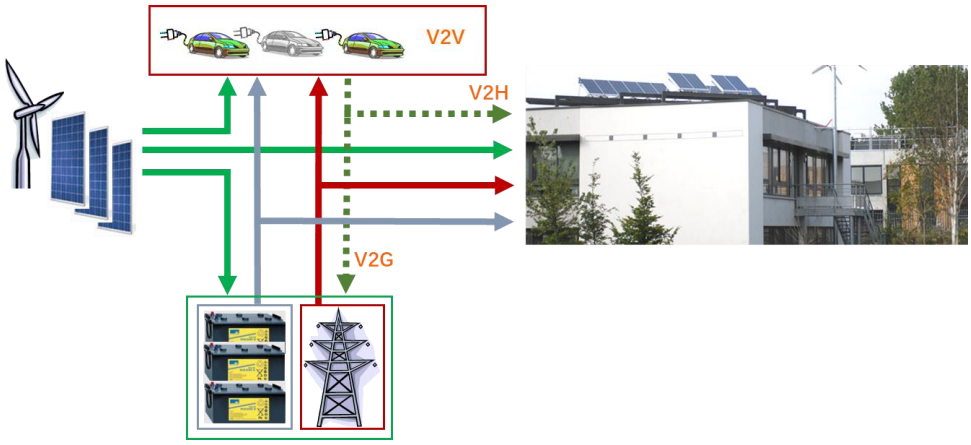

Figure 37. V2G, V2H, and V2V framework.

V2G technology has a bright development prospect brought by the EV integration in the power grid [103], which can bring many services to the power grid and also maximize the renewable energy source integration [104, 105]. The implementation of V2G technology requires the active participation of EV owners. However, EV owners worry about the disadvantages of participating in the V2G program, such as battery degradation. If EV owners are unwilling to participate, this can be a huge social barrier for the implementation of V2G technology. Therefore, we need to find suitable solutions, such as the introduction of V2G energy management strategies and appropriate incentives.

The spread of EVs will increase the grid load during the EV charging process. However, the expected penetration of EVs opens up the possibility for the implementation of V2G [102, 106]. In most cases, the goals of V2G management are to maximize profits, reduce emissions, and improve power quality of the grid.

V.2.2. Major benefits of vehicle to grid

The major benefits of V2G will be further discussed in detail, which includes ancillary services, active power support, reactive power compensation, and support for renewable energy resources.

V.2.2.1 Ancillary services

Unidirectional V2G provides the “load only” ancillary services to the power grid by controlling the EVs charging rates upon request from the power grid operators. Ancillary services can be classified into two categories, power grid regulation, and spinning reserve. The power grid regulation provides frequency regulation to satisfy the generation and load demand. The grid operators usually take direct real-time control to respond to the grid demand by increasing or decreasing the generation. Nevertheless, the power balance can be achieved by utilizing the unidirectional V2G technology to adjust the EV load demand under two operating modes, which are “regulation up” mode and “regulation down” mode. In unidirectional V2G technology, grid-connected EVs are considered as dynamic loads, where the charging rate of the EVs is regulated up and down to meet the preference operating point.With the aim to provide ancillary services, all the optimal unidirectional V2G scheduling shows high profits for the participated aggregators, especially for the proposed fuzzy optimization which is approximately six percent higher than the other optimization techniques.

V.2.2.2 Active power support

Another V2G service utilizes the excessive EVs energy which is more than the normal use of EVs to provide active power support for the power grid. The active power support requires EVs to discharge the batteries' energy. Therefore, it could only be accomplished using bidirectional V2G. The goal of this service is to flatten the grid load profile by “peak load shaving” and “load leveling”. Peak power is usually needed for a short period of time throughout a day. Therefore, it will be more economical to supply the peak load demand from the distributed sources, e.g. the grid-connected EVs. During the peak load period, EVs can be used to supply energy to the power grid to shave off the peak load, which can help to reduce the applied stress on power system components and the EV owners will get higher revenues. During the off-peak hours, EV owners can charge their EV batteries with lower energy prices.

Active power support is an important service of V2G and it can attain the premium benefits. One of the advantages is the loss reduction. The overall power losses will be reduced by maintaining the power system operating capacity at a lower level. Traditionally, power system is constructed to meet the highest peak of the load demand. Thus, the power equipment is under-utilized during the off-peak hour. The implementation of peak load shaving technique by utilizing the V2G technology can maximize the power equipment capacity and prevent additional equipment upgrade costs. In addition, shifting EVs charging time to off-peak hours is a good method to avoid power system overloading and equipment aging.

V.2.2.3 Reactive power compensation

Reactive power compensation is a technique to provide voltage regulation in the power grid. Reactive power support also provides power factor correction, which reduces the current flows from generation and power losses in the power line.

Furthermore, this service can reduce the loading of power equipment, which leads to an increase in power system operating efficiency.

The conventional method for reactive power compensation is achieved by drawing reactive power from a distribution generator or static Volt–Ampere Reactive compensator.

In most cases, a capacitive reactive power is needed for power grid compensation. Therefore, grid-connected EV can provide the reactive power compensation service due to the capacitive reactive power reserved in the DC-link capacitor. Since the reactive power compensation is provided by the DC-link capacitor of the EV bidirectional battery charger, this service will not cause any degradation to the battery lifespan. The reactive power compensation is done by controlling the switching of the AC/DC converter with various control strategies.

V.2.2.4 Support for renewable energy resources

Energy generation and transportation sector are the two major sources of CO_2 emission, which threaten the public health and environment. The deployment of renewable energy generation can protect the environment. However, the power generation of renewable energy sources is strongly dependent on environmental factors. The intermittent and unpredictable are the mains drawbacks of renewable energy resources.

The integration of EVs in the power system could be a solution to the issues above. The intermittency issue of renewable energy resources can be solved by utilizing a fleet of EVs as energy backups or energy storage. The EV fleets act as the energy backups to supply necessary power when the renewable energy generation is insufficient. Meanwhile, they act as energy storage to absorb the excessive power generated by renewable energy resources which would be curtailed. Research has shown that larger renewable energy capacity can be accommodated into the power system with more grid-connected EV battery capacity. Therefore, EV can improve the economics of the renewable energy generation industry. With proper energy management between renewable energy resources and EV, the future power grid will be cleaner and more sustainable.

V.2.3. Challenges of vehicle to grid

V2G implementation will bring plenty of advantages and flexibility to the power grid. Nonetheless, V2G is a new technology that has not matured. Many economical, technical, and social challenges need to be overcome in order to adopt the V2G technology.

V.2.3.1 Battery degradation

Battery cells will deteriorate gradually with the battery charging and discharging cycles. The irreversible chemical reaction in the battery will increase the internal resistance and reduce the battery useable capacity. The battery aging rate depends on many factors, which include the charging and discharging rates, voltage, depth of discharge, and temperature. The participations of EVs in the V2G technology require more battery charging and discharging cycles which are likely to result in quicker battery degradation. V2G control strategy is developed to prevent the abusive use of EV batteries. The balance between the financial factor and the battery technical factor is crucial to optimize the benefits for power utility and EV owners.

V.2.3.2 High investment cost

Another challenge to the V2G implementation is the high investment cost required to upgrade the power system. Improvements in hardware and software infrastructure are needed for the V2G implementation. Each EV that participates in the V2G system will require a bidirectional battery charger. A bidirectional battery charger is hardware that consists of a complex controller and high-tension cabling with tight safety requirements. In addition, V2G has the potential to increase energy loss, which is another unfavorable issue in the power system as it has a direct relationship to economic disadvantage. The V2G implementation requires frequent charge and discharge cycles and these processes involve energy conversions which will contribute to more conversion losses. Multiple energy conversions for a large fleet of EVs charging and discharging processes can denote serious energy losses to the power system.

V.2.3.3 Social barriers

The participation of a large number of EVs is crucial requirements for the V2G implementation. However, the social barrier has prevented the public acceptance of V2G technology, which appears to be a huge challenge for V2G adoption. In most cases, EV owners will ensure a guaranteed amount of energy stored in the EV battery for emergency use and unpredicted journey. Since taking part in the V2G technology requires them to share the EVs batteries energy with the power grid, this will create a range of anxiety among the EV owners. The lack of a charging facility makes the situation becomes worse. In order to reduce the social barriers for V2G implementation, a well-planned EV charging

network is necessary. In addition, V2G management control needs to consider the EV SOC level. V2G connectivity needs to be cut off when the EV SOC is lower than an initially preset percentage. This is to ensure the EV battery has enough energy for daily driving usage.

V.3. DC microgrid structure with integrated V2G

A microgrid based on DC common bus is considered due to its superior better current control because there is no negative and zero sequence currents [32]. The design of EV charging station including V2G is based on DC microgrid. As shown in Figure 38, the DC microgrid is composed of four parts: PV sources, a storage system, a public grid connection, and EVs.

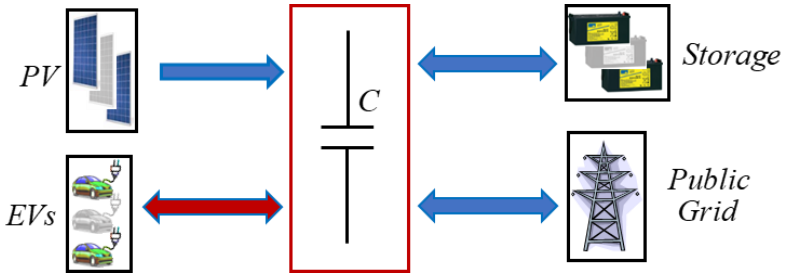

Figure 38. DC microgrid with integrated V2G.

DC microgrid power flow is shown in Figure 39: 'PV' represents PV sources, 'PG' represents the public grid, 'S' represents the storage system, 'EV' represents EVs. The real-time power priority is shown by the arrow. For example, PV sources firstly support EVs, secondly charge storage, then thirdly inject into the public grid.

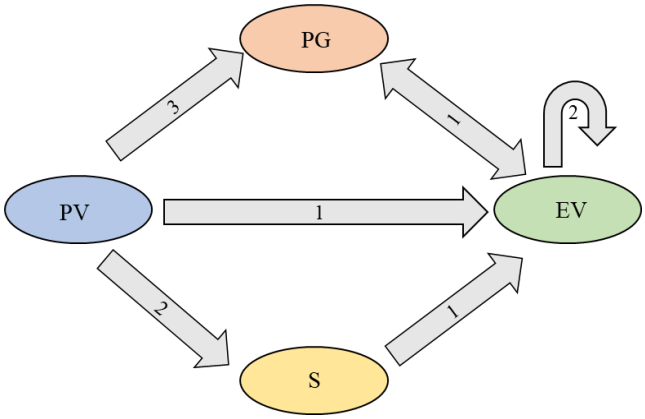

Figure 39. DC microgrid power flow.

According to the "*peak*" periods and "valley" periods of the public grid, the energy flow of the DC microgrid can be divided into two cases. During the "*valley*" periods of the public grid, the electricity produced by PV sources is first used to charge EVs. Storage is the second-ranked energy source for charging EVs; in addition, it is also used to absorb excess energy produced by PV sources. The public

grid is the third-ranked energy source for charging EVs, and it can buy excessive energy from PV sources. During the "peak" periods of the public grid, the order of charging EVs is the same as the "*valley*" periods of the public grid, and the difference is that V2G is achievable during this period. If the energy produced by PV sources is still surplus after supplied to the EVs, in order to adjust the peak-valley difference of the public grid, PV sources can inject excess energy into the public grid. In addition, the energy released by EVs can be injected into the public grid. Considering the energy cost, the order of injecting energy into the public grid is PV sources firstly, then EVs batteries.

During the period of V2G, in order to ensure the power balance of the public grid, the energy injected into the public grid, namely p_{inject_G}, should be limited. It may be assumed that the maximum power injected into the public grid cannot exceed the estimated PV power under STC, namely P_{PV_STC}, which is shown in (5. 1), where p_{PV} is PV power that can be injected into the public grid, p_{EV_total} is the power that EVs can output. c_{PV} is the coefficient of PV power, and c_{EV} is the coefficient of the energy that EVs can release.

$$p_{\text{inject\_G}} = P_{\text{PV\_STC}} = c_{\text{PV}} p_{\text{PV}} + c_{\text{EV}} p_{\text{EV\_total}} \text{ , with } c_{\text{PV}}, c_{\text{EV}} \in [0,1] \quad (5.\ 1)$$

V.4. Power flow management: G2V and V2G algorithm

According to users' wishes and the actual situation of EVs batteries, EVs can be divided into two types, only accept to charge, i.e. G2V, and only accept to discharge, i.e. V2G. The stored energy of the EV battery is E, the maximum energy that EVs can discharge is $E_{discharge}$, and the maximum energy that EVs can be charged is E_{charge}, which can be calculated by (5. 2)and (5. 3), respectively.

$$\begin{cases} E_{charge} = E \cdot (SOC_{EV\_final\_\lim} - SOC_{EV\_in}) & \text{if } SOC_{EV\_in} < SOC_{EV\_final\_\lim} \\ 0 & \text{if } SOC_{EV\_in} = SOC_{EV\_final\_\lim} \end{cases} \quad (5.\ 2)$$

$$\begin{cases} E_{discharge} = E \cdot (SOC_{EV\_in} - SOC_{EV\_final\_\lim}) & \text{if } SOC_{EV\_in} > SOC_{EV\_final\_\lim} \\ 0 & \text{if } SOC_{EV\_in} = SOC_{EV\_final\_\lim} \end{cases} \quad (5.\ 3)$$

This section presents two algorithms for power flow management of G2V and V2G, which are demonstrated within an EV charging station to simultaneously support multiple EVs.

V.4.1. Immediate charge/discharge algorithm (ICDA)

ICDA means that after the EV is successfully connected to the charger, as long as the EV operating power is within the EV power limit, the EV can be charged/discharged immediately, without considering other restrictions. The flow chart of ICDA is shown in Figure 40.

When a new EV arrives, if there is a free charger, the charger is directly allocated to the EV. By comparing the EV operating power with the power limit of the EV charging station, it is determined whether the EV enters the waiting state or can be directly charged/discharge until $SOC_{EV\_final\_\lim}$ is reached, and finally, the EV leaves the EV charging station at the time set by the user. The EV power limit is calculated according to the state of the EV charging station. If there are no free chargers when the EV arrives, the EV can choose to leave directly or wait until a free charger appears.

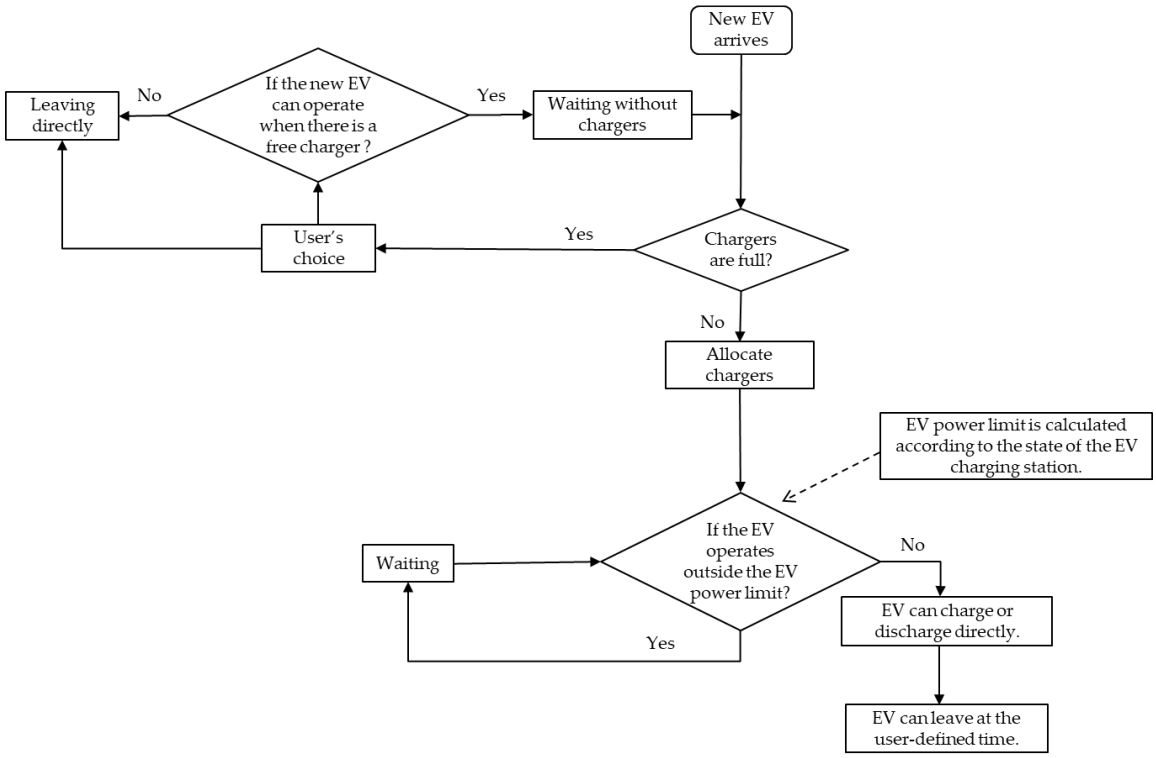

Figure 40. Flow chart of ICDA.

V.4.2. Dynamic searching peak and valley algorithm (SPVA)

The method to estimate the optimal start operating time is shown in Figure 41. As shown in Figure 41, the EV estimator is the related function of EV information and grid power information. The purpose of SPVA is to estimate the optimal start operating time of EVs by searching the "*peak*" periods and "*valley*" periods of the public grid.

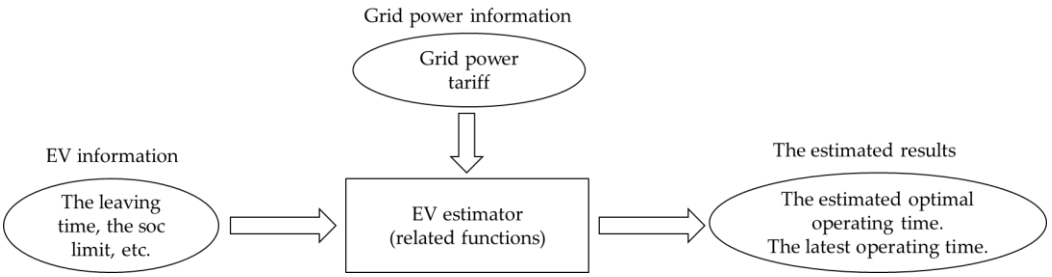

Figure 41. Method to estimate the optimal start operating time.

The flow chart of SPVA is shown in Figure 42. When a new EV arrives, the EV estimator calculates the optimal operating time of EVs. After the EV is connected to the charger, the EV remains to wait until the optimal operation time appears.

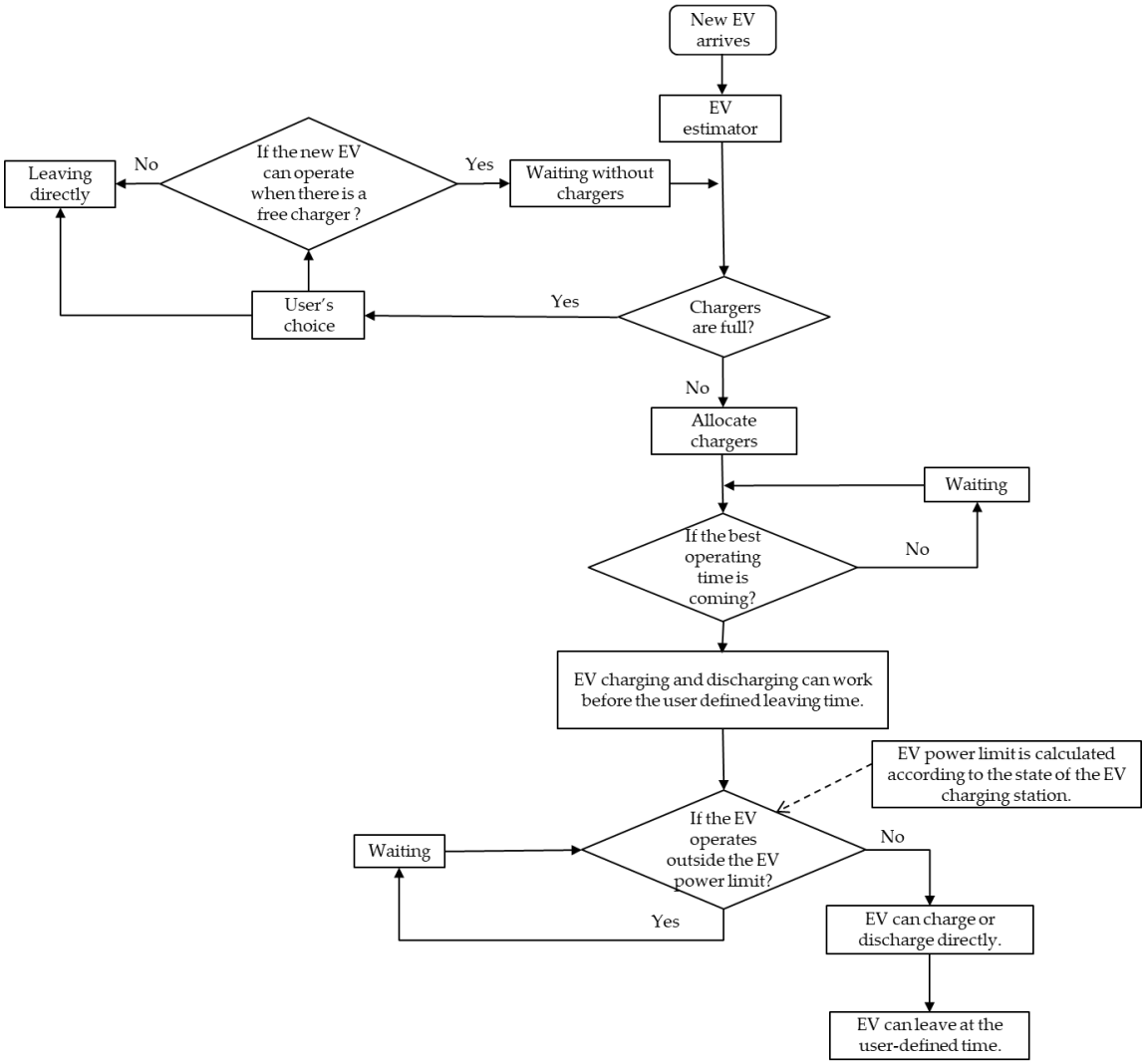

Figure 42. Flow chart of SPVA.

V.5. Simulation results and analyses

In the DC microgrid system, PV sources include 400 PV panels (40 in parallel and 10 in series), and its power under standard conditions is 100kW [97]. The storage voltage and capacity are 300V and 300Ah, respectively. The public grid is a low-voltage three-phase network with a frequency of 50 Hz. The charging method of lithium-ion batteries in EVs is CC/CV, while the discharge is constant power. The battery energy of EV is about 24kWh, namely J_{EV_ERF}. There are three charging modes in the charging station: fast mode whose maximal charging power is 83kW, namely P_{FAST_MAX}; average mode whose maximal charging power is 27kW, namely P_{AVER_MAX}; and slow mode whose maximal charging power is 7kW, namely P_{SLOW_MAX}.

V.5.1. Simulation conditions and assumptions

In order to ensure the validity of the simulation, it is assumed that all EVs have the same battery characteristics. We can configure different battery characteristics, such as capacity, according to the EV model [107], which will be mentioned in future research. Figure 43 shows the real solar irradiance and PV cell temperature from 8:00 to 22:00 on May 28, 2019, at Compiegne, France.

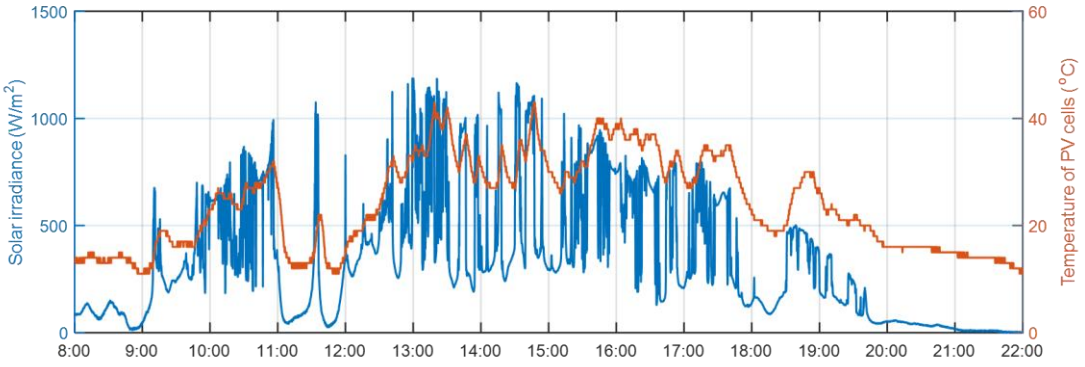

Figure 43. Solar irradiance and PV cell temperature.

Figure 44 shows the tariff of the public grid from 8:00 to 22:00. It exists two grid "*peak*" periods 11:00-13:00 and 18:00-20:00, and the tariff is fixed during the two time-periods. The closer the time point to these two time-periods, the higher the tariff to absorb power from the public grid.

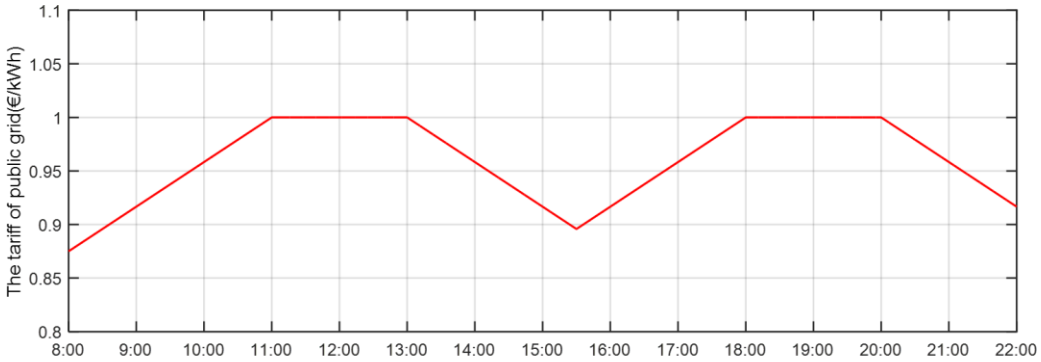

Figure 44. Energy tariff of the public grid.

The simulation parameters of the system are detailed in Table 13 [97], where P_{DIS} is the constant discharge power, which was chosen 89.6kW, I_{S_MAX} is the storage current limitation, SOC_{MIN} and SOC_{MAX} are the *soc* lower limit and the *soc* upper limit, respectively, C_{ERF} is the capacity of the storage, and v_{C_REF} is the rated voltage of DC bus.

Table 13. Simulation parameters of the system.

Parameter	**Value**	**Parameter**	**Value**
P_{FAST_MAX}	83kW	I_{S_MAX}	115A
P_{AVER_MAX}	27kW	SOC_{MIN}	20%
P_{SLOW_MAX}	7kW	SOC_{MAX}	80%
P_{DIS}	89.6kW	C_{ERF}	300Ah
Number of chargers	5	v_{C_REF}	400V
J_{EV_ERF}	24kWh	P_{PV_STC}	100kW

The power limits of the point of common coupling of the EV charging station with the public grid are shown in Table 14. Since loads of the public grid are different according to different periods, the power limits are set accordingly to ensure the stability of the public grid. There are two types of power limits: grid injection power limit and grid supply power limit. In the "*peak*" periods of the public grid, the injection power limit is 100kW, the supply power limit is -10kW, and in other periods, the injection power limit is 50kW, and the supply power limit is -50kW.

Table 14. Power limits of the public grid.

Period	**8:00-11:00**	**11:00-13:00**	**13:00-18:00**	**18:00-20:00**	**20:00-22:00**
Grid injection power limit (kW)	50	100	50	100	50
Grid supply power limit (kW)	-50	-10	-50	-10	-50

The simulation parameters of EVs are shown in Table 15. The three charging modes for EVs, i.e. fast mode, average mode, and slow mode, are considered. When a new EV arrives, the user can choose waiting or departure if there is no free charger. 'CH' represents 'charge', 'DCH' represents 'discharge', 'F' represents 'fast mode', 'A' represents 'average mode', 'S' represents 'slow mode', 'W' represents 'waiting', and 'D' represents 'departure'. $Ordinal_{EV}$ represents the ordinal number of EVs.

Table 15. Simulation parameters of EVs.

$Ordinal_{EV}$	**1st**	**2nd**	**3rd**	**4th**	**5th**	**6th**	**7th**	**8th**
$T_{arrive}(100s)$	17	20	87	198	213	331	336	343
$T_{depart}(100s)$	42	75	204	311	222	388	405	400
$SOC_{EV\_in}(\%)$	66	87	47	21	49	37	12	44
$SOC_{EV\_final\_\lim}(\%)$	11	97	1	78	82	87	9	40
Type	DCH	CH(F)	DCH	CH(S)	CH(A)	CH(A)	DCH	DCH
Choice	W	W	W	D	D	W	D	W

Table 15. Simulation parameters of EVs. (Continue)

$Ordinal_{EV}$	**9th**	**10th**	**11th**	**12th**	**13th**	**14th**	**15th**	**16th**
$T_{arrive}(100s)$	356	375	382	398	428	462	471	484
$T_{depart}(100s)$	449	464	423	460	431	601	495	499
$SOC_{EV\_in}(\%)$	48	38	41	40	26	37	17	66
$SOC_{EV\_final\_\lim}(\%)$	26	81	44	92	19	27	65	80
Type	DCH	CH(S)	CH(A)	CH(A)	DCH	DCH	CH(S)	CH(F)
Choice	W	W	D	D	W	W	W	D

In this case, in order to reflect the effectiveness of the algorithm, the EV number is randomly given 16, and 'Type' and 'Choice' are randomly generated by an algorithm. T_{arrive} represents the time each EV arrives at the charging station. T_{depart} represents the time each EV leaves the charging station. SOC_{EV_in} represents the initial soc_{EV}, $SOC_{EV\_final\_\lim}$ represents the limit value of soc_{EV} when the EV departures that set by users. According to the willingness of users, EVs come to charging stations for two purposes: being charged and discharging.

V.5.2. Simulation results under ICDA

The first simulation case works under ICDA and the EV can directly be charged/discharge within the EV power limit. As shown in Figure 45, the steady DC bus voltage is 400V within the simulation period, which proves that the power management strategy works well to balance the powers under ICDA.

Figure 46 shows the storage *soc* and distribution coefficient k under ICDA. The *soc* of storage is limited between 20% and 80% to extend storage life [108]. $k=1$ means only the storage is working and $k=0$ means only the public grid is working. $0<k<1$ means the storage and the public grid are working simultaneously.

Storage current evolution under ICDA is shown in Figure 47. The storage current is between -115A and 115A to reduce the damage of the storage. The value -115A is the maximum discharge current of batteries, while the value 115A is the maximum current for batteries to be charged. The simulation result shows that the current is successfully limited.

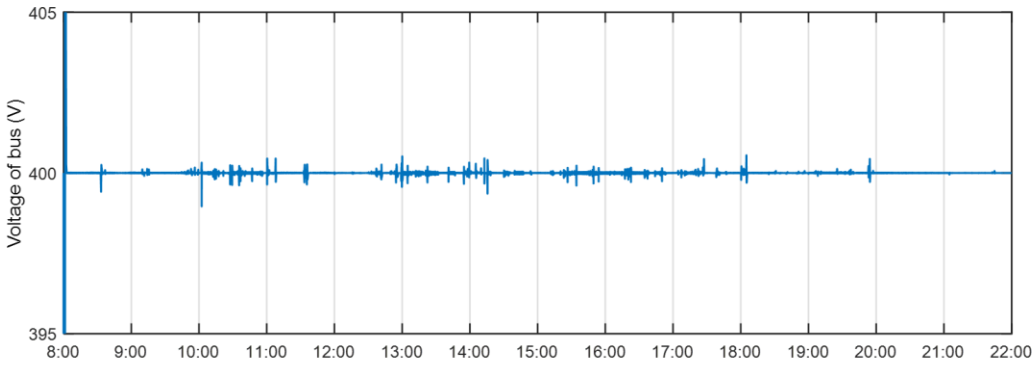

Figure 45. DC bus voltage evolution under ICDA.

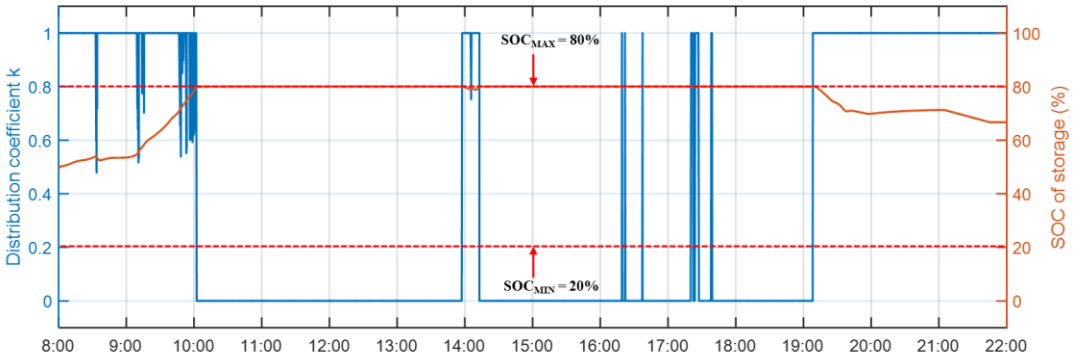

Figure 46. Storage *soc* and distribution coefficient K under ICDA.

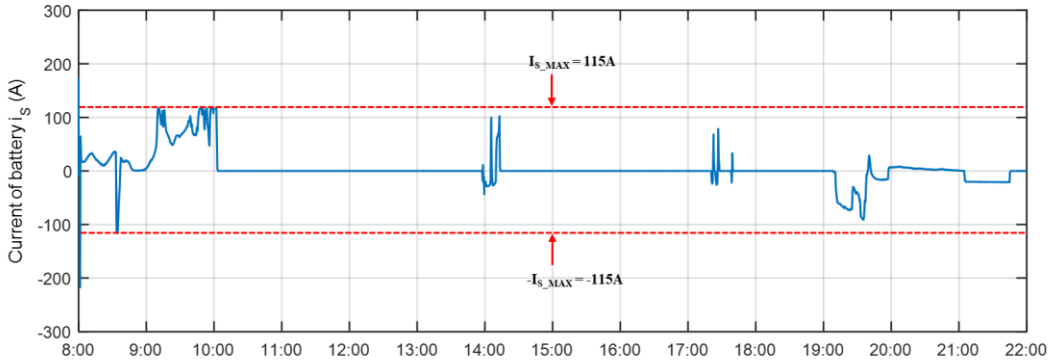

Figure 47. Storage current evolution under ICDA.

The power flow of DC microgrid under ICDA is shown in Figure 48. PV source can switch freely between PV-constrained production control and PV-MPPT control [109]. The power $p_{EVs} < 0$ means that EVs show a total tendency to discharge, $p_{EVs} > 0$ means that EVs show a total tendency to be charged. During the "*peak*" periods of the public grid: 11:00-13:00 and 18:00-20:00, the injection power limit is 100kW, and the supply power limit is -10kW to prevent the public grid from overloading. During the *"valley"* periods of the public grid, the injection power limit is 50kW, and the supply power limit is -50W. Setting different power limits according to the "peak" periods and *"valley"* periods of the public grid is beneficial to improve the stability of the public grid, which also respects the power flow given in Figure 39.

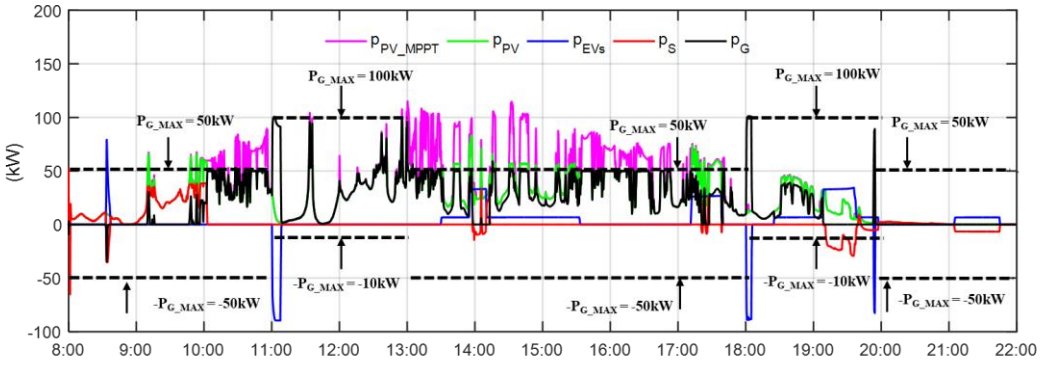

Figure 48. Power flow of DC microgrid under ICDA.

Figure 49 shows the parking periods of EVs. The parking periods of EVs are different according to the willingness of users. From EV_charger_1 to EV_charger_5 represent EVs connected to chargers 1 to 5, respectively, e.g. EV_charger_1 represents the ordinal number and parking periods of the EVs connected to the charger 1.

The power evolutions of EVs under ICDA are shown in Figure 50. If the power is positive, it means that the EV is being charged; if it is negative, it means that the EV discharges. Figure 51 shows the soc_{EV} evolutions under ICDA.

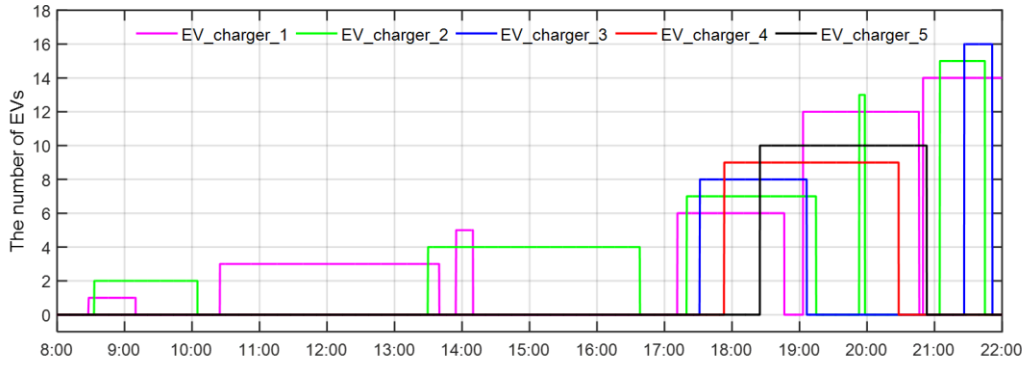

Figure 49. Parking periods of EVs at each charger.

Figure 50. Power evolutions under ICDA.

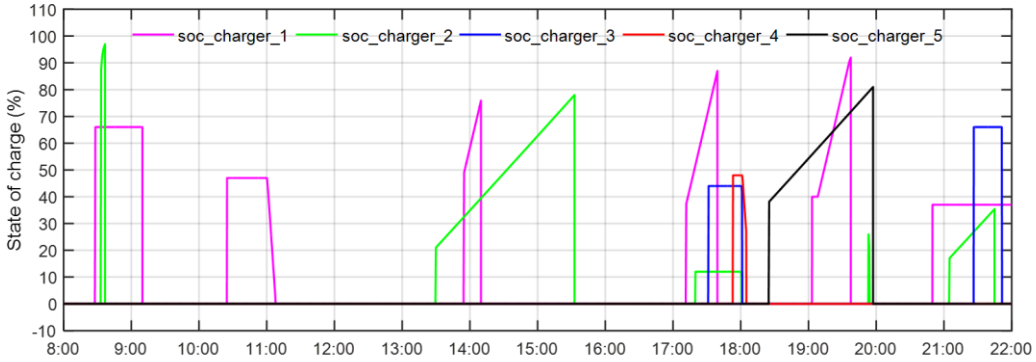

Figure 51. State of charge soc_{EV} evolutions under ICDA.

The operating time of EVs connected to charger 1 is shown in Figure 52. $t_{EV\_charger\_1}$ represents parking periods of EVs connected to charger 1. $t_{EV\_operate}$ represents the start operating time of EVs. t_{EV_arrive} represents the arrival time of EVs. t_{EV_depart} represents the departure time of EVs.

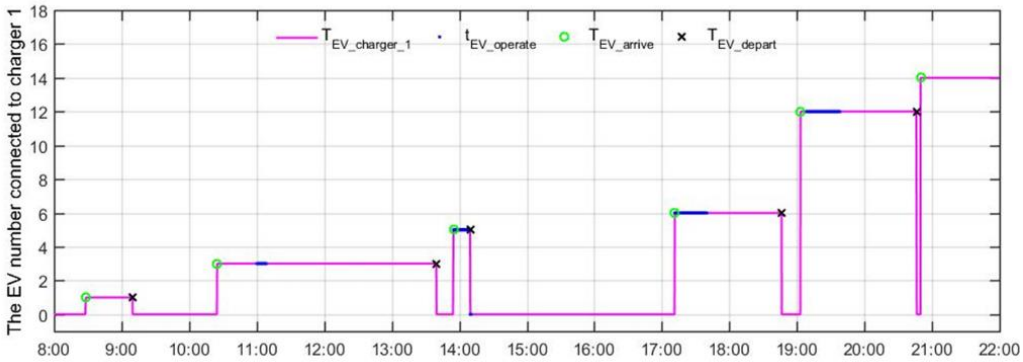

Figure 52. Operating time of EVs connected to charger 1 under ICDA.

As shown in Figure 52, EVs connected to charger 1 in chronological order are 1st, 3rd, 5th ,6th ,12th ,14th. After an EV arrives at the charging station, when the power is met, the charging/discharging operation begins. EVs that immediately start charging/discharging operations after arriving at the charging station are 5th, 6th, 12th, while the 3rd EV enters the waiting state after arriving at the charging station, then discharges when power is met. Moreover, the 1st and 14th did not discharge until they left because of unsatisfactory power.

The operating time of EVs connected to charger 2 is shown in Figure 53. As shown in Figure 53, EVs connected to charger 2 in chronological order are 2nd, 4th, 7th, 13th, 15th. EVs that immediately start charging/discharging operations after arriving at the charging station are the 2nd, the 4th, the 13th, the 15th EVs, while the 7th EV enters the waiting state after arriving at the charging station, then discharges when power is met.

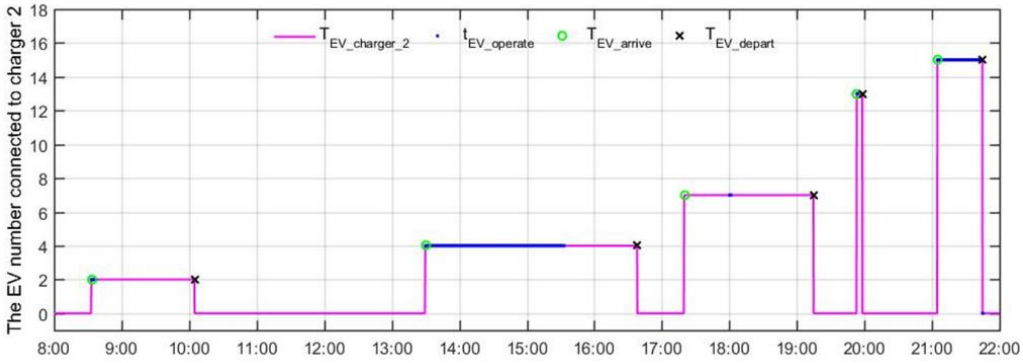

Figure 53. The operating time of EVs connected to charger 2 under ICDA.

The operating time of EVs connected to charger 3 is shown in Figure 54. As shown in Figure 54, EVs connected to charger 3 in chronological order are the 8th and the 16th EVs. The 8th EV enters the waiting state after arriving at the charging station, then discharges when power is met, while the 16th EV did not charge until it left because of unsatisfactory power.

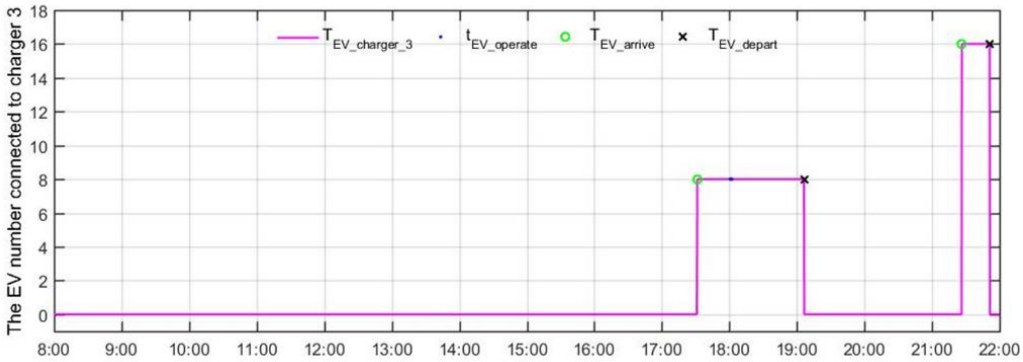

Figure 54. The operating time of EVs connected to charger 3 under ICDA.

The operating time of EVs connected to charger 4 is shown in Figure 55. As shown in Figure 55, the EV connected to charger 4 is the 9th EV. The 9th EV enters the waiting state after arriving at the charging station, then discharges when power is met.

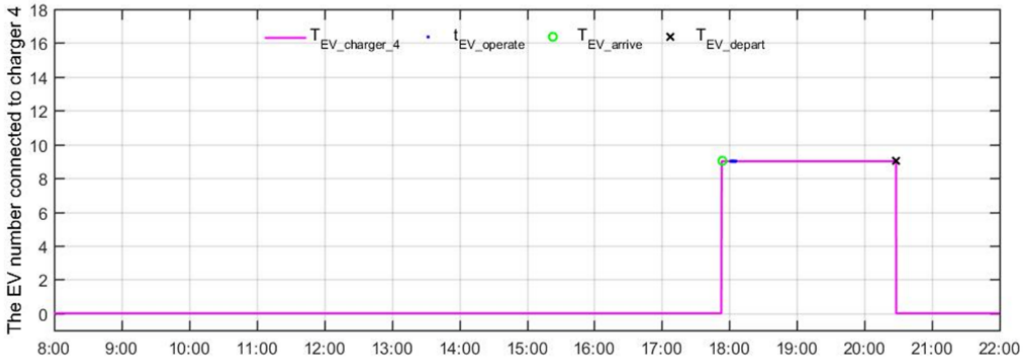

Figure 55. The operating time of EVs connected to charger 4 under ICDA.

The operating time of EVs connected to charger 5 is shown in Figure 56. EV connected to charger 5 is the 10th EV, which immediately starts charging/discharging operations after arriving at the charging station.

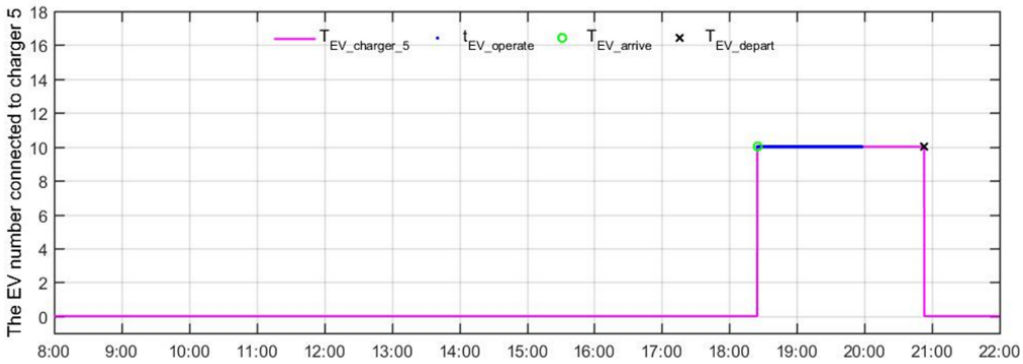

Figure 56. The operating time of EVs connected to charger 5 under ICDA.

The recording of EV charging under ICDA is shown in Figure 57. The ratings arrive_N1, park_N2, finish_N3, not_finish_N4, and depart_N5 are respectively the number of EVs arrived at the charging station, the number of EVs parking at the charging station, the number of EVs that have completed operations, the number that has not completed operations, and the number of EVs leaving directly. The rating *arrive_N*1 is expressed by (5. 4):

$$arrive\_N1 = park\_N2 + finish\_N3 + not\_finish\_N4 + depart\_N5 \quad (5.\ 4)$$

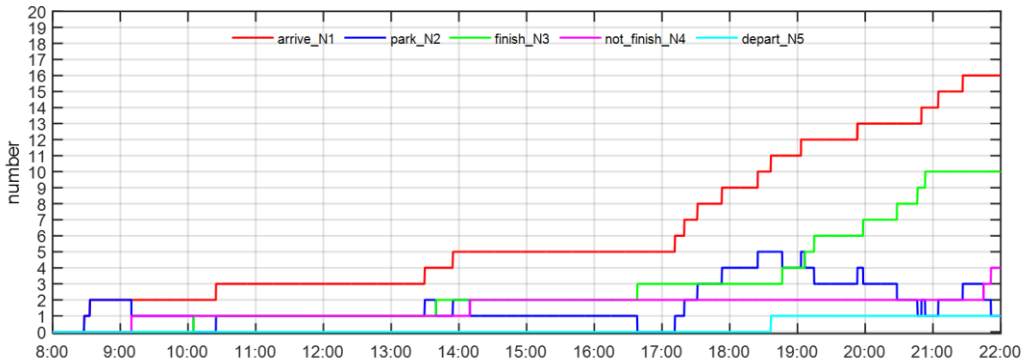

Figure 57. Recording of EV charging under ICDA.

V.5.3. Simulation results under SPVA

The second simulation works under SPVA and the EV cannot be charged/discharged until the estimated optimal start operating time of EVs is given by searching the *"peak"* periods and *"valley"* periods of the public grid; $t_{EV\_best\_st}$ represents the optimal start operating time, and $t_{EV\_latest\_st}$ represents the estimated latest operating time.

As shown in Figure 58, the steady DC bus voltage is 400V within the simulation period, which proves that the power management strategy works well to balance the powers under SPVA.

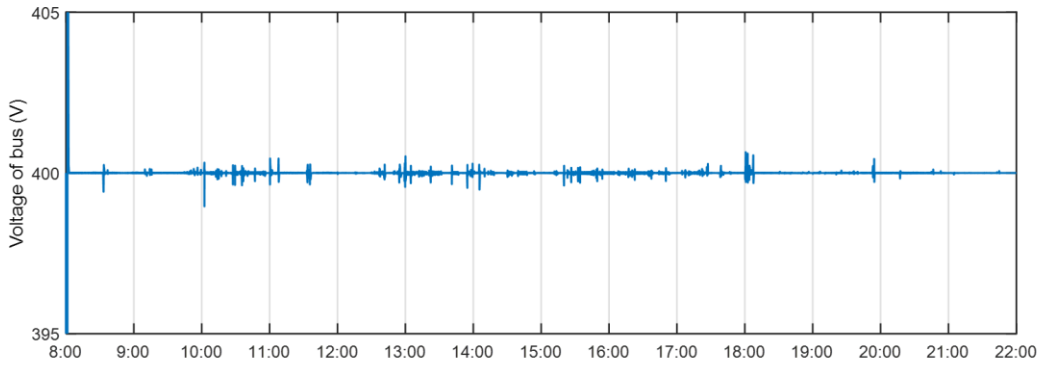

Figure 58. DC bus voltage evolution under SPVA.

Figure 59 shows the storage *soc* and distribution coefficient *k* under SPVA. The evolutions of the state of charge *soc* and distribution coefficient *k* show the feasibility of SPVA and respect the power flow given in Figure 39.

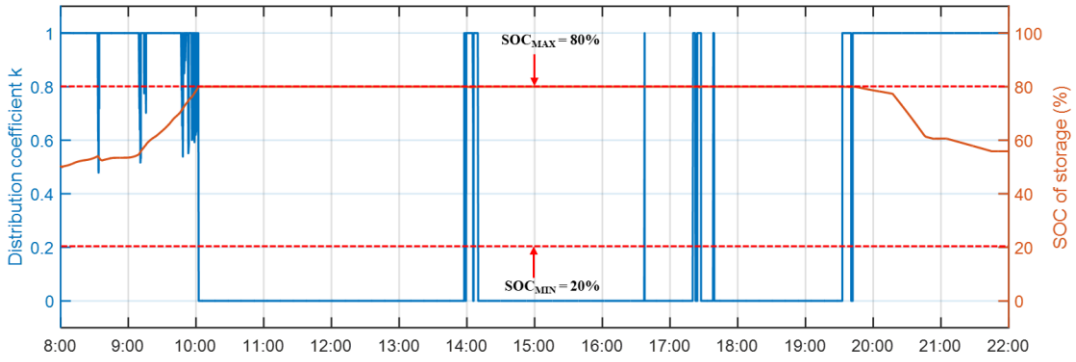

Figure 59. Storage *soc* and distribution coefficient *k* under SPVA.

Storage current evolution under SPVA is shown in Figure 60. As already mentioned, the absolute value of the storage current is limited to 115A, and the simulation result shows that the current is successfully limited.

The power flow of DC microgrid under SPVA is shown in Figure 61. The grid power is within the imposed power limits during the simulation period, respecting the power flow given in Figure 39. Setting different power limits of the public grid in the *"valley"* period and the "*peak*" period provides a guarantee for the stability of the public grid.

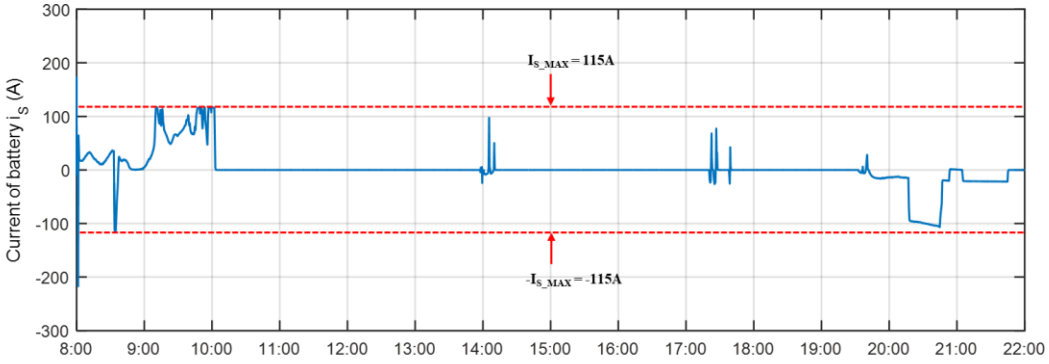

Figure 60. Storage current evolution under SPVA.

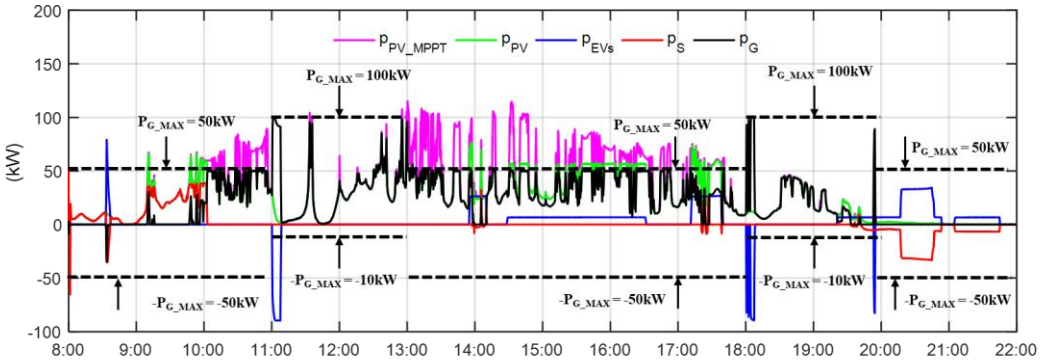

Figure 61. Power flow of DC microgrid under SPVA.

Figure 62 shows the parking periods of EVs. In order to compare the two algorithms, all the information about EVs in case 1 and case 2 are the same.

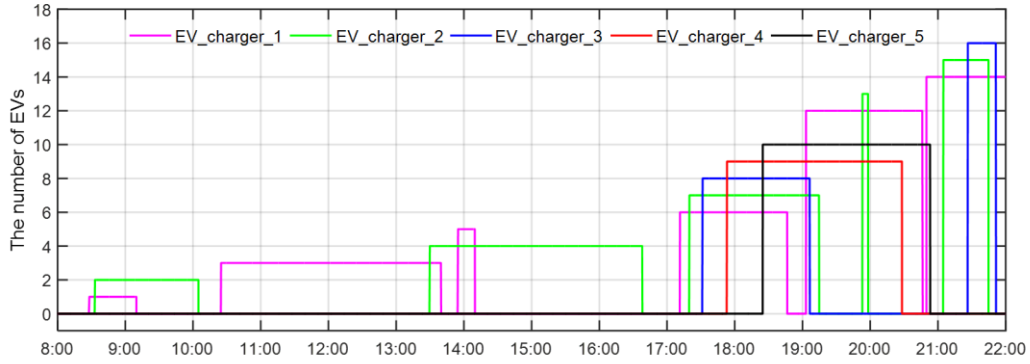

Figure 62. Parking periods of EVs at each charger.

The theoretical optimal start operating time and latest start operating time of EVs are shown in Table 16, which can be calculated by the EV charging station based on T_{arrive}, T_{depart}, SOC_{EV_in}, $SOC_{EV\_final\_\lim}$, charging modes, and discharge power.

Table 16. Theoretical optimal start operating time and latest start operating time of EVs.

$Ordinal_{EV}$	**1st**	**2nd**	**3rd**	**4th**	**5th**	**6th**	**7th**	**8th**
$t_{EV\_best\_st}(100s)$	36.69	20.00	108.00	233.15	213.00	331.00	360.01	360.01
$t_{EV\_latest\_st}(100s)$	36.70	72.83	199.56	237.28	213.00	371.33	404.71	399.61

Table 16. Theoretical optimal start operating time and latest start operating time of EVs. (Continue)

$Ordinal_{EV}$	**9th**	**10th**	**11th**	**12th**	**13th**	**14th**	**15th**	**16th**
$t_{EV\_best\_st}(100s)$	360.01	408.56	382.00	442.40	428.00	462.00	471.00	497.42
$t_{EV\_latest\_st}(100s)$	446.88	408.56	421.99	442.41	430.33	600.04	471.00	497.43

The power evolutions under SPVA are shown in Figure 63. Compared with Figure 13, the 4th and the10th EVs are farther away from the "*peak*" periods of the public grid, while the 12th EV directly avoids the "*peak*" periods of the public grid, thereby preventing the public grid from overloading, meanwhile reducing charging costs, which proves the effectiveness and superiority of SPVA. Figure 64 shows the soc_{EV} evolutions under SPVA.

The operating time of EVs connected to charger 1 is shown in Figure 65. Compared with Figure 52, due to SPVA, the 12th EV did not choose to be charged immediately after arrival but waited for the optimal start operating time, which saved the user's charging costs and avoided adding peak loads to the public grid.

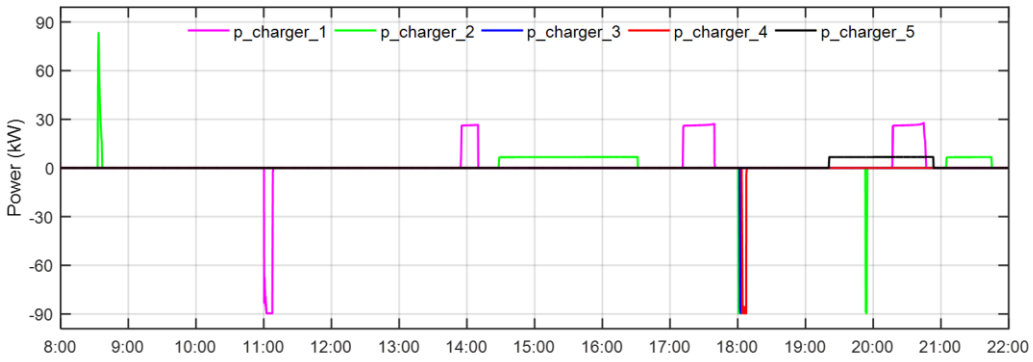

Figure 63. Power evolutions under SPVA.

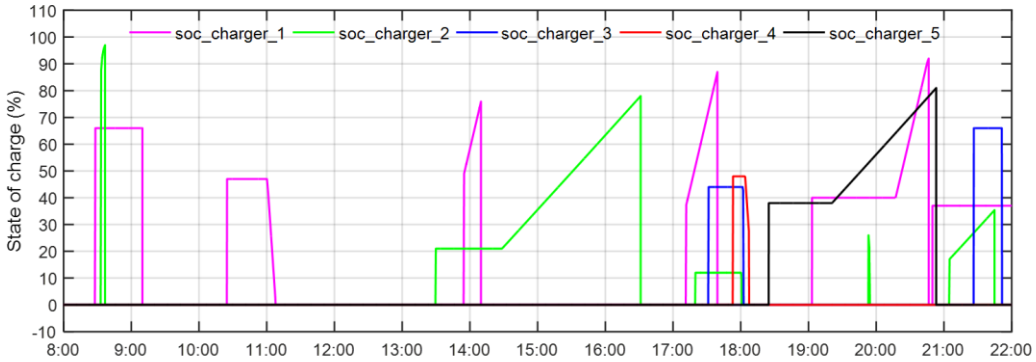

Figure 64. State of charge soc_{EV} evolutions under SPVA.

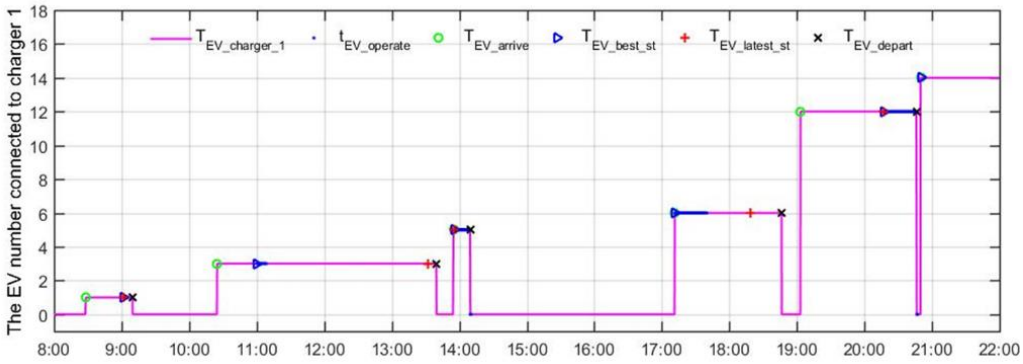

Figure 65. Operating time of EVs connected to charger 1 under SPVA.

The operating time of EVs connected to charger 2 is shown in Figure 66. Compared with Figure 53, due to SPVA, the 4th EV did not choose to be charged immediately after arrival but waited for the optimal start operating time.

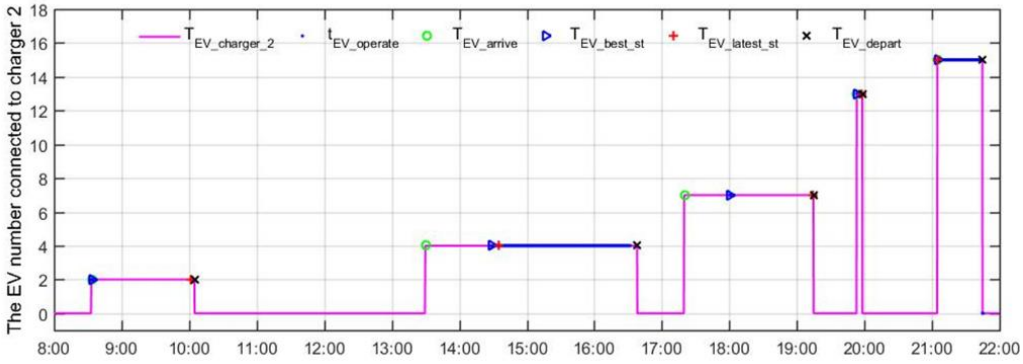

Figure 66. Operating time of EVs connected to charger 2 under SPVA.

The operating time of EVs connected to charger 3 is shown in Figure 67, and the 8th and the 16th EVs have the same operation results as Figure 54.

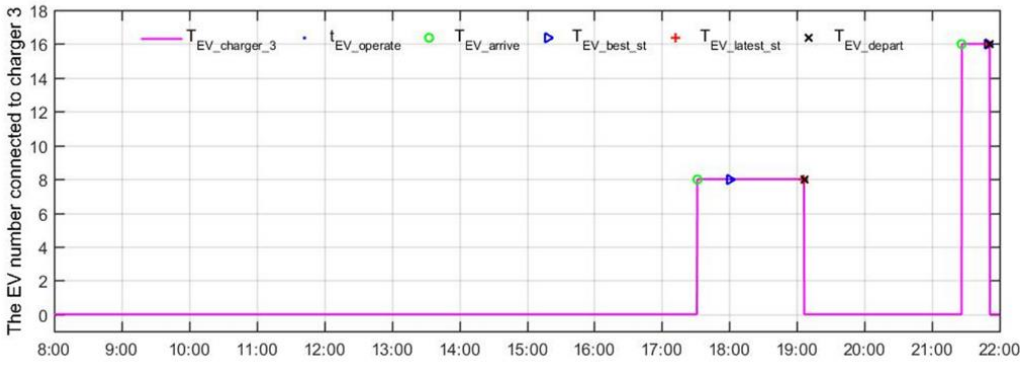

Figure 67. Operating time of EVs connected to charger 3 under SPVA.

The operating time of EVs connected to charger 4 is shown in Figure 68. The operating time of EVs connected to charger 5 is shown in Figure 69 and the 9th EV has the same operation result as Figure 56. Compared with Figure 56, due to SPVA, the 10th EV did not choose to be charged immediately after arrival but waited for the optimal start operating time.

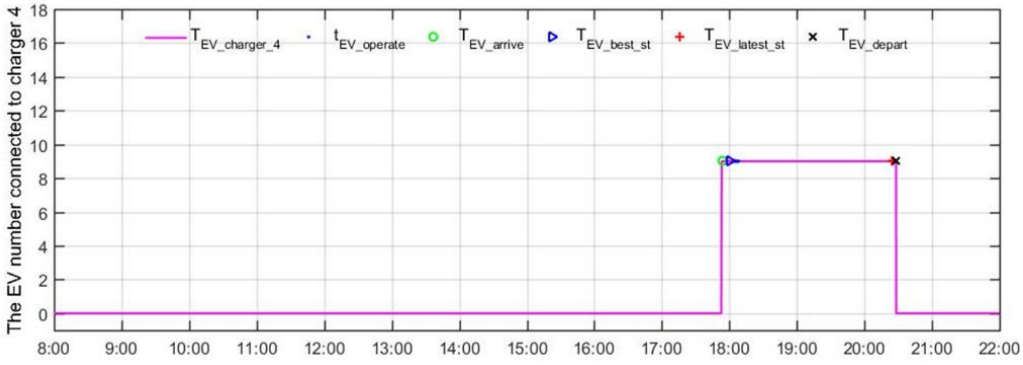

Figure 68. Operating time of EVs connected to charger 4 under SPVA.

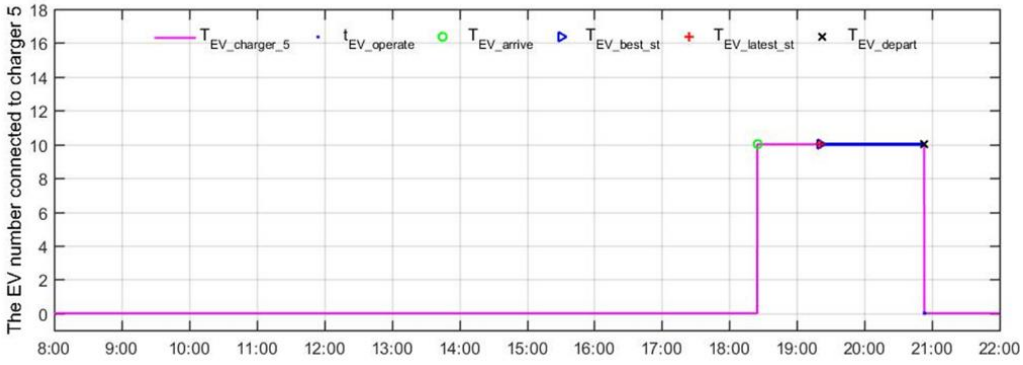

Figure 69. Operating time of EVs connected to charger 5 under SPVA.

The recording of EV charging under SPVA is shown in Figure 70, which respects (5. 4).

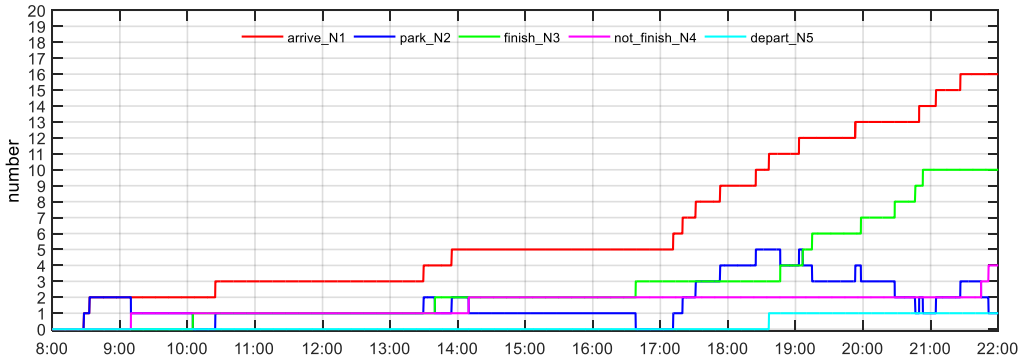

Figure 70. Recording of EV charging under SPVA.

V.5.4. Comparison and analyses of the two simulation cases

The simulation results of ICDA and SPVA are shown in Table 17, where D_{cp} represents the completion degree of EVs, calculated by (5. 5):

$$D_{cp} = \left| \frac{soc_{EV\_final} - SOC_{EV\_in}}{SOC_{EV\_final\_lim} - SOC_{EV\_in}} \right| * 100\% \qquad (5.\ 5)$$

The parameter soc_{EV_final} represents the soc_{EV} when EVs leave the charging station. $D_{cp}(1)$ and $D_{cp}(2)$ are the completion degree of EVs under ICDA and SPVA, respectively.

Under the two algorithms, the completion degree of EVs is the same under ICDA and SPVA, as shown in Table 18.

Table 17. Simulation results of ICDA and SPVA

$Ordinal_{EV}$	**1st**	**2nd**	**3rd**	**4th**	**5th**	**6th**	**7th**	**8th**
$Type\ (1)$	DCH	CH	DCH	CH	CH	CH	DCH	DCH
$D_{cp}(1)$	0%	100%	100%	100%	81.65%	100%	100%	100%
$Type\ (2)$	DCH	CH	DCH	CH	CH	CH	DCH	DCH
$D_{cp}(2)$	0%	100%	100%	100%	81.65%	100%	100%	100%

Table 17. Simulation results of ICDA and SPVA. (Continue)

$Ordinal_{EV}$	**9th**	**10th**	**11th**	**12th**	**13th**	**14th**	**15th**	**16th**
$Type\ (1)$	DCH	CH	CH	CH	DCH	DCH	CH	CH
$D_{cp}(1)$	100%	100%	0%	100%	100%	0%	38.33%	0%
$Type\ (2)$	DCH	CH	CH	CH	DCH	DCH	CH	CH
$D_{cp}(2)$	100%	100%	0%	100%	100%	0%	38.33%	0%

One note that there are 11 EVs with a completion degree of 100%, the 1st, the 11th, the 14th, and the 16th EV with a completion degree of 0%, among which, the 11th EV directly left after arriving at the charging station because the charging station could not meet the user need. The 5th EV with a completion degree of 81.65%, and the 15th EV with a completion degree of 38.33%.

Table 18. Results comparison of ICDA and SPVA.

Algorithms	**ICDA**	**SPVA**
EV number	16	16
Number of finishing CH or DCH	11	11
Energy cost of public grid power $(c€)$	-280.4216	-294.1568

The comparison between the two algorithms highlights that the energy cost of the public grid under ICDA is higher than that under SPVA. Thus, the power management strategy can run well under SPVA, ease the pressure on the public grid at the "*peak*" periods, and reduce the energy cost of the public grid.

V.6. Conclusions

The object of this chapter is to propose a power management strategy with integrated V2G to reduce the peak pressure of the public grid while meeting the needs of users, and then to verify it. Firstly, the concept, major benefits, and challenges of V2G are described, and then DC microgrid structure with integrated V2G is proposed, which provides a basis for power flow management of G2V and V2G algorithm. The SPVA is proposed to judge the optimal charging/discharging start time of EVs, through its arrival time, departure time, soc_{EV_in}, and $soc_{EV\_final\_\lim}$, to achieve peak shaving and valley filling while reducing the cost of the public grid. In addition, in order to better maintain the stability of the public grid, the "*peak*" periods and *"valley"* periods of the public grid correspond to different power limits. Simulation results show that the charging station based on a DC microgrid can well operate considering the EV charging/discharging behaviours; the proposed SPVA is highly effective in reducing the cost of the public grid by calculated the optimal start operating time of EVs, meanwhile ensuring the stability of the public grid.

General conclusion and perspectives

The energy crisis accelerates the transformation of traditional energy sources based on fossil energy to clean and low-carbon modern energy. Distributed energy which is more efficient and environmentally friendly than traditional energy will play a key role in the power system. Distributed energy is a small power system that integrates smart grid, energy storage, and other technologies with small power generation technology as the core. Distributed energy has both economic and ecological benefits, can meet users' multiple energy needs, and can optimize supply and demand integration of resource allocation.

This thesis firstly studied a real-time power management strategy for an EV charging station. The EV charging system topology is presented and common problems during an EV charging process are discussed. The proposed power management deals with the uncertainties of EV users' behaviour considering its arbitrary and random choices through the human-machine interface. The simulation results obtained under MATLAB/Simulink verify the feasibility of the proposed management strategy that presents a good performance in terms of precise control. Then, SROA for an EV charging station based on a DC microgrid is presented to maximize the utilization of available power to meet user needs, meanwhile, taking into consideration the intermittency of the PV source, the capacity limitation of the storage, and the power limitation of the public grid. Simulation results show that compared with RBA, the proposed SROA respect the user's choice while reducing total charging time, increasing the full rate, and maximizing the available power utilization, which shows the feasibility and effectiveness of SROA. Finally, this thesis proposes a suitable power management strategy for the EV charging station with integrated V2G. A dynamic SPVA, based on energy management, is proposed for an EV charging station to mitigate the impact on the public grid, while reducing the energy cost of the public grid. The proposed SPVA can determine the optimal charging/discharging start time of EV in consideration of all of the initial state of charge SOC_{EV_in}, charging modes, arrival time, departure time, and the peak periods. Simulation results demonstrate the proposed SPVA effectiveness, which can guarantee the balance of the public grid, meanwhile satisfy the charging demand of EV users, and most importantly, reduce the public grid energy cost.

After concluding the main research work of this thesis, the originality and main scientific contributions of this thesis conclude as given below.

Firstly, a microgrid-based EV charging station topology is proposed. The microgrid is composed of PV sources, an electrochemical storage system, a public grid connection, chargers associated with their parking spots, and a DC common bus. The PV system can operate in MPPT mode and power-constrained mode. The public grid can operate under its power constraints obtained from the public grid operator in real-time. The storage system operates under its power and capacity constraints to protect the over-

charging and, over-discharging for long-life support. The five chargers in five parking spots are designed to respect the real small charging station.

Secondly, in order to ensure the stability of EV charging stations and meet users' satisfaction, a real-time power management strategy for an EV charging station and a real-time interface is investigated. The management strategy fully considers the randomness and unpredictability of users' choices based on power availability. Meanwhile, the real-time power management strategy considers the constraints of the physical components of the microgrid. The real-time interface can deal with microgrid's sources and interact with users. When an EV arrives, the user can set his/her choice through the interface according to the microgrid's current condition. This management strategy deals with the uncertainties of EV users' behaviours. The arrival time of EVs and the initial SOC_{EV} are randomly and non-schedulable to emulate the real condition of EV arrival. An EV charging algorithm is presented to deal with the uncertainties of EV user behaviours. Users may choose three charging modes: fast mode, average mode, and slow mode. In addition, it is also considered that the user can disconnect the EV from the charger at any time.

Thirdly, RBA and SROA algorithms are proposed for EV shedding and restoration. Compared with RBA, SROA respects the user's choice while reducing total charging time, increasing the full rate, and maximizing the available power utilization, which provides an effective technical means for the stable operation of an EV charging station based on the microgrid. In addition, the SROA has certain reference significance for reducing the impact of EV charging on the peak load of the public grid.

Fourthly, an EV charging station model combined with V2G based on a DC microgrid is proposed. This model makes use of EV's "*load-source*" character to bring benefits to users while meeting user needs.

Fifthly, a suitable power management strategy for the EV charging station with integrated V2G is proposed. In the strategy, the priority order for charging EVs is PV sources, the storage system, the public grid. During the "*peak*" periods of the public grid, the DC microgrid discharges to the public grid, and the discharge priority order is PV sources and then the EVs considering the discharge cost. The SPVA is proposed to calculate the optimal charging/discharging start time of EVs to achieve the effect of peak shaving and valley filling, while meeting the charging requirements of EVs, taking into account the EV arrival time, departure time, soc_{EV_in}, and $soc_{EV\_final\_\lim}$. Most importantly, it reduces the cost of the public grid, which is beneficial to the public grid and EV users.

Last but not least, a reasonable electricity price mechanism is set which provides the possibility for SPVA. In order to protect the stability of the public grid, the charge/discharge power limits are different in accordance with the "*peak*" periods and "*valley*" periods of the public grid.

The accomplished work during this thesis opens up several perspectives, which are also the key points needed to be improved.

Firstly, with the popularity of EVs, there will be certain rules for EVs arriving at the charging station every day, thus, the EV prediction system will be designed which can predict the current situation of EVs based on the EV data of the past few days. In addition, PV data can be predicted based on the weather forecast. With these two predictions, EV charging stations will have predictions about the usage of the public grid and batteries, which can better control the system and improve the stability of the system, laying a solid foundation for the realization of fully intelligent EV charging stations in the future.

Secondly, the energy management strategy of the EV charging station based on DC microgrid is currently only tested in simulation. The ultimate goal is to apply it in experimental. So, in the next step, the management strategy needs to be tested on the experimental platform and then applied to the actual EV charging station.

Thirdly, in the opinion of the charging station manager, minimizing the total cost of the charging station is an issue that must be considered, so optimization algorithms based on the proposed energy management strategy considering the degradation of battery storage, the loss of EV batteries, and the life of PV, will be applied to minimize the total operation energy costs of EV charging stations. Optimization techniques based on machine learning and artificial intelligence can be considered.

Fourthly, in the long-term plan, the energy of microgrid combined with EVs will be optimized, and the renewable energy access will be optimized. This will not only adjust the balance of the public grid, but also reduce the investment in the construction of a rotating reserve for the public grid.

Fifthly, the time period we currently consider for V2G is from 8:00 to 22:00, but in reality, part of the energy of EVs can be sent back to the public grid at night. Therefore, 24-hour V2G should be studied in the future.

To sum up, although the proposed EV charging station model combined with/without V2G accompanied by corresponding energy management strategies only stay on the basis of simulation, but it provides a foundation and guiding significance for the construction of future EV charging stations.

References

[1] IEA(2020), *Global EV Outlook 2020, IEA, Paris* https://www.iea.org/reports/global-ev-outlook-2020.

[2] Khan W., Ahmad F., and Alam M.S., *Fast EV charging station integration with grid ensuring optimal and quality power exchange.* Engineering Science and Technology, an International Journal, 2019. **22**(1): p. 143-152.

[3] Un-Noor F., et al., *A Comprehensive Study of Key Electric Vehicle (EV) Components, Technologies, Challenges, Impacts, and Future Direction of Development.* Energies, 2017. **10**(8).

[4] Szinai J.K., et al., *Reduced grid operating costs and renewable energy curtailment with electric vehicle charge management.* Energy Policy, 2020. **136**: p. 111051.

[5] Chen T., et al., *A Review on Electric Vehicle Charging Infrastructure Development in the UK.* Journal of Modern Power Systems and Clean Energy, 2020. **8**(2): p. 193-205.

[6] Lutsey N. and Hall D., *Emerging best practices for electric vehicle charging infrastructure*. 2017.

[7] (EIA) U.S.E.I.A., *International Energy Outlook*. 2019: Washington, DC: Office of Energy Analysis, U.S. Department of Energy.

[8] Pearre N.S. and Ribberink H., *Review of research on V2X technologies, strategies, and operations.* Renewable and Sustainable Energy Reviews, 2019. **105**: p. 61-70.

[9] Zhang R. and Fujimori S., *The role of transport electrification in global climate change mitigation scenarios.* Environmental Research Letters, 2020. **15**(3): p. 034019.

[10] Daina N., Sivakumar A., and Polak J.W., *Electric vehicle charging choices: Modelling and implications for smart charging services.* Transportation Research Part C: Emerging Technologies, 2017. **81**: p. 36-56.

[11] Chan C.C., *The Rise & Fall of Electric Vehicles in 1828–1930: Lessons Learned [Scanning Our Past]*. Proceedings of the IEEE, 2013. **101**(1): p. 206-212.

[12] Lieven T., *Policy measures to promote electric mobility – A global perspective.* Transportation Research Part A: Policy and Practice, 2015. **82**: p. 78-93.

[13] Kempton W., Perez Y., and Petit M., *Public Policy for Electric Vehicles and for Vehicle to GridPower*.* Revue d'économie industrielle, 2014(148): p. 263-290.

[14] Li W., et al., *Public Preference for Electric Vehicle Incentive Policies in China: A Conjoint Analysis.* Int J Environ Res Public Health, 2020. **17**(1).

[15] Tu J.-C. and Yang C., *Key Factors Influencing Consumers' Purchase of Electric Vehicles.* Sustainability, 2019. **11**(14).

[16] Yong J.Y., et al., *A review on the state-of-the-art technologies of electric vehicle, its impacts and prospects.* Renewable and Sustainable Energy Reviews, 2015. **49**: p. 365-385.

[17] Yang F., et al., *Predictive modeling of battery degradation and greenhouse gas emissions from U.S. state-level electric vehicle operation.* Nature Communications, 2018. **9**(1): p. 2429.

[18] Hu X., et al., *Battery warm-up methodologies at subzero temperatures for automotive applications: Recent advances and perspectives.* Progress in Energy and Combustion Science, 2020. **77**: p. 100806.

[19] Rahman M.A., Wang X., and Wen C., *A review of high energy density lithiu• air battery technology.* Journal of Applied Electrochemistry, 2013. **44**: p. 5-22.

[20] Owusu P.A. and Asumadu-Sarkodie S., *A review of renewable energy sources, sustainability issues and climate change mitigation.* Cogent Engineering, 2016. **3**(1).

[21] Moghaddam Z., et al., *Smart Charging Strategy for Electric Vehicle Charging Stations.* IEEE Transactions on Transportation Electrification, 2018. **4**(1): p. 76-88.

[22] Bamisile O., et al. *Smart Micro-Grid: An Immediate Solution to Nigeria's Power Sector Crisis*. in *2019 IEEE Innovative Smart Grid Technologies - Asia (ISGT Asia)*. 2019.

[23] Baloch M.H., et al., *Hybrid energy sources status of Pakistan: An optimal technical proposal to solve the power crises issues.* Energy Strategy Reviews, 2019. **24**: p. 132-153.

[24] Arndt C., et al., *Faster Than You Think: Renewable Energy and Developing Countries.* Annual Review of Resource Economics, 2019. **11**(1): p. 149-168.
[25] Shamshirband M., Salehi J., and Gazijahani F.S., *Decentralized trading of plug-in electric vehicle aggregation agents for optimal energy management of smart renewable penetrated microgrids with the aim of CO2 emission reduction.* Journal of Cleaner Production, 2018. **200**: p. 622-640.
[26] Zhuk A., et al., *Managing peak loads in energy grids: Comparative economic analysis.* Energy Policy, 2016. **88**: p. 39-44.
[27] Brown T.W., et al., *Response to 'Burden of proof: A comprehensive review of the feasibility of 100% renewable-electricity systems'.* Renewable and Sustainable Energy Reviews, 2018. **92**: p. 834-847.
[28] Wang D., et al., *Review of key problems related to integrated energy distribution systems.* CSEE Journal of Power and Energy Systems, 2018. **4**(2): p. 130-145.
[29] Tan K.M., Ramachandaramurthy V.K., and Yong J.Y., *Integration of electric vehicles in smart grid: A review on vehicle to grid technologies and optimization techniques.* Renewable and Sustainable Energy Reviews, 2016. **53**: p. 720-732.
[30] Zidan A. and Gabbar H.A., *Chapter 8 - Design and control of V2G*, in *Smart Energy Grid Engineering*, Gabbar H.A., Editor. 2017, Academic Press. p. 187-205.
[31] Sechilariu M. and Locment F., *Connecting and Integrating Variable Renewable Electricity in Utility Grid*. 2016. p. 1-33.
[32] Sechilariu M. and Locment F., *Urban DC microgrid: intelligent control and power flow optimization*. 2016: Butterworth-Heinemann.
[33] Wurtz F. and Delinchant B., *"Smart buildings" integrated in "smart grids": A key challenge for the energy transition by using physical models and optimization with a "human-in-the-loop" approach.* Comptes Rendus Physique, 2017. **18**(7): p. 428-444.
[34] Mac Kinnon M.A., Brouwer J., and Samuelsen S., *The role of natural gas and its infrastructure in mitigating greenhouse gas emissions, improving regional air quality, and renewable resource integration.* Progress in Energy and Combustion Science, 2018. **64**: p. 62-92.
[35] Badal F.R., et al., *A survey on control issues in renewable energy integration and microgrid.* Protection and Control of Modern Power Systems, 2019. **4**(1): p. 8.
[36] Locment F., Sechilariu M., and Forgez C. *Electric vehicle charging system with PV Grid-connected configuration*. in *2010 IEEE Vehicle Power and Propulsion Conference*. 2010.
[37] Hirsch A., Parag Y., and Guerrero J., *Microgrids: A review of technologies, key drivers, and outstanding issues.* Renewable and Sustainable Energy Reviews, 2018. **90**: p. 402-411.
[38] Funke S.Á., et al., *How much charging infrastructure do electric vehicles need? A review of the evidence and international comparison.* Transportation Research Part D: Transport and Environment, 2019. **77**: p. 224-242.
[39] Kostopoulos E.D., Spyropoulos G.C., and Kaldellis J.K., *Real-world study for the optimal charging of electric vehicles.* Energy Reports, 2020. **6**: p. 418-426.
[40] Tampubolon M., et al., *Constant voltage and constant current control implementation for electric vehicles (evs) wireless charger.* Journal of Physics: Conference Series, 2018. **1007**.
[41] Vu V., Tran D., and Choi W., *Implementation of the Constant Current and Constant Voltage Charge of Inductive Power Transfer Systems With the Double-Sided LCC Compensation Topology for Electric Vehicle Battery Charge Applications.* IEEE Transactions on Power Electronics, 2018. **33**(9): p. 7398-7410.
[42] Lin C.P., et al., *SOH Estimation and SOC Recalibration of Lithium-Ion Battery with Incremental Capacity Analysis & Cubic Smoothing Spline.* Journal of The Electrochemical Society, 2020. **167**(9).
[43] Thomson S.J., et al. *Design and Prototype Modelling of a CC/CV Electric Vehicle Battery Charging Circuit*. in *2018 International Conference on Circuits and Systems in Digital Enterprise Technology (ICCSDET)*. 2018.
[44] Tomaszewska A., et al., *Lithium-ion battery fast charging: A review*. eTransportation, 2019. **1**: p. 100011.
[45] Wang D., Locment F., and Sechilariu M., *Modelling, Simulation, and Management Strategy of an Electric Vehicle Charging Station Based on a DC Microgrid.* Applied Sciences, 2020. **10**(6).

[46] Haque A., Kurukuru V.S.B., and Khan M.A. *Energy Management Strategy for Grid Connected Solar Powered Electric Vehicle Charging Station*. in *2019 IEEE Transportation Electrification Conference (ITEC-India)*. 2019.
[47] Mahmud K., et al., *Integration of electric vehicles and management in the internet of energy*. Renewable and Sustainable Energy Reviews, 2018. **82**: p. 4179-4203.
[48] Weiss H.J., Winkler T., and Ziegerhofer H., *Large lithium-ion battery-powered electric vehicles@ From idea to reality.* 2018 ELEKTRO, 2018: p. 1-5.
[49] Dang Q., *Electric Vehicle (EV) Charging Management and Relieve Impacts in Grids.* 2018 9th IEEE International Symposium on Power Electronics for Distributed Generation Systems (PEDG), 2018: p. 1-5.
[50] Sun B., Tan X., and Tsang D.H.K., *Optimal Charging Operation of Battery Swapping and Charging Stations With QoS Guarantee.* IEEE Transactions on Smart Grid, 2018. **9**(5): p. 4689-4701.
[51] Bashiri M. and Bahadori N. *Optimized plan of charging stations for management of demands: An emerging need of hybrid electric vehicle*. in *2016 Future Technologies Conference (FTC)*. 2016.
[52] Chaudhari K., et al., *Hybrid Optimization for Economic Deployment of ESS in PV-Integrated EV Charging Stations.* IEEE Transactions on Industrial Informatics, 2018. **14**(1): p. 106-116.
[53] Tao J., et al. *Pricing strategy and charging management for PV-assisted electric vehicle charging station*. in *2018 13th IEEE Conference on Industrial Electronics and Applications (ICIEA)*. 2018.
[54] Mohsenian-Rad H. and ghamkhari M., *Optimal Charging of Electric Vehicles With Uncertain Departure Times: A Closed-Form Solution.* IEEE Transactions on Smart Grid, 2015. **6**(2): p. 940-942.
[55] Xing H., et al., *Decentralized Optimal Scheduling for Charging and Discharging of Plug-In Electric Vehicles in Smart Grids.* IEEE Transactions on Power Systems, 2016. **31**(5): p. 4118-4127.
[56] Locment F. and Sechilariu M., *Modeling and Simulation of DC Microgrids for Electric Vehicle Charging Stations.* Energies, 2015. **8**(5): p. 4335-4356.
[57] Bobanac V. and Pandzic H. *Lithium-ion batteries: Experimental research and application to battery swapping stations*. in *2018 IEEE International Energy Conference (ENERGYCON)*. 2018.
[58] Gong Q., et al., *PEV Charging Control Considering Transformer Life and Experimental Validation of a 25 kVA Distribution Transformer.* IEEE Transactions on Smart Grid, 2015. **6**(2): p. 648-656.
[59] Saldaña G., et al., *Electric Vehicle into the Grid: Charging Methodologies Aimed at Providing Ancillary Services Considering Battery Degradation.* Energies, 2019. **12**(12).
[60] Bandpey M.F. and Firouzjah K.G., *Two-stage charging strategy of plug-in electric vehicles based on fuzzy control.* Computers & Operations Research, 2018. **96**: p. 236-243.
[61] Xu Z., et al., *A Hierarchical Framework for Coordinated Charging of Plug-In Electric Vehicles in China.* IEEE Transactions on Smart Grid, 2016. **7**(1): p. 428-438.
[62] Pflaum P., Alamir M., and Lamoudi M.Y., *Probabilistic Energy Management Strategy for EV Charging Stations Using Randomized Algorithms.* IEEE Transactions on Control Systems Technology, 2018. **26**(3): p. 1099-1106.
[63] Hsu Y., et al., *On an Electric Scooter With G2V/V2H/V2G and Energy Harvesting Functions.* IEEE Transactions on Power Electronics, 2018. **33**(8): p. 6910-6925.
[64] Ahamed M.H.F., et al. *Modelling and simulation of a solar PV and battery based DC microgrid system*. in *2016 International Conference on Electrical, Electronics, and Optimization Techniques (ICEEOT)*. 2016.
[65] Bhandari Y., et al. *Reducing fuel consumption in microgrids using PV, batteries, and generator cycling*. in *IEEE International Conference on Electro-Information Technology , EIT 2013*. 2013.
[66] Sechilariu M., Locment F., and Darene N. *Social Acceptance of Microgrids Dedicated to Electric Vehicle Charging Stations*. in *2018 7th International Conference on Renewable Energy Research and Applications (ICRERA)*. 2018.

[67] Sechilariu M., et al., *Electromobility framework study: infrastructure and urban planning for EV charging station empowered by PV-based microgrid.* IET Electrical Systems in Transportation, 2019. **9**(4): p. 176-185.
[68] Locment F. and Sechilariu M. *Energetic Macroscopic Representation and Maximum Control Structure of electric vehicles charging photovoltaic system*. in *2010 IEEE Vehicle Power and Propulsion Conference*. 2010.
[69] Locment F. and Sechilariu M., *DC microgrid for future electric vehicle charging station designed by Energetic Macroscopic Representation and Maximum Control Structure.* 2014 IEEE International Energy Conference (ENERGYCON), 2014: p. 1454-1460.
[70] Marcincin O. and Medvec Z., *Concept of charging stations for electric cars.* Proceedings of the 2014 15th International Scientific Conference on Electric Power Engineering (EPE), 2014: p. 169-172.
[71] Wu Y., et al., *Demand side energy management of EV charging stations by approximate dynamic programming.* Energy Conversion and Management, 2019. **196**: p. 878-890.
[72] Bae S. and Kwasinski A., *Spatial and Temporal Model of Electric Vehicle Charging Demand.* IEEE Transactions on Smart Grid, 2012. **3**(1): p. 394-403.
[73] Xia Y., et al., *An EV Charging Demand Model for the Distribution System Using Traffic Property.* IEEE Access, 2019. **7**: p. 28089-28099.
[74] Trigueiro dos Santos L., Sechilariu M., and Locment F., *Optimized Load Shedding Approach for Grid-Connected DC Microgrid Systems under Realistic Constraints.* Buildings, 2016. **6**(4).
[75] Tran Dang K., et al. *Load shedding and restoration real-time optimization for DC microgrid power balancing*. in *2016 IEEE International Energy Conference (ENERGYCON)*. 2016.
[76] Wang B., et al. *A simple PV constrained production control strategy*. in *2012 IEEE International Symposium on Industrial Electronics*. 2012.
[77] Ferro G., et al., *An optimization model for electrical vehicles scheduling in a smart grid.* Sustainable Energy, Grids and Networks, 2018. **14**: p. 62-70.
[78] Nguyen D.T. and Le L.B. *Optimal energy trading for building microgrid with electric vehicles and renewable energy resources*. in *ISGT 2014*. 2014.
[79] Lu X., et al. *Multi-objective optimal scheduling of a DC micro-grid consisted of PV system and EV charging station*. in *2014 IEEE Innovative Smart Grid Technologies - Asia (ISGT ASIA)*. 2014.
[80] Wang D., Locment F., and Sechilariu M. *Shedding and restoration algorithms for an EV charging station to maximize available power*. in *2020 22nd European Conference on Power Electronics and Applications (EPE'20 ECCE Europe)*. 2020.
[81] Chekired D.A., Khoukhi L., and Mouftah H.T., *Decentralized Cloud-SDN Architecture in Smart Grid: A Dynamic Pricing Model.* IEEE Transactions on Industrial Informatics, 2018. **14**(3): p. 1220-1231.
[82] Hoang D.T., et al., *Charging and Discharging of Plug-In Electric Vehicles (PEVs) in Vehicle-to-Grid (V2G) Systems: A Cyber Insurance-Based Model.* IEEE Access, 2017. **5**: p. 732-754.
[83] Lee B., et al., *An Isolated/Bidirectional PWM Resonant Converter for V2G(H) EV On-Board Charger.* IEEE Transactions on Vehicular Technology, 2017. **66**(9): p. 7741-7750.
[84] Li F., et al., *Method to improve charging power quality of electric vehicles.* The Journal of Engineering, 2019. **2019**(16): p. 2706-2709.
[85] Rahmani-Andebili M., *Vehicle-for-grid (VfG): a mobile energy storage in smart grid.* IET Generation, Transmission & Distribution, 2019. **13**(8): p. 1358-1368.
[86] Shi R., et al. *A robust economic dispatch of residential microgrid with wind power and electric vehicle integration*. in *2016 Chinese Control and Decision Conference (CCDC)*. 2016.
[87] Alam M.J.E., Muttaqi K.M., and Sutanto D., *Effective Utilization of Available PEV Battery Capacity for Mitigation of Solar PV Impact and Grid Support With Integrated V2G Functionality.* IEEE Transactions on Smart Grid, 2016. **7**(3): p. 1562-1571.
[88] Sovacool B.K., et al., *The neglected social dimensions to a vehicle-to-grid (V2G) transition: a critical and systematic review.* Environmental Research Letters, 2018. **13**(1): p. 013001.
[89] Zhao Y., Noori M., and Tatari O., *Vehicle to Grid regulation services of electric delivery trucks: Economic and environmental benefit analysis.* Applied Energy, 2016. **170**: p. 161-175.
[90] Sechilariu M., *Intelligent Energy Management of Electrical Power Systems.* Applied Sciences, 2020. **10**: p. 2951.

[91] Locment F. and Sechilariu M. *DC microgrid for future electric vehicle charging station designed by Energetic Macroscopic Representation and Maximum Control Structure*. in *2014 IEEE International Energy Conference (ENERGYCON)*. 2014.
[92] Turker H. and Bacha S., *Optimal Minimization of Plug-In Electric Vehicle Charging Cost With Vehicle-to-Home and Vehicle-to-Grid Concepts.* IEEE Transactions on Vehicular Technology, 2018. **67**(11): p. 10281-10292.
[93] Li H., et al. *Research on multi-objective optimization coordination of plug-in hybrid electric vehicle and distributed generation*. in *2015 5th International Conference on Electric Utility Deregulation and Restructuring and Power Technologies (DRPT)*. 2015.
[94] Sarker M.R., Olsen D.J., and Ortega-Vazquez M.A., *Co-Optimization of Distribution Transformer Aging and Energy Arbitrage Using Electric Vehicles.* IEEE Transactions on Smart Grid, 2017. **8**(6): p. 2712-2722.
[95] Shi Y., et al., *Model Predictive Control for Smart Grids With Multiple Electric-Vehicle Charging Stations.* IEEE Transactions on Smart Grid, 2019. **10**(2): p. 2127-2136.
[96] Aluisio B., et al., *Optimal operation planning of V2G-equipped Microgrid in the presence of EV aggregator.* Electric Power Systems Research, 2017. **152**: p. 295-305.
[97] Ashique R.H., et al., *Integrated photovoltaic-grid dc fast charging system for electric vehicle: A review of the architecture and control.* Renewable and Sustainable Energy Reviews, 2017. **69**: p. 1243-1257.
[98] Wang D., Sechilariu M., and Locment F., *PV-Powered Charging Station for Electric Vehicles: Power Management with Integrated V2G.* Applied Sciences, 2020. **10**(18).
[99] Shi L., Lv T., and Wang Y., *Vehicle-to-grid service development logic and management formulation.* Journal of Modern Power Systems and Clean Energy, 2018. **7**(4): p. 935-947.
[100] Mao T., Zhang X., and Zhou B., *Modeling and Solving Method for Supporting 'Vehicle-to-Anything' EV Charging Mode.* Applied Sciences, 2018. **8**(7).
[101] Wang Y., et al. *Integration of V2H/V2G hybrid system for demand response in distribution network*. in *2014 IEEE International Conference on Smart Grid Communications (SmartGridComm)*. 2014.
[102] Mwasilu F., et al., *Electric vehicles and smart grid interaction: A review on vehicle to grid and renewable energy sources integration.* Renewable and Sustainable Energy Reviews, 2014. **34**: p. 501-516.
[103] Xiang Y., et al., *Electric vehicles in smart grid: a survey on charging load modelling.* IET Smart Grid, 2019. **2**(1): p. 25-33.
[104] Kempton W. and Tomić J., *Vehicle-to-grid power fundamentals: Calculating capacity and net revenue.* Journal of Power Sources, 2005. **144**(1): p. 268-279.
[105] Ahmad F., Alam M.S., and Asaad M., *Developments in xEVs charging infrastructure and energy management system for smart microgrids including xEVs.* Sustainable Cities and Society, 2017. **35**: p. 552-564.
[106] Ahmadian A., et al., *Plug-in electric vehicle batteries degradation modeling for smart grid studies: Review, assessment and conceptual framework.* Renewable and Sustainable Energy Reviews, 2018. **81**: p. 2609-2624.
[107] Boglou V., et al., *A Fuzzy Energy Management Strategy for the Coordination of Electric Vehicle Charging in Low Voltage Distribution Grids.* Energies 2020. **13**: p. 3709.
[108] Marra F., et al. *Demand profile study of battery electric vehicle under different charging options*. in *2012 IEEE Power and Energy Society General Meeting*. 2012.
[109] Bai W., Sechilariu M., and Locment F., *DC Microgrid System Modeling and Simulation Based on a Specific Algorithm for Grid-Connected and Islanded Modes with Real-Time Demand-Side Management Optimization.* Applied Sciences, 2020. **10**(7).